Enzyme Diffusion and Cellulose Breakdown in the Bioremediation of Medical Waste

by

Douglas B. Hudgins

Thesis submitted to the Faculty of the

Virginia Polytechnic Institute and State University

in partial fulfillment of the requirements for the degree of

MASTER OF SCIENCE

in

Mechanical Engineering

APPROVED:

Alan A. Kornhauser, Chairman

Charles F. Reinholtz

Richey M. Davis

May, 1994
Blacksburg, Virginia

c.2

LD
5655
V855
1994
H834
c.2

Enzyme Diffusion and Cellulose Breakdown in the Bioremediation of Medical Waste

by

Douglas B. Hudgins

Committee Chairman: Alan A. Kornhauser
Mechanical Engineering

Abstract

The disposal of infectious medical waste has become a major environmental concern. New disposal methods are currently being investigated; one of these is a bioremediation process which utilizes enzymes in a batch reactor to render the waste noninfectious. The success of this biological process depends on (among other things) two mechanisms: the diffusion of the disinfecting enzymes into small crevices within the waste stream and the breakdown of cellulose-derived material by cellulase enzymes.

It was found that the waste stream contained a variety of small crevices which could possibly contain pathogens. Circulation in these crevices was restricted by their small openings and one must rely on diffusion of enzymes to disinfect their interiors. Numerical models for the diffusion of enzymes within one-dimensional and re-entrant crevices were developed and a method for comparing various re-entrant crevices was presented. From these models a conservative method for determining approximate disinfection times for the crevices was described. It was determined from this conservative method that most crevices within the waste will either be disinfected during the process or shortly thereafter.

This biological process also utilizes cellulases to breakdown the paper within the waste stream. Small-scale simulated waste experiments were conducted with cellulases to determine the increase in maximum mixable solids concentration and the mass reduction of the waste due to cellulase activity. The addition of cellulases to the slurry more than doubled the waste concentration which could be agitated and reduced the agitator shaft power by as much as 50% when compared to the simulated waste tests with no cellulase. Significant mass reduction was also observed with the addition of cellulases to the slurries. Small-scale breakdown experiments were conducted with and without cellulases using newsprint as the substrate. These experiments were performed to determine the influence of cellulose hydrolysis by cellulases on agitator power. A simple mathematical model was developed and presented which described this phenomenon.

Acknowledgments

To begin with, I would like to thank my advisor, Dr. Alan Kornhauser for his help and insight into this research. Without his guidance and knowledge, this work would not have been possible. His patience and suggestions in writing this report were also greatly appreciated.

I must thank Dr. Charles Reinholtz for his knowledge and organization of the entire bioremediation project, without this my research would not have been pursued. I also thank him for his willingness to help me with any problem at a moment's notice.

I thank Dr. Richey Davis for his advise and Chemical Engineering expertise. His guidance and background in Chemical Engineering kept this research moving in the right direction.

Thanks to Mr. Clark Fuqua and Mr. T.D. Steele for their support and funding of this research. Their enthusiasm for this project made the work that much more exciting.

I would like to thank Anil Garg, Travis Walker, and Charlie Douglass for their help and understanding of the mechanical system. I would also like to thank them for their remarks and humor in the lab.

Thanks to Steven Hall, Mark Vaughan, and Liz Devaney for their patience in conducting numerous experiments. Their humor and comments, though not always welcome, made this research more enjoyable.

I would also like to thank my lab partners, Brian Lattimer, Mike Alexandrian, Frank Cantelmi, Yagna Mukkamala, and Brian Kafka for the camaraderie we shared in the Flow Lab.

Many years of thanks to my roommate and friend, Troy Mutter. I will always remember the five years we shared apartments together in Richmond and in Blacksburg. I wish him and his new bride Valerie the best and consider him the brother that I never had.

Special thanks to the members of the Light Year Club (a.k.a. B.P.'s): Craig Dempsey, Miller Williams, Dr. Harrison Steeves, Stephen Hiner, and Dave Braine. The many weekend flyfishing trips were a much needed break from my graduate studies. These trips in my eyes were truly worthless.

Last of all, but most important, I would like to thank my parents, Dr. and Mrs. H. Bland Hudgins. I give credit to them for all that I am and have today. Their love and support during my graduate studies as well as during my entire life provide the foundation for all my goals in my career as an engineer and as a person.

Table of Contents

			page
1	Introduction		1
	1.1	Motivation	1
		1.1.1 Medical Waste -- A Disposal Problem	2
		1.1.2 Biological Process Summary	2
		1.1.3 Mechanical System Summary	4
	1.2	Research Overview	7
		1.2.1 Enzyme Crevice Penetration	8
		1.2.2 Cellulose Breakdown	9
	1.3	Literature Review	11
		1.3.1 Diffusion	12
		1.3.2 Cellulose Hydrolysis Due to Cellulases	14
Part I	**Enzyme Crevice Penetration Due to Molecular Diffusion**		17
2	One-Dimensional Diffusion Model		18
	2.1	Development of Fundamental One-Dimensional Model	19
		2.1.1 Fick's Second Law of Diffusion	19
		2.1.2 No Concentration Gradient in Radial Direction	21
	2.2	Determination of Diffusion Coefficient	21
		2.2.1 Experimentally Measured Coefficient	22
		2.2.2 Stokes-Einstein Equation	24
	2.3	One-Dimensional Crevice Analysis	26
		2.3.1 Worst Case Scenario	26
		2.3.2 Boundary Conditions	27
		2.3.3 One-Dimensional Model Exact Solution	29
		2.3.4 One-Dimensional Model Results	29

page

2.3.5 Disinfection Time Versus Penetration Time 32

2.3.6 Crevice Disinfection After Process Time 33

2.3.7 Example Disinfection Time Calculation 38

3 Re-entrant Crevice Diffusion Models 41

3.1 Re-entrant Crevice Characterization 42

3.1.1 Porous Media 42

3.1.2 Re-entrant Crevices 43

3.2 Development of Fundamental Two-Dimensional Model 43

3.3 Exact Solution for Sector Crevice 46

3.4 Rectangular Crevice Models 48

3.4.1 Rectangular Crevice Notation 49

3.4.2 Alternating Direction Implicit Method 51

3.5 Rectangular Crevice Comparison to Sector Crevice 52

3.5.1 Characteristic Length 53

3.5.2 Sector - Rectangular Volume Analysis 54

3.5.3 Dimensionless Volume 57

3.6 Rectangular-Sector Comparison 58

4 Diffusion Conclusions 63

4.1 One-Dimensional Model Conclusions 63

4.2 Re-entrant Model Conclusions 64

4.3 Future Work 65

Part II Cellulose Breakdown within the Batch Reactor 67

5 Overview of Cellulose 68

5.1 Molecular Structure of Cellulose 68

5.2 Basics of Cellulose Hydrolysis by Cellulases 70

5.3 Composition of Various Paper Types in Medical Waste 75

5.3.1 Composition of Wood 75

page

5.3.2 Basics of Wood Pulp 76

5.3.3 Activity of Cellulases on Paper in the Batch Reactor 77

6 Cellulose Hydrolysis Experimentation 78

6.1 Maximum Mixable Solids Concentration Experiments 78

6.1.1 Simulated Medical Waste Sample 79

6.1.2 Experimental Apparatus and Setup 79

6.1.3 Experimental Procedure 80

6.1.4 Simulated Medical Waste Results 82

6.2 Influence of Cellulose Hydrolyzation on Agitator Power 87

6.2.1 Experimental Procedure 87

6.2.2 Paper Breakdown Results 90

7 Cellulose Hydrolysis Model 96

7.1 Model Theory 96

7.2 Method for Determining Coefficients and Time Constants 99

7.3 Model Results 101

8 Cellulose Breakdown Conclusions 108

8.1 Simulated Waste Experiments 108

8.2 Newsprint Experiments 110

9 Review and Summary 112

9.1 Enzyme Diffusion Review and Summary 112

9.2 Guidelines for Determining Disinfection of Crevices 115

9.3 Summary of Cellulose Breakdown Conclusions 116

Appendix A Diffusion Solutions 118

A.1 One-Dimensional Diffusion Solutions 118

A.1.1 One-Dimensional Diffusion During Batch Process 118

A.1.2 One-Dimensional Diffusion (Post-Batch) 122

A.2 Re-entrant Sector Exact Solution 125

		page
Appendix B	Diffusion Computer Codes	128
B.1	One-Dimensional Diffusion Computer Codes	128
	B.1.1 Code Listing for Batch Process	128
	B.1.2 Code Listing for Post-Batch Diffusion	130
B.2	Two-Dimensional Diffusion Computer Codes	132
	B.2.1 Code Listing for Sector Crevice	132
	B.2.2 Code Listing for Shape 1	139
	B.2.3 Code Listing for Shape 2	146
Appendix C	Experimental Verification of Diffusion Assumption	155
Appendix D	Sector-Rectangular Comparison for Shape 2	160
References		163
Bibliography		167
Vita		168

List of Figures

		page
Figure 1.1	Mechanical System Schematic.	6
Figure 2.1	Differential Control Volume.	20
Figure 2.2	One-Dimensional Crevice Problem.	28
Figure 2.3	Solute Concentration at the Back Wall (L = 0.64 cm) (Incorrect Diffusion Coefficient Range).	30
Figure 2.4	Enzyme Concentration at the Back Wall (L = 0.64 cm).	31
Figure 2.5	Enzyme Penetration After a One Hour Diffusion Time.	36
Figure 2.6	Back Wall (L = 0.64 cm) Enzyme Concentration.	37
Figure 2.7	Killing of HPV-2 for 0.1% Protease, pH 8.5.	39
Figure 3.1	Sector Crevice Problem Definition.	45
Figure 3.2	Concentration Versus Time for a Sector Crevice.	48
Figure 3.3	Rectangular Crevice Notation (Shape 1).	49
Figure 3.4	Rectangular Crevice Notation (Shape 2).	50
Figure 3.5	Rectangular Crevices with Characteristic Length.	54
Figure 3.6	Rectangular-Sector Transformation.	56
Figure 3.7	Sector Crevice Concentration for Various Dimensionless Volumes.	58
Figure 3.8	Transient Concentration for $Vo = 30$ Corresponding to Shape 1 and the Worst Case for Shape 2.	60
Figure 3.9	Time Versus Volume Comparison for $\theta = 0.1$ (Shape 1).	61
Figure 5.1	Beta Configuration Found in Cellulose.	69
Figure 5.2	Cellulose Structure.	70
Figure 5.3	Linkage of L-amino acids in the Formation of an Enzyme.	71
Figure 5.4	Cellulose Degradation by Cellulases.	74
Figure 6.1	Shaft Power Versus Time for Simulated Medical Waste With and Without Cellulase.	83

		page
Figure 6.2	Shaft Power Versus Waste Concentration With and Without Cellulase.	85
Figure 6.3	Shaft Power Versus Time for 1% Newsprint With and Without Cellulase.	91
Figure 6.4	Shaft Power Versus Time for 2% Newsprint With and Without Cellulase.	92
Figure 6.5	Shaft Power Versus Time for 4% Newsprint With and Without Cellulase.	93
Figure 7.1	Power Reduction Over Time Due to Mechanical Agitation.	103
Figure 7.2	Power Reduction Over Time Due to Mechanical Agitation and Cellulase Activity.	104
Figure 7.3	Coefficients and Constants Relationship With Paper Concentration.	105
Figure 7.4	Model Comparison With Experimental.	107
Figure D.1	Sector - Shape 2 Comparison for a Length Ratio of 0.25.	160
Figure D.2	Sector - Shape 2 Comparison for a Length Ratio of 0.50.	161
Figure D.3	Sector - Shape 2 Comparison for a Length Ratio of 0.75.	162

List of Tables

		page
Table 2.1	Protease Diffusion Coefficient Summary.	25
Table 5.1	Amino Acid Composition of the Endo and Exo-glucanases of *Trichoderma viride.*	72
Table 5.2	Average Composition of Wood.	75
Table 6.1	Simulated Medical Waste Composition.	79
Table 6.2	Mass Reduction of Simulated Waste Samples.	86
Table 6.3	Mass Reduction of Paper Samples.	94
Table 7.1	Power Coefficients and Constants for Various Paper Concentrations.	102

1
Introduction

1.1 Motivation

Infectious medical waste disposal is a growing problem in today's society. There are only a few licensed methods for disposal of such waste with the most common method being incineration. However, there is a growing interest in the development of new technologies to dispose of infectious medical waste. One of the current new technologies being investigated is a bioremediation process. This process uses enzymes to treat the infectious medical waste as well as breakdown some of the cellulose material and render the waste suitable for disposal in sanitary landfills. This process has substantial benefits when compared to other alternatives because it has no harmful emissions and is more environmentally friendly.

Success of the bioremediation process depends on (among other things) two mechanisms: the diffusion of the disinfecting enzymes into small crevices within the waste stream and the breakdown of cellulose-derived material by cellulase enzymes. The enzymes which disinfect the waste need to reach all cavities within the waste in adequate numbers to reduce the number of pathogens in the waste stream to acceptable levels. Also, the cellulase enzyme needs to breakdown paper substantially so that more waste can be disposed of per cycle of the system. This work investigates these two areas of concern.

This section will orient the reader to the waste problem and this new technology by covering the following topics:

- Medical waste - a disposal problem
- The biological process summary
- The mechanical system summary

1.1.1 Medical Waste -- A Disposal Problem

The disposal of waste has become a major concern. Infectious medical waste has become an even greater problem due to the regulations which most states place on hospitals concerning the disposal of such waste. Each year 150,000 tons of medical waste are produced in the state of Virginia [1, Malloy]. Currently, in Virginia the only method of disposal permitted by the regulations is incineration. The amount of waste generated in Virginia exceeds the capacity of the states licensed incinerators due to a moratorium on new construction and/or installation of incinerators in the state. The moratorium was placed on new construction and/or installation due the increasing environmental concerns over air emissions and the residual ash produced by these incinerators. In order to dispose of this waste, hospitals ship the excess waste across state lines.

In addition to disposal limitations in Virginia, questions are being raised around the use of incinerators due to environmental concerns. The ash which is produced from incineration is carcinogenic and is therefore considered toxic -- another waste disposal problem [1, Malloy]. Hershkowitz [2] notes that substandard on-site incinerators generate up to 3 million tons of ash every year. Air emissions of incinerators are also another environmental concern. Therefore, there has been an increased interest in the development of new disposal methods in Virginia in addition to other states. Currently, new regulations are being drafted which would allow safe alternative systems to operate in Virginia. This is where the new bioremediation technology developed by Virginia institutions becomes applicable.

1.1.2 Biological Process Summary

A Virginia company along with Virginia universities has developed a unique method to disinfect medical waste. This technology disinfects the waste stream and therefore allows the waste, once treated, to be disposed of in a sanitary landfill similar to household garbage. The method is known as bioremediation which is defined as follows: "The

remediation of danger due to hazardous waste through the application of biological agents." In this technology enzymes at proper temperature and pH are used to kill the harmful microbes as well as decompose the cellulose derivative material such as paper, gauze, sponges, etc. The "recipe" used is a mixture of protease and cellulase enzymes. The protease enzymes are used to disinfect and the cellulase enzymes are used to hydrolyze the cellulose within the waste stream. This section gives an overview of the biological process and also lists the additional steps in the bioremediation process needed to treat the waste entirely. It also discusses the significance of using cellulase enzymes during the biological process.

This process takes place in a slurry of water, waste, and enzymes in a large tank, a simple batch reactor, which is agitated constantly. In order for these enzymes to do their job, they must be in a favorable environment. In other the words, the pH and temperature of the slurry must be monitored and controlled at all times in order for the enzymes to be at optimum activity. To complicate matters, the optimum pH for the cellulase and protease enzymes is not the same. Therefore, the actual treatment of the waste within the reactor occurs in a two step process. The paper is hydrolyzed initially at a pH of 4.3 and temperature of 50°C. After sufficient hydrolyzation time, the pH is adjusted to 9.0, the protease is added and after a time still to be determined, the disinfection process is completed.

In addition to the biological process, the bioremediation process incorporates several other steps to treat the waste entirely. These other steps include shredding the waste to reduce the size of the particles and expose more surfaces to the enzymes, separating the water from the waste after the biological process is completed, disposing of the water effluent to the sewer, and disposing of the remaining waste to a municipal waste landfill. This is a summary of the entire bioremediation process.

Now that a basic overview of entire bioremediation process has been covered, the purpose of the cellulase enzymes can be better understood. The cellulase enzymes serve no purpose in the actual neutralization of harmful "bugs". However, these enzymes serve three significant purposes.

- They act as a viscosity modifier in the batch reactor.
- They reduce some of the cellulose entirely to glucose.
- They ensure access of other enzymes to all microbe-containing materials.

Firstly, the cellulase reduces the viscosity of the slurry by attacking the long strands of cellulose within paper. The enzymes break the paper into smaller pieces, thus reducing the viscosity of the mixture over time. This allows for higher solids concentrations to be treated in the reactor in one batch, since studies have shown that as much as 60 percent of medical waste is paper [3, Carpenter]. Secondly, by reducing some of the cellulose entirely to glucose which is soluble in water, the mass of the waste stream as it leaves the system is reduced. This mass is lost because the water/sugar effluent is sent directly to the sewer and does not remain in the waste which is sent to the landfill. Also additional mass is lost due to some of the small cellulose strands passing through the screen during the water separation stage of the process. This separation stage occurs after the waste has been disinfected. Thirdly, the cellulase enzymes remove any cellulose-derived material which may be blocking the entrance to voids within the waste stream. These enzymes actually "clean" the waste so that all surface are exposed to the protease enzymes which disinfect the waste.

1.1.3 Mechanical System Summary

The bioremediation process sounds like a unique environment-friendly process of using naturally occurring enzymes to treat harmful waste, but this raises the question, how does

the waste travel from red-coded infectious waste to unrecognizable harmless refuse. This required the design of a mechanical system. This system needed to be safe to operate, relatively simple, and adaptable to various hospital locations, needs, etc. The mechanical system has the following components:

- hopper
- shredder/sizing screen
- agitated tank
- slurry pump
- separator
- HEPA filter with exhaust fan

The mechanical system schematic is shown in Figure 1.1.

The first component in the system is the hopper. The operator deposits the redbags in the hopper which feeds the shedder. It also can hold more than one bag so that the operator can fill the hopper completely and attend to other responsibilities while the waste is being shredded.

The shredder/sizing screen combination is the next component in the mechanical system. In the regulations previously mentioned, one of the requirements for disposal is that the waste be unrecognizable after treatment. The system satisfies this criterion by reducing the particle size to approximately 1.27 cm (1/2 in) by a shredder/sizing screen combination. The mesh size of the screen is such that only the desired size particles pass through while the larger particles recirculate and remain until they have reached the desired particle size. This shredder is fed manually via a hopper and empties directly into the batch reactor which is positioned under the shredder.

Connected to the hopper are the HEPA filter and exhaust fan. This combination keeps the hopper and shedder under negative pressure so that the operator will not be exposed to any harmful pathogens during the process. This ensures a safe working environment for all the employees at the hospital.

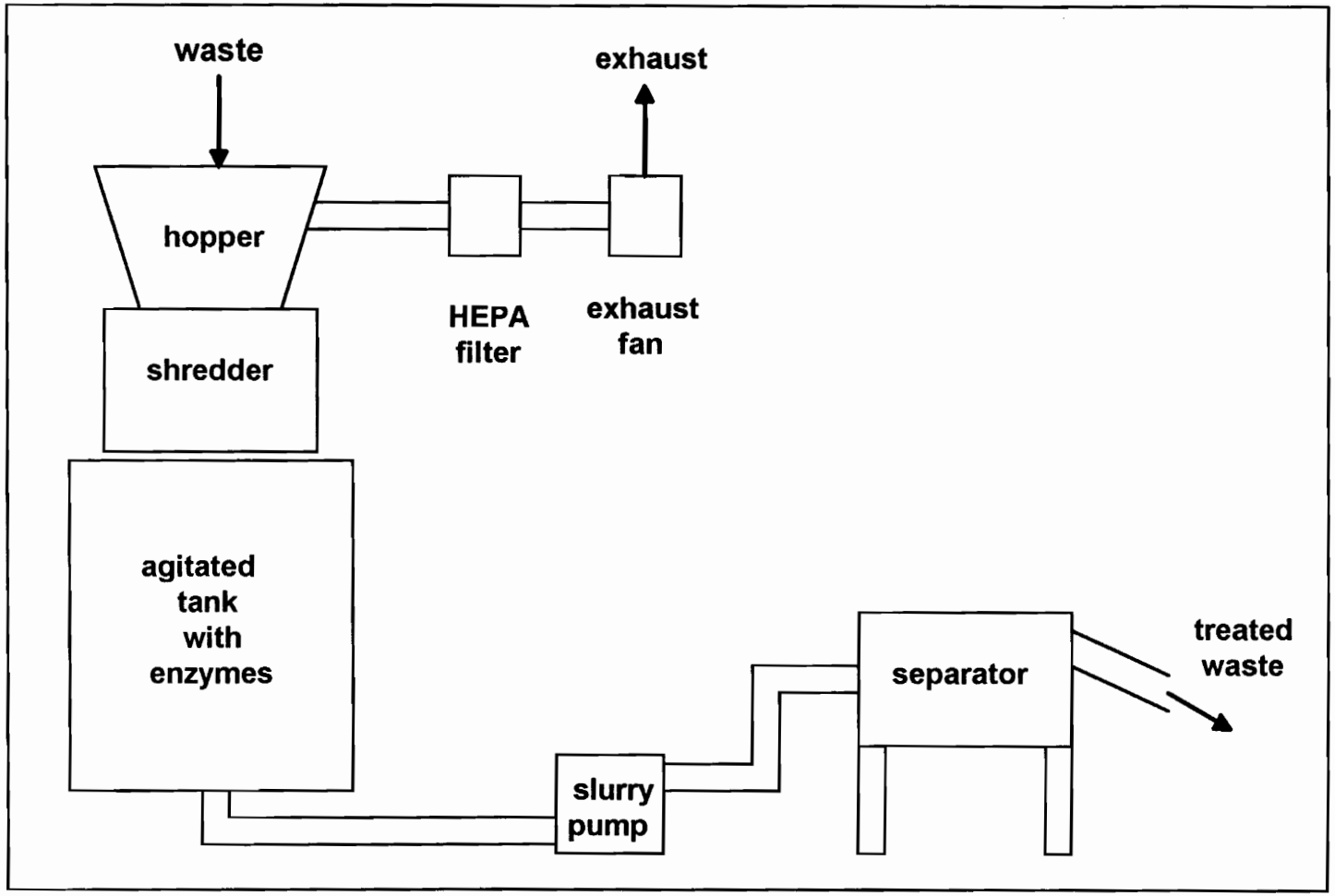

Figure 1.1 - Mechanical System Schematic.

The agitated tank is probably the most important component in the system because this is where the disinfection of the waste occurs. Before waste is actually fed into the hopper, the tank has been filled with water, base, and cellulase enzymes at the appropriate temperature for optimum cellulase activity. The acid is used in order to lower the pH to the desired value for optimum cellulase activity. Once the setup of the tank is complete, waste is metered into the tank until the agitator power reaches a maximum set level and waste addition subsides. The hydrolyzation process is allowed to continue for an additional hour to maximize the hydrolyzation of the cellulose material. Once this is achieved, base is added to increase the pH to the desired level for optimum protease activity and the protease enzymes are introduced to begin the disinfection. After disinfection has occurred, the water must be removed from the waste.

The slurry pump transports the disinfected slurry to the separator. This pump has the capability to pump very viscous slurries with solids concentrations up to 15% by weight. The pump is actually a chopper pump which reduces the particle size of the remain waste even further. This aids in meeting the requirement that the waste be unrecognizable after treatment.

The waste is dewatered by a hydraulic press separator which allows some of the smaller particles within the slurry to pass to the sewer. After the waste stream has be dewatered, there is an 85% reduction in volume in the waste stream. Now, the resulting mass of solids can be disposed of in an ordinary sanitary landfill.

1.2 Research Overview

With the design of the entire mechanical system, there were several areas of research which had to be investigated in order to validate the bioremediation system. There were two specific objectives in this research:

- Determine the degree of enzyme penetration into small voids or crevices within the waste stream.

- Investigate the effect the hydrolyzation of paper has on the agitator power as well as the maximum mixable solids concentration within the slurry.

These two topics were separated into two parts within this paper:

- Part I - Enzyme Crevice Penetration Due to Molecular Diffusion.

- Part II - Cellulose Breakdown Enhanced by Cellulase Enzyme.

1.2.1 Enzyme Crevice Penetration

Within the waste stream generated at a hospital, there are a number of large crevices such as bottles, tubes, etc., which could possibly be infected with virus, bacteria, or the like. Due to the shredding process within the system, most of these large voids will be eliminated. However, in the approximate 1.27 cm (1/2 in) pieces to which the waste stream is reduced, some small crevices remain, some of which include small hypodermic needles, tubes, small pieces of sponge, etc. These types of crevices are potentially difficult to disinfect due to insufficient penetration of the enzyme-rich solution into the small opening.

The protease enzymes ability to disinfect is due largely to the agitation of the slurry because this agitation constantly keeps enzymes at the surface of particles which need to be treated. If the opening to a crevice is small enough, say the inside diameter of a hypodermic needle, there is no fluid motion in or out of the crevice. Therefore, the only possible path for the protease to penetrate such a crevice would be due to molecular diffusion of the enzymes through the crevice opening. The purpose of this research was to determine the degree of protease penetration into these types of voids and the amount of time needed to disinfect these areas completely.

The research developed one-dimensional and two-dimensional models which simulate the various crevice types. The one-dimensional model accounted for any long, slender crevice such as tubes or needles. The two-dimensional model presented more of a problem, since there are an infinite number of shapes and sizes of crevices which could occur within the waste; so, two of the most frequently occurring shapes in the waste stream were modeled These two shapes were a sector-shaped crevice which had an exact solution and rectangular-shaped crevice which were modeled using a finite difference technique. The rectangular crevice diffusion rates were compared with the sector crevice model by analyzing a group of dimensionless parameters. From this comparison it was determined that by using the exact solution and this group of parameters, diffusion rates of most rectangular shapes could be approximated with the exact solution.

Most of the diffusion work was numerical analysis but, some experiments were conducted. The experimental method which was implemented failed to give accurate diffusion measurements. This method utilized capillary tubes within an agitated bath of dye with a known diffusion coefficient. This test was conducted in order to determine if there was an enhanced diffusion coefficient due to turbulence from mixing. A detailed procedure of this method and the reasons for its failure, as well as an alternative method suggested by Davis [4] are presented in Appendix C.

1.2.2 Cellulose Breakdown

Cellulose contained in paper, gauze, sponges, etc. is a major component in the make-up of medical waste. Due to the cellulase enzyme as well as mechanical agitation, there is a considerable amount of breakdown of the cellulose derivative material. Research was conducted in a small-scale test vessel with an agitator in order to quantify the degree and rate of breakdown. This was done in order to determine the effect cellulose breakdown has on agitator power and maximum mixable solids concentration in the slurry.

Research was done to determine the variation in agitator power due to the decomposition of paper. It was determined that different types of paper decompose differently due to the variation in molecular structure and composition. Each type of paper has its own breakdown rate depending on the paper's origin and the type of cellulases present in the slurry. The variation among types of paper was a concern since the paper composition of the waste stream from hospitals is an unknown. Therefore, most tests were run with newsprint, which is probably the most difficult paper type to breakdown due to its low cellulose content.

From this work breakdown models were developed for two types of decomposition: the breakdown due to mechanical agitation and cleavage of hydrogen bonds and the breakdown enhanced by the hydrolyzation of cellulose due to the addition of cellulase enzyme. Hydrolyzation is defined as the breakdown of a substance into a weak acid or weak base in the presence of water. These models will help in the design of additional bioremediation systems as well as help in the fundamental understanding of the viscosity reduction capabilities of cellulase.

In addition to the agitator power models, tests were conducted to determine the maximum solids concentration which could be treated in one batch. This information was essential in the design of the system in order to determine the tank size which would be capable of treating the amount of waste generated by a specific hospital each day. These tests were performed with simulated medical waste in two liter batches. Waste was metered into the tank at a rate scaled down to meet the predicted waste output of the shredder in the actual system. Tests were conducted with and without cellulase to determine the increase in solids concentration made possible by the enzyme hydrolysis within the slurry. As a result of these tests, data was obtained on the approximate reduction in volume and mass of the waste stream.

1.3 Literature Review

On the subject of this research, there were two areas in the literature which needed to be investigated:

- Diffusion of enzymes.
- The enhancement of cellulose breakdown due to cellulase enzymes.

Very little work has been done on the diffusion of specific enzymes. However, much work has been conducted on the broad topic of diffusion. The fundamental equations which describe diffusion phenomena and mass transfer extensively have been covered in numerous texts and will not be covered in this section. These fundamental equations governing the diffusion of enzymes were developed in the body of this paper. In this literature review, two topics of previous work were covered.

- Diffusion of protease enzymes in aqueous solutions.
- Experimental test methods using capillary tubes or similar one-dimensional volumes to evaluate molecular diffusivity rates.

In reference to literature in the area of cellulose hydrolyzation, much work has been published on the breakdown of cellulose into reduced sugars and similar topics, but very little has been written on cellulose hydrolyzation and its resulting influence on agitator power or its influence on maximum mixable solids concentration. Three topics of previous work dealing with cellulose hydrolyzation were covered in this section.

- The use of cellulases.
- Cellulose hydrolyzation by enzymes and its influence on agitator power.
- The use of cellulases to reduce cellulose to fermentable sugars in municipal solid waste.

1.3.1 Diffusion

This research is concerned with the binary diffusion of protein enzymes through solvents very similar to water. Two papers of previous work are cited by Ottesen and Svendsen [5] and Shane et al. [6]. Both of the paper's authors observed the diffusion of different protein types: Ottesen and Svendsen - serine proteases and Shane et al. - pancreatic proteases.

Ottesen and Svendsen described and compared various serine proteases known as subtilisins which originated from strains of *Bacillus subtilis* or related bacteria. The enzymes which are used in this bioremediation process originate from the same strains. In their work Ottesen and Svendsen compared three subtilisins: Subtilisin Carlsberg, Subtilisin BPN', and Subtilisin Novo. They indicated that these three enzymes were almost identical in amino acid composition and therefore, should have very similar diffusion rates. They listed the binary liquid diffusion coefficient as 9.07×10^{-7} cm^2/s for Subtilisin BPN' at 20° C for a solvent of water. However, they did not indicate the method used to determine this diffusion coefficient.

Diffusion of protein enzymes other than subtilisins have been studied as well. Shane et al. described the effect of a solvent gradient on protein diffusion. They evaluated the apparent diffusion rates of α-chymotrypsin across porous membranes as a function of the methanol concentration and methanol concentration gradient. The solvent used was a water-methanol mixture and α-chymotrypsin is a pancreatic protease. In this work the experiments were conducted with the water-methanol mixture at uniform concentration and with a methanol concentration gradient across the membrane. They conducted these experiments using a diffusion cell technique. They listed a diffusion coefficient of 1.02×10^{-6} cm^2/s for this particular protein in water at 20° C. Therefore, this previous work by Shane et al. and Ottesen and Svendsen was of value to this research due to principals of enzymatic diffusion in a solvent and for the measured values of diffusion coefficient which were used to evaluate the numerical models.

Several methods were listed in the literature to experimentally measure the mutual diffusion coefficient at infinite dilution. These methods include the diaphragm cell [7, Northrop and Anson], the Taylor dispersion method [8, Taylor], the capillary tube method, and various optical technique such as light scattering [9, Cummins and Pike] and holography [10, Heflinger et al.]. This literature review concentrates on the capillary method because two methods using capillary tubes were suggested to validate the diffusion only assumption in this research. The capillary tube method was described by the following authors:

- Anderson and Saddington [11]
- Mills and Kennedy [12]
- Mills [13]

Anderson and Saddington first introduced the capillary tube method. Their method used a narrow, thick-walled capillary, sealed at one end. This tube was filled with a labeled species and then lowered vertically, open end upward, into a large volume of inactive solution. Diffusion of the labeled species from the capillary into the inactive, unagitated solution was allowed to take place and, after an appropriate time, the capillary tube was removed. The amount of labeled species remaining in the capillary was then measured and the diffusion coefficient was determined from this data as described by the authors.

Mills and Kennedy describe a similar method. They suggested that the process of immersing the capillaries in the large bulk of solution might be expected to produce losses by mechanical convection. However, their results proved these losses to be small and confirmed that these losses could be neglected.

The problem of stirring the bulk solution outside the capillary seemed to be more important than the immersing process. If the bath is unstirred the concentration at the top of the column is not always zero. However, if the solution is stirred at a gradually increasing speed, turbulence will eventually develop across the end of the capillary and some labeled material will be removed from the tube by this means. Mills designed an

experiment in which the liquid flowing across the top of the capillary tube was arranged to have a streamline or laminar form. The data from his experiment showed that diffusion coefficients using this method agreed with those on the same system from diaphragm cell measurements only when the streamline flow rate was between 1 and 3 mm/s. By controlling the streamline flow rate between these limits the precision of successive measurements improved from the usual ±2 percent or worse, to ±0.8 percent. He stated that further improvements in precision of this conventional technique are limited by the accuracy with which the contents of the capillary (about 10μl volume) can be analyzed.

1.3.2 Cellulose Hydrolysis Due to Cellulases

The use of cellulases to decompose cellulose to a reduced form has been explored since the early 1900's. Seilliere [14] investigated the breakdown of cellulose by snail digestive juices. However, it was not until the early 1950's that activities of cellulases were observed in chemical detail using highly purified preparations. Reese et al. [15] studied the degradation of soluble cellulose derivatives by fungal-derived strains of cellulase. From this origin the use of cellulases had expanded to the following uses by the mid-1970's detailed by Emert et al. [16]:

- Digestive aids
- Food processing:
  - Nutrient availability
  - Texture modification
  - Pulp removal
- Microbial growth for single cell protein
- Saccharification of cellulose
- Plant cell wall removal:
  - Tissue culture
  - Fusion of protoplasts

More recently, efforts have concentrated on the use of cellulases in the saccharification and fermentation of cellulose material to ethanol. The work in this area was detailed in papers by such authors as Ramachandran and Hashim [17], Roy et al. [18], and Philippidis et al. [19].

The present research demonstrated the use of cellulases to enhance the cellulose breakdown in order to reduce the viscosity and maximize the amount of material added to the reactor. There have been some research efforts in the area of agitation intensity and its influence on cellulase activity. However, this work was concerned with the effect the intensity had on cellulose hydrolysis rate and not the reduction in solution viscosity over time due to cellulose hydrolysis.

Mukataka et al. [20] experimented with the effect of agitation intensity on the production of reduced sugars using *Trichoderma reesei* QM9414 under sufficiently dissolved oxygen concentration. These experiments were conducted on three different cellulose-derived substrates: Whatman No. 1 filter paper, carboxymethyl cellulose, and cellobiose. They evaluated the activity of the enzyme by measuring the amount of reduced sugars in the supernatant fluid obtained after the removal of solids for the filter paper and carboxymethyl cellulose. For the cellobiose they measured the release of glucose in the supernatant fluid. Each of these tests were conducted at different values of tip velocity ranging from 0.3 to 1.7 m/s in a 1.2 L working volume. They determined that the optimum tip velocity for all three substrates was about 1.0 m/s which corresponded to 300 rpm for an impeller with a diameter of 66 mm. The activity actually decreased for tip velocities above this value for all substrates. However, the optimum range was between 0.7 and 1.4 m/s. Work by Wase et al. [21] also has shown the reduction in cellulase activity for reactors which encounter intense mixing. These studies were conducted with cellulases derived from fungal strains other than *Trichoderma reesei*.

Research on cellulose hydrolysis of waste materials has only been conducted on that of solid municipal wastes. The research in this area has mainly been concerned with the use of cellulases to reduce the paper, cardboard, etc. in the municipal waste to fermentable sugars for fuel production. Tiraby et al. [22] measured influence of enzyme and substrate concentration on the enzymatic saccharification of municipal wastes. The municipal wastes used were cleared of glass and metal and the particle size was reduced to 4-5 cm

by mechanical grinding. The average composition was determined as follows (in percentage of dry matter):

- cellulose 41%
- hemicellulose 14%
- lignin 16%
- fat 4%
- total nonextractibles (plastics, ashes, etc.) 21%

For the enzyme concentration experiments, they found a nearly linear correlation between enzyme concentration and sugar yields at 24 and 48 hours. Sattler et al. [23] also detailed similar results except that Sigmacell 50 and pretreated poplar wood were use as the substrate instead of municipal waste. For the substrate concentration experiments detailed by Tiraby and others, the enzyme concentration was kept at 10 mg enzyme/g substrate and the substrate concentration was raised. In their experiments, 6, 8, or 10% slurries were hydrolyzed to the same extent. At 15 and 20%, a decrease in saccharification rate was observed. They attributed this decrease due to substrate and/or product inhibition. During the cellulose breakdown some of the cellulase adsorbs to the substrate. At high substrate concentration more cellulase might possibly adsorb to the material and the saccharification rate is reduced due to substrate inhibition. Product inhibition results from the accumulation of reduced sugars and glucose in solution. With higher substrate concentration, one would expect that the concentration of reduced sugars and glucose would be greater in solution. Thus, the chemical reaction of hydrolysis approaches equilibrium and the saccharification rate decreases. Most other research in the area of municipal waste hydrolysis has been in the area of acid hydrolysis and therefore, was not covered in this literature review.

Part I

Enzyme Crevice Penetration Due to Molecular Diffusion

2

One-Dimensional Diffusion Model

As previously mentioned, there will be a number of long, slender, tube-like shapes within the waste stream. The most frequently occurring of these slender objects will be hypodermic needles. The needles can be modeled as a simple one-dimensional diffusion problem where diffusion occurs along the axial direction of the needle. Diffusion refers to the net transport of material within a single phase in the absence of mixing (by mechanical means or by convection) [24, Reid et al.]. In this case the material was an enzyme transported in water or a liquid with a viscosity similar to water in the axial direction of the needle.

The enzymes are needed in the slurry to kill the pathogens in the waste stream. These pathogens may also be present in the needles. The diffusion of enzyme into the needles needed to be studied to determine the time required to disinfect the needles. Therefore, there were two topics which needed to be addressed concerning the one-dimensional problem: the diffusion of enzyme into the needle and the disinfection of the crevice once the enzyme is present.

This chapter describes the diffusion of enzyme in a one-dimensional crevice as well as the disinfection of these needles by enzymes. These two topics are covered in three sections:

1. Development of Fundamental One-Dimensional Model
    - -Fick's Second Law of diffusion
    - -No concentration gradient in radial direction

2. Determination of Diffusion Coefficient
    - -Experimentally measured coefficient
    - -Stokes-Einstein equation

3. One-dimensional Crevice Analysis
    - -Worst case scenario

-Boundary conditions
-One-dimensional model exact solution
-One-dimensional model results
-Disinfection time vs penetration time
-Crevice disinfection after process time
-Example disinfection time calculation

2.1 Development of Fundamental One-Dimensional Model

In order to determine the degree of enzyme penetration into the hypodermic needles, the fundamental equations had to be derived. These equations are derived from Fick's first and second laws. This section derives these equations and lists the assumptions used in the model.

In the ideal system, this enzyme needed to penetrate into the narrow needle in order to innoculate any type of harmful virus or bacteria within. In all the models discussed, the following assumptions were made:

- The crevice which needed to be disinfected was filled with a liquid and this solvent had similar properties to water.
- The enzyme/water-like solution was at the appropriate pH and temperature for optimum enzyme activity.
- The concentration of enzyme at the opening of the crevice was constant and equivalent to the enzyme concentration in the slurry.

2.1.1 Fick's Second Law of Diffusion

The one-dimensional diffusion model for the hypodermic needle was defined by Fick's second equation of diffusion. This equation was developed for a simple transient diffusion process. Fick's second equation was derived by combining his first equation with a mass-balance equation for a differential control volume. Fick's first law of diffusion is:

$$J_e = -D(\frac{dC_e}{dx}) \tag{2.1}$$

where J_e is the flow of solute in units of mass, or mole, per unit area per unit time, D is the diffusion coefficient of the solute in a particular solvent, and C_e is the concentration of solute.

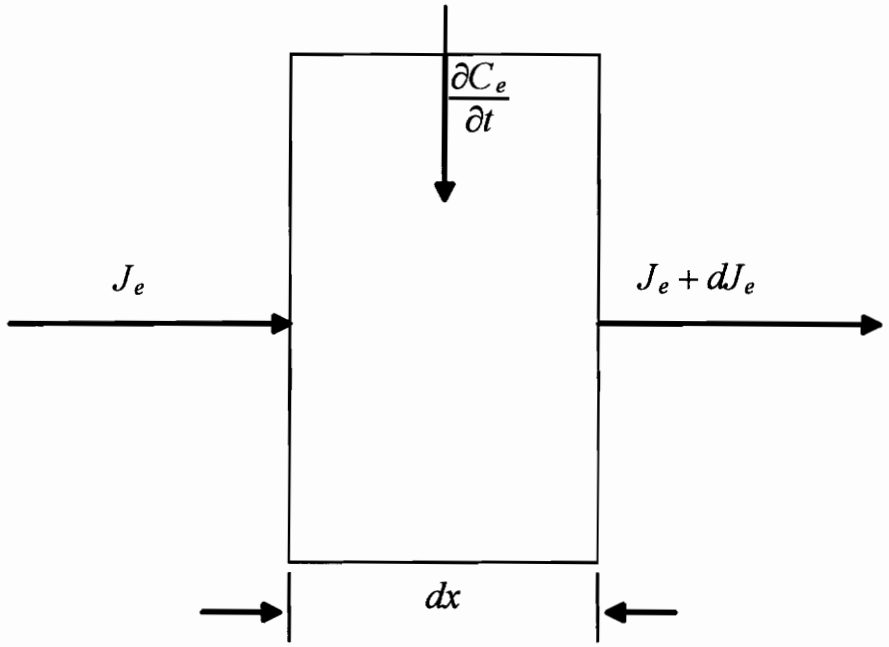

Figure 2.1 - Differential Control Volume.

Now, by referring to Figure 2.1, it can be seen that the mass balance requires that the increase in concentration per unit time be equal to the mass flux into the control volume minus the mass flux out of the control volume resulting in the following.

$$\frac{\partial C_e}{\partial t} = -\frac{\partial J_e}{\partial x} \tag{2.2}$$

Substituting equation 2.1 into equation 2.2 results in Fick's second law for constant or average diffusion coefficient.

$$\frac{\partial C_e}{\partial t} = D\frac{\partial^2 C_e}{\partial x^2} \tag{2.3}$$

This was the differential equation which needed to be solved in order to determine enzyme penetration times for all one-dimensional crevices.

2.1.2 No Concentration Gradient in Radial Direction

In order for crevices such as hypodermic needles to be modeled as one-dimensional crevices, the concentration gradient was assumed to be zero in the radial direction:

$$\frac{\partial C_e}{\partial r} = 0 \tag{2.4}$$

This assumption can be made since the entire cylindrical area of the needle was exposed to the solute (enzyme) concentration at $x = 0$. Therefore, the solute proceeded uniformly in the x-direction and there was no need to include the radial direction term.

2.2 Determination of Diffusion Coefficient

The diffusion coefficient is a measurement of the rate that a specific substance (enzyme) moves through a given solution. The coefficient is a function of the solute and solvent of the solution and can be measured experimentally or predicted using one of several different empirical correlations. In order to estimate accurate enzyme penetration times, the diffusion coefficient for a binary mixture of enzyme and water had to be determined.

The diffusion coefficient is defined by Fick's first law as the proportionality constant between the diffusion flux and diffusion potential. For an isothermal, isobaric binary system, the diffusion coefficients are defined by

$$J_A^V = -D_{AB}\frac{dC_A}{dx} \tag{2.5}$$

$$J_B^V = -D_{AB}\frac{dC_B}{dx} \tag{2.6}$$

where J_A^V is the flux of A relative to a plane of no net volume flow, J_B^V is the flux of B relative to a plane of no net volume flow, D_{AB} is the binary diffusion coefficient, and C_A and C_B are the concentration of A and B, respectively. As shown in equations 2.5 and 2.6, when fluxes are expressed in relation to a plane of no net volume flow, the diffusion potential is the concentration gradient. At low concentrations of B, D_{AB} is independent of concentration. This is known as the inifinite dilution criteria. A more detailed discussion on diffusion fluxes, potentials, and coefficients has been given by Reid et al. [24], Bird et al. [25], and Cussler [26].

2.2.1 Experimentally Measured Coefficient

Experimental measurement of the diffusion coefficient of the particular enzyme/water solution was necessary in order to evaluate the enzymatic diffusion. The experimental techniques employed can take months to perform accurately and needed an operator who was experienced in these techniques, neither of which was an option in this research. Therefore, the literature was searched to find the diffusion coefficient needed for the models.

The enzyme which was used in the bioremediation process is produced by Novo Nordisk Industri and was described in their literature as an endoprotease that hydrolyzes a wide range of peptide bonds with no clear bond preferences [27, Boyce]. The origin of the enzyme was from the strains of *Bacillus subtilis* or others in this genus which classifies the enzyme as a Subtilisin. This enzyme will be referred to as subtilisin Novo in this section.

A diffusion coefficient for a protease enzyme with water as a solvent was found in the literature. This data was determined experimentally using an optical technique not disclosed in the paper. The enzyme detailed was specifically Subtilisin BPN' which is a

serine protease originating from strains of *Bacillus subtilis* or related bacteria [5, Ottesen and Svendsen]. This particular enzyme was produced by Nagase & Co., Ltd.,. Ottensen states that the amino acid sequence of subtilisin Novo was completely identical to the sequence of subtilisin BPN'. In other words, it could be assumed that the enzyme used by Ottesen and Svendsen was approximately the same size as the enzyme used in this bioremediation process. Therefore, the diffusion coefficient for subtilisin Novo was assumed to be comparable to the coefficient listed for subtilisin BPN'.

The diffusion coefficient for a binary mixture of subtilisin protease enzyme and water was measured to be 9.07×10^{-7} cm^2/s [5, Ottesen and Svendsen]. This measurement was determined at a solution temperature of 20°C. Since the slurry in the bioremediation process tank will be at 50°C, the effect of a temperature change on the diffusion coefficient was considered. There were two correction methods listed in the literature for a change in solution temperature. The first method was used in the Wilke-Chang and Tyn-Calus correlations for the binary liquid diffusion coefficient at infinite dilution [24, Reid et al.] and will be referred to in this text as the Wilke-Chang temperature correction method. In the Wilke-Chang method, the affect of temperature was accounted for by assuming

$$\frac{D^o_{AB}\eta_B}{T} = const \tag{2.7}$$

where D^o_{AB} is the binary liquid diffusion coefficient at infinite dilution, η_B is dynamic viscosity of the solvent, and T is the temperature of the solution. Using this correction factor, the binary diffusion coefficient at 50°C was 1.83×10^{-6} cm^2/s.

The second method was developed by Tyn [24, Reid et al.] and therefore will be referred to as the Tyn temperature correction method in this paper. He reviewed the various proposed techniques to correlate infinitely dilute binary diffusion coefficients with temperature. He suggested

$$\frac{D^o_{AB}(T_2)}{D^o_{AB}(T_1)} = \left(\frac{T_c - T_1}{T_c - T_2}\right)^n \tag{2.8}$$

where $D^o_{AB}(T_2)$ and $D^o_{AB}(T_1)$ are the diffusion coefficients at temperature 1 and temperature 2, respectively, and T_c is the critical temperature of the solvent. The parameter n was related to the heat of vaporization of the solvent at T_b (solvent), and for water $n = 6$ [24, Reid et al.]. Based on this method, the temperature corrected diffusion coefficient was 1.54×10^{-6} cm^2/s. The two values of 1.54×10^{-6} and 1.83×10^{-6} cm^2/s were the diffusion coefficients which were used throughout this research.

2.2.2 Stokes-Einstein Equation

Along with the experimental value listed, it was also valuable to determine a theoretical diffusion coefficient for comparison. There were several theoretical equations as well as predictive methods listed in the literature for determining approximate diffusion coefficients. Probably the simplest theoretical equation involved the analysis of large spherical molecules diffusing in a dilute solution. The equation utilized the particle diameter of the spheres as well as the solvent viscosity. It resulted from hydrodynamic theory explained in Bird et al. [25]. This is known as the Stokes-Einstein equation:

$$D^o_{AB} = \frac{RT}{6\pi\eta_B r_A} \tag{2.9}$$

where D^o_{AB} is the binary liquid diffusion coefficient at infinite dilution, R is the universal gas constant, T is the temperature, η_B is the dynamic viscosity of the solvent, and r_A is the radius of the "spherical solute" [24, Reid et al.]. Although this fixed relation was derived for a very special situation, it was used as a "ball park" value to check the experimental value listed in the previous section. This assumption that the enzyme molecules are spherical in nature was validated in Ottesen and Svendsen [5] and therefore, the Stokes-Einstein equation is an appropriate theoretical approximation for the binary diffusion coefficient.

In order to approximate the diffusion coefficient from the Stokes-Einstein equation, the diameter of a subtilisin enzyme had to be determined. Information provided through Novo

Nordisk Bioindustrial indicated that most enzyme diameters fall within the range of 50 to 100 Angstroms. This range translated to a range of 5.0×10^{-7} to 1.0×10^{-6} cm.

Using this data along with the viscosity of water at 50°C resulted in a theoretical diffusion coefficient range of 1.73×10^{-6} to 8.65×10^{-7} cm^2/s corresponding to an enzyme diameter of 50 and 100 Angstroms. These theoretical data agree quite well with the experimental values given in Section 2.2.1. A summary of the diffusion coefficient values is shown in Table 2.1.

Table 2.1 - Protease Diffusion Coefficient Summary

Experimental Value at 20°C	9.07×10^{-7} cm^2/s
Corrected to 50°C (Tyn Method)	1.54×10^{-6} cm^2/s
Corrected to 50°C (Wilke-Chang Method)	1.83×10^{-6} cm^2/s
Stokes-Einstein Equation for 50 Angstrom Sphere (50°C)	1.73×10^{-6} cm^2/s
Stokes-Einstein Equation for 100 Angstrom Sphere (50°C)	8.65×10^{-7} cm^2/s

2.3 One-Dimensional Crevice Analysis

In order to determine if all one-dimensional voids would be exposed to the protease enzyme, a worst case scenario was hypothesized. Once the worst case was determined, appropriate boundary conditions were placed on the problem. As a result, an exact solution for the one-dimensional, transient case was determined and theoretical diffusion times were calculated.

2.3.1 Worst Case Scenario

It was assumed that the worst case scenario would be a needle, 1.27 cm long, which was open at both ends. As discussed in Section 1.1.3, the waste stream particles are reduced to a maximum size of 1.27 cm (1/2 in) in any dimension by the shredder in the initial step of the mechanical system. Therefore, the maximum length of a hypodermic needle or any other long, slender crevice which needed to be disinfected was 1.27 cm (1/2 in). There was also the possibility that the needle openings could either become closed or plugged. However, it was determined that both ends of the needle will be open to the slurry enzyme concentration.

In order to diffuse enzymes into the needles, the ends of the needles needed to be open to the slurry. Therefore, the possible problem of blockage needed to be analyzed There were two possible causes for closing of the crevice entrance:

- Pluggage due to paper, cotton gauze, dried blood, or a number of other organic materials within the waste stream.
- Blockage due to the shearing motion of the shredder blades which might cause the needle opening to deform and close off the needle opening.

These two causes for blockage needed to be addressed. In the event of blockage due to waste material, the assumption was made that these organics were either cellulose-derived

waste or protein-containing organics and therefore, were either hydrolyzed by the cellulase enzymes or the protease enzymes. As discussed in Section 1.1.2, the waste was treated with the cellulase before the protease disinfection began; thus resulting in removal of any blockage of crevices due to cellulose derivative material. As for the protein based substances such as blood, there was no data available for the breakdown rate due to protease enzyme. If the blockage due to blood occurred at the opening of the crevice only and not throughout the entire crevice length, then it could be assumed that the exposure of the crevice opening to the cellulase/water solution loosened and removed the dried blood before the protease enzyme was added. Therefore, pluggage of the crevice opening due to waste material was neglected in this research.

The other type of obstruction of the crevice opening was a result of pinching or crimping of the needle during the shredding process. Tests were conducted which subjected hypodermic needles to shearing and cutting action similar to the actual shredding process. The needles tested were standard disposable Cournand-style. Needle gauges of 21, 19, and 17 were tested. These needles exhibited no noticeable deformation of the crevice openings and therefore, crimping of the needles due to size reduction should not be experienced in the actual process.

According to these assumptions, the worst case, one-dimensional crevice was determined to be a 1.27 cm (1/2 in) hypodermic needle which was open to the slurry at both ends.

2.3.2 Boundary Conditions

In section 2.2 Fick's second law of diffusion was set up. In order to solve the one-dimensional problem, appropriate boundary conditions needed to be placed on the governing equation. As discussed in Section 2.3.1, the crevice length was 1.27 cm which was open at both ends. Therefore, due to symmetry, this needle was modeled as a 0.64 cm (1/4 in) crevice which was open to enzyme at only one end. This meant that in order

to determine if complete enzyme penetration had occurred throughout the entire crevice, diffusion times were evaluated at the blocked end or back wall of the needle. This corresponded to the following governing equation which was previously shown (Equation 2.3),

$$\frac{\partial C_e}{\partial t} = D_{AB}\frac{\partial^2 C_e}{\partial x^2} \tag{2.3}$$

boundary conditions,

$$C_e(x,t) = C_\infty \text{ for } x = 0, t > 0 \tag{2.10}$$

$$\frac{\partial C_e(x,t)}{\partial x} = 0 \text{ for } x = L, t > 0 \tag{2.11}$$

and initial condition.

$$C_e(x,t) = 0 \text{ for } 0 \le x \le L, t = 0 \tag{2.12}$$

where C_∞ is the protease enzyme concentration in the slurry and L is the length of the crevice. The assumptions of no turbulence within the crevice and infinite turbulence outside the crevice were satisfied by equations (2.3) and (2.10), respectively. Figure 2.2 illustrates the one-dimensional crevice with the boundary conditions shown from above.

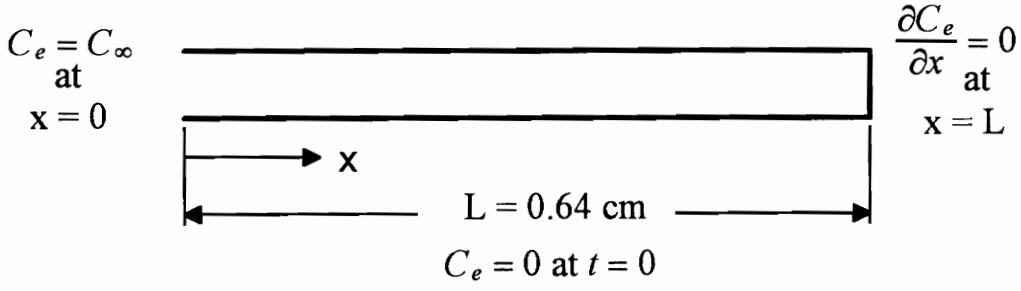

Figure 2.2 - One-Dimensional Crevice Problem.

2.3.3 One-Dimensional Model Exact Solution

Once the governing equation and boundary conditions were specified, the exact solution for the enzyme concentration at any place within the crevice at any specified time was solved using separation of variables. For this one-dimensional case, a number of solution methods could have been employed, however the rigorous solution using separation of variables is shown in Appendix A. The exact solution is:

$$\theta(x,t) = 1 + \frac{2}{L}\sum_{m\to 1}^{\infty} -\frac{1}{\beta_m}\sin(\beta_m x)\exp(-D_{AB}\beta_m^2 t) \qquad (2.13)$$

where

$$\theta(x,t) = \frac{C_e(x,t)}{C_\infty}$$

$$\beta_m = \frac{(2m-1)\pi}{2L}$$

and L is the length of the crevice. Now, actual enzyme penetration times were determined from the computer code (Appendix B) for any location within the crevice, with the most important position being at the back wall.

2.3.4 One-Dimensional Model Results

In the initial work conducted on this problem, a diffusion coefficient range was assumed based upon diffusion coefficients for electrolyte solutions. This one-dimensional model was determined before the diffusion coefficient information in Section 2.2 was located. Therefore, a diffusion coefficient range of $5.0\text{x}10^{-5}$ to $5.0\text{x}10^{-6}$ cm^2/s was assumed, which was typical for most electrolyte solutions. However, the diffusion coefficient was highly dependent on the particle size of the solute, and the size of the ions in electrolyte solutions were much smaller than the size of enzymes. For this reason the diffusion coefficient range first used in the analysis was high (this can be seen by comparing the range

from above with Table 2.1) and the enzyme diffusion times were incorrect. The initial calculations were for a 1.27 cm (1/2 in) open-ended needle which was modeled as a needle 0.64 cm in length with no diffusion flux at one end and open to the enzyme slurry concentration at the other. Figure 2.3 shows the dimensionless enzyme concentration, $\theta(L,t)$, at the back wall of the 0.64 cm needle or crevice. In this initial model shown in Figure 2.3, the time to diffuse one-tenth of the slurry enzyme concentration to the center of a 1/2" needle open at both ends ranged from fifteen minutes to just under three hours depending on the diffusion coefficient used. Therefore, by using these models it seemed as though the enzyme concentration which diffused into the needle would be sufficient to disinfect the entire crevice during the batch process based upon the disinfection data which will be presented in Section 2.3.7.

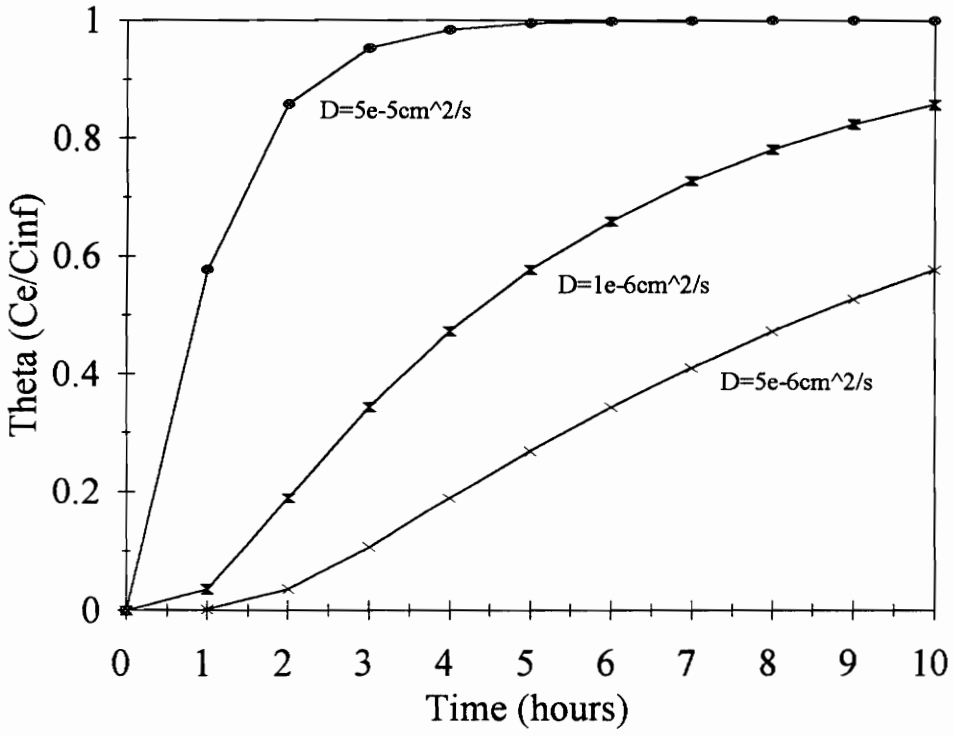

Figure 2.3 - Solute Concentration at the Back Wall (L = 0.64 cm) (Incorrect Diffusion Coefficient Range).

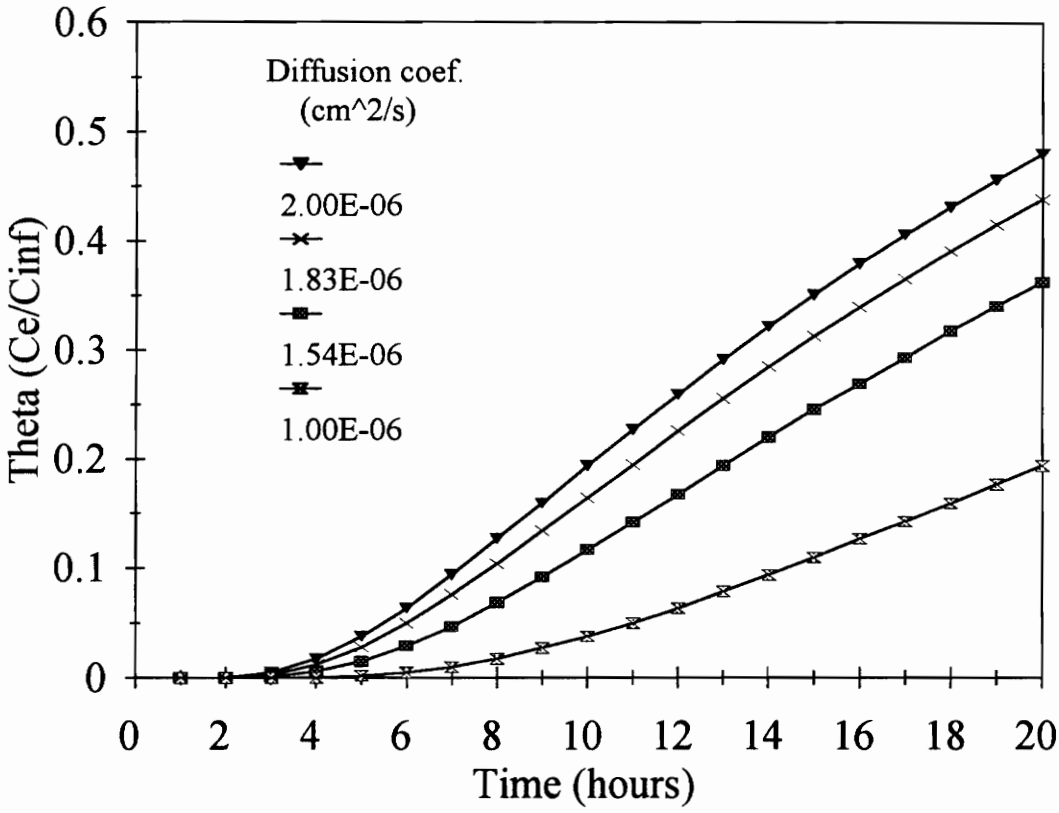

Figure 2.4 - Enzyme Concentration at the Back Wall (L = 0.64 cm).

Upon further review of diffusion coefficient data, enzyme diffusion coefficient values were determined as covered in Section 2.2 and shown in Table 2.1. Therefore, a new analysis of the hypodermic needle case was conducted using the more accurate diffusion coefficient range. Using the same exact solution shown in equation (2.12) and the new diffusion coefficient values suggested in Table 2.1, resulted in the curves depicted in Fig. 2.4. Once again, Fig. 2.4 shows the dimensionless enzyme concentration, $\theta(L,t)$, at the back wall of the 0.64 cm needle similar to that shown in Fig. 2.3. The time to diffuse one-tenth of the slurry enzyme concentration with the more accurate diffusion coefficient was greatly increased as compared to the results in Fig. 2.3. As Fig. 2.4 illustrates, the time for $\theta(L,t)$ to be equal to 0.1 ranged from 7 to 15 hours depending on which diffusion coefficient was chosen from Table 2.1 to evaluate the solution. Therefore, if

crevice disinfection needed to be completed during the protease treatment stage in order for licensing of the system, then the slurry protease concentration or the process time would have to be increased.

Currently, the protease enzyme process time has not been set. The process time will probably range between one and three hours. Due to the slow diffusion rates for liquid binary mixtures, the entire crevice was not exposed to protease even after three hours and therefore, the entire crevice was not disinfected after the protease process time. However, the entire crevice will be exposed to protease enzyme some time after dewatering of the waste. Disinfection will occur after separation if the protease, which is already present within the crevice, is allowed to equilibrate throughout the crevice. This subject is covered in Section 2.3.6.

2.3.5 Disinfection Time Versus Penetration Time

Up until now in this report, the words, enzyme penetration time and crevice disinfection time, have been used interchangeably. However, these two should not be confused. Enzyme penetration time is the amount of time needed for a specified concentration of enzyme to reach a specified distance within the crevice. Crevice disinfection time is the sum of enzyme penetration time and the amount of time needed for the enzyme to neutralize the microbes once the enzyme is at this specified distance. Now, what is meant by disinfection? By definition for this research, infectious medical waste is said to be "disinfected" when there has been a six log reduction in the number of microbes present in the waste stream [28, Therien]. These definitions have been considered in the next section to determine actual kill times within the crevice. Some of the data from Fig. 2.4 was used in order to determine actual crevice disinfection because the protease has to diffuse to a specified area before the enzymes can disinfect this region.

The Department of Veterinary Medicine at Virginia Polytechnic Institute and State University has been conducting disinfection or kill time tests on virus and bacteria. Toth

[29] has been conducting the experiments on viral disinfection with enzymes and Sriranganathan [30] has been conducting the experiments on bacterial disinfection with enzymes. Some of their results have been used along with the diffusion model results in order to determine actual crevice disinfection times.

2.3.6 Crevice Disinfection After Process Time

As discussed in Section 2.3.4, the entire crevice was not exposed to protease enzyme during the process time and the entire crevice was not completely disinfected. After the enzyme process time, the waste was dewatered, but it can be assumed that the enzyme/water solution remains inside the needles. It was assumed that this enzyme/water solution remained at the same pH but at a reduced temperature. Therefore, there will be additional disinfection after the waste is removed from the slurry because the enzymes will remain active. This analysis was done to determine the amount of time needed to disinfect the crevice after the batch process was complete.

The concentration distribution of enzyme which remained within the crevice is determined by the solution to the differential equation in Section 2.3.4. This distribution varies depending on the batch process time, slurry enzyme concentration, etc. This results in a new one-dimensional problem with different boundary conditions and initial conditions than described in Section 2.3.4. This new diffusion problem, once solved, illustrates how the initial concentration distribution approaches some equilibrium concentration throughout the entire crevice after the batch process is completed. The initial condition to this new problem was the solution to the differential equation in Section 2.3.4. This initial condition is the concentration distribution within the crevice after the batch process was completed. Once this new diffusion problem was solved, the diffusion data was used along with the "germ" kill rate data to determine the amount of time that was needed to elapse before the entire crevice was disinfected. The approximate time to disinfect the

crevice was determined to be one day; so it is probable that the waste will still be in the dumpster at the hospital when complete disinfection is achieved.

This new problem was described with the same governing equation (2.3)

$$\frac{\partial C_e(x,t)}{\partial t} = D_2 \frac{\partial^2 C_e(x,t)}{\partial x^2} \tag{2.3}$$

and new boundary conditions equations

$$\frac{\partial C_e(x,t)}{\partial x} = 0 \text{ for } x = 0, t > 0 \tag{2.14}$$

$$\frac{\partial C_e(x,t)}{\partial x} = 0 \text{ for } x = L, t > 0 \tag{2.15}$$

The initial condition for this problem was taken from the solution of the initial one-dimensional problem described in Section 2.3.3 and shown in Fig. 2.2. This initial condition is as follows:

$$C_e(x,T) = C_\infty - \frac{2C_\infty}{L} \sum_{m\to 1}^{\infty} \frac{1}{\gamma_m} \sin(\gamma_m x) e^{-D_1 \gamma_m^2 T} \tag{2.16}$$

where $$\gamma_m = \frac{(2m-1)\pi}{2L}$$

D_1 is the diffusion coefficient for the protease enzyme at the process temperature, and T is the batch or protease process time. Equation (2.16) is the enzyme concentration distribution within the crevice after the batch process time. These equations were solved much as before, with the details shown in Appendix A. This resulted in an exact solution for the concentration distribution versus time given the initial concentration distribution described by Equation (2.16). The exact solution is:

$$\theta(x,t) = 1 - \frac{2}{L^2}\left[2 \sum_{m\to 1}^{\infty} \sum_{n\to 1}^{\infty} e^{-D_2\beta_m^2 t}\cos(\beta_m x)\frac{e^{-D_1\gamma_n^2 T}}{\gamma_n^2 - \beta_m^2} + \sum_{n\to 1}^{\infty} \frac{e^{-D_1\gamma_n^2 T}}{\gamma_n^2} \right] \quad (2.17)$$

where

$$\theta(x,t) = \frac{C_e(x,t)}{C_\infty}$$

$$\beta_m = \frac{m\pi}{L}$$

$$\gamma_n = \frac{(2n-1)\pi}{2L}$$

D_1 is the diffusion coefficient corresponding to the batch temperature, D_2 is the diffusion coefficient corresponding to the ambient temperature, and T is the enzyme treatment batch time.

As one can see, this solution was highly dependent on the initial condition or the initial process time. Figure 2.5 illustrates this initial condition for a protease process time of one hour. This figure shows the dimensionless enzyme concentration within the crevice for the entire one-dimensional diffusion field for the protease diffusion coefficient range of $1x10^{-6}$ to $2x10^{-6}$ cm^2/s. Only about one-third of the 0.64 centimeter crevice has been exposed to enzyme, therefore, in order for the entire crevice to be disinfected, enzyme from the open end of the crevice must be allowed to diffuse to the opposite end during the post-batch equilibrium time. The post-batch equilibrium time is defined as the time for the enzyme concentration within the crevice to reach equilibrium which will be less than 40 hours.

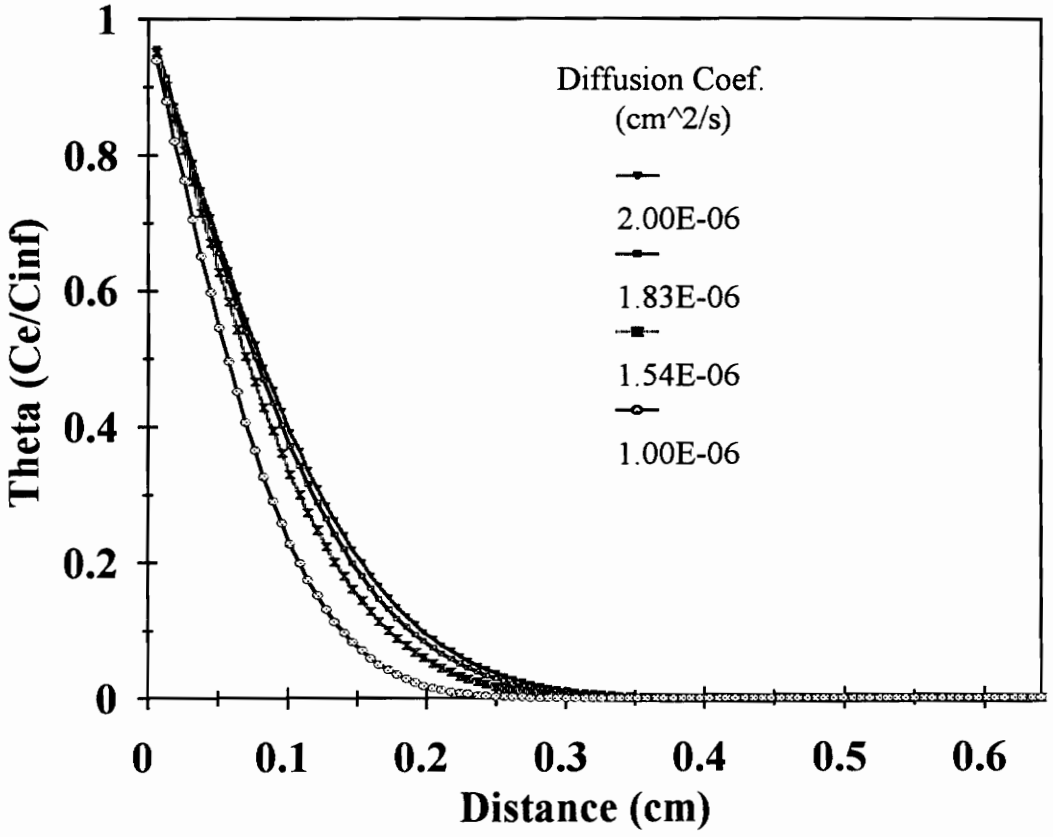

Figure 2.5 - Enzyme Penetration after a One Hour Diffusion Time.

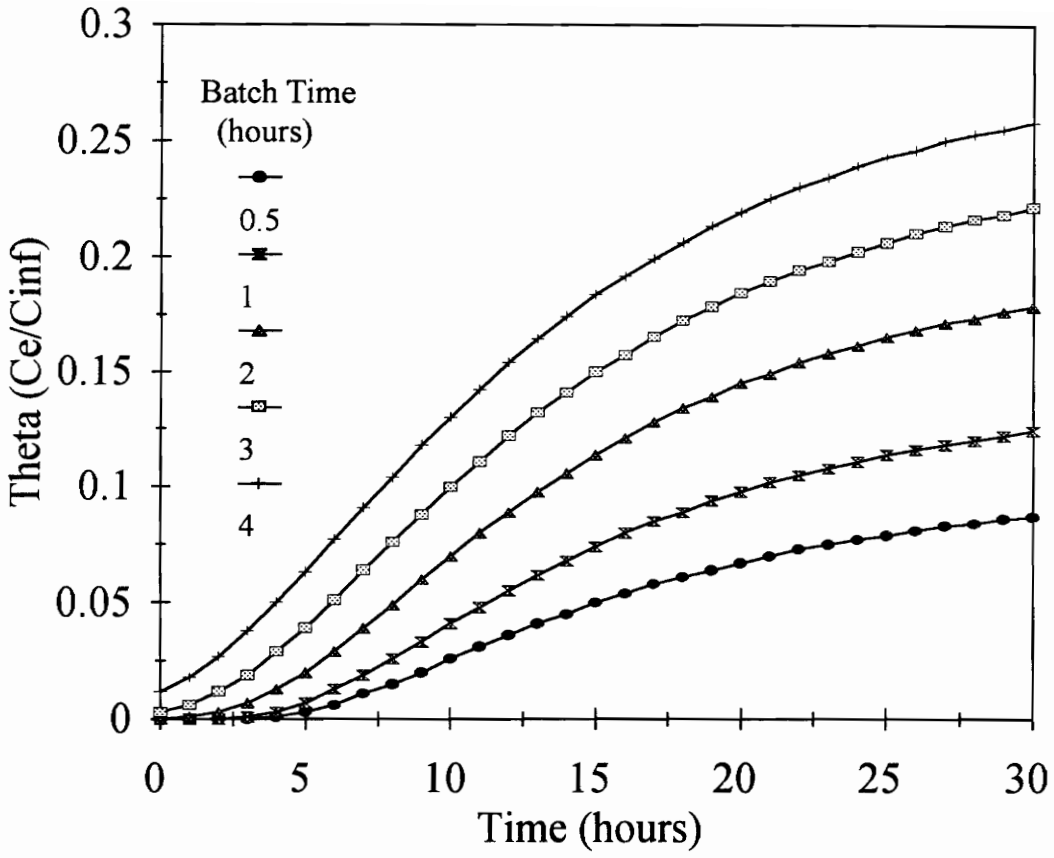

Figure 2.6 - Back Wall (L = 0.64 cm) Enzyme Concentration.

The most conservative viewpoint was to observe the concentration of enzyme at the back wall of the crevice as the enzyme concentration approaches equilibrium. This data was plotted in Fig. 2.6. This figure illustrates the back wall dimensionless concentration, $\theta(L,t)$, versus time after processing for various batch times. As one would expect, the figure shows that the longer the initial batch time, the greater the initial protease concentration and the greater the back wall enzyme concentration. This figure uses a batch protease diffusion coefficient (1.83×10^{-6} cm^2/s) corresponding to 50°C for the initial condition and a protease diffusion coefficient (1.00×10^{-6} cm^2/s) corresponding to 25°C for the post-batch diffusion. Ambient temperature was used for the model, since it was assumed that after the waste was placed in a dumpster and then disposed of in a landfill, the waste was at the ambient temperature.

Now that the diffusion data was available, approximate disinfection times were evaluated using the *in vitro* disinfection data of Toth and Sriranganathan. In order for the disinfection times to be determined a couple of parameters must be set. These variables were the initial slurry protease concentration and the protease process time. Due to the scope of this research and the fact that all the data on *in vitro* disinfection times has not been determined, a series of curves has not been generated for crevice disinfection times. However, these data will be easy to generate once all the information is available from The Department of Veterinary Medicine. An example disinfection time calculation is presented in the next section.

2.3.7 Example Disinfection Time Calculation

Since all the data on *in vitro* disinfection times has not yet been generated, the disinfection times within the hypodermic needle can not be determined. This section gives a conservative example disinfection time calculation so that once the *in vitro* disinfection time data is completed, the crevice disinfection curves can be prepared by following this conservative example. Reasons are given in this section for the conservatism of this sample calculation. This section also describes some of the results from Toth on disinfection of the Human Polio Virus (HPV-2).

Toth observed the killing of HPV-2 at various temperatures by a specific protease enzyme. Figure 2.7 illustrates the number of HPV-2 versus time for a 0.1% protease concentration at a pH of 8.5 for various temperatures. According to Fig. 2.7 for example at 50° C, 0.1% protease reduced the number of HPV-2 from 10^6 per ml to 10^2 per ml in 30 minutes where as at 35°C, 0.1% protease reduced the number of HPV-2 from 10^6 per ml to 10^2 per ml in three hours. One would expect the kill time to increase as the temperature of the solution decreased since the optimum activity of protease is around 50° C. Toth also stated that the limit of detection of the testing equipment was approximately 10^2 per ml, so the minimum number of virus for all temperatures might even be lower than 100.

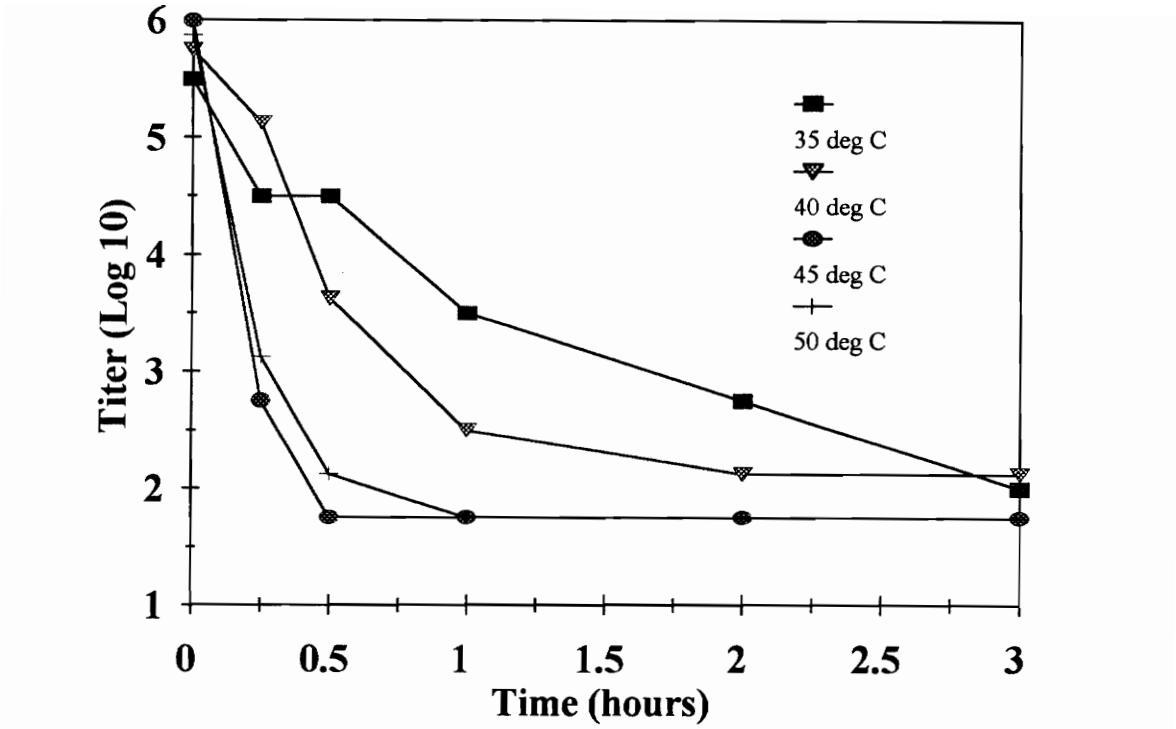

Figure 2.7 - Killing of HPV-2 for 0.1% Protease, pH 8.5.

For the sample calculation, a few parameters needed to be set. The slurry protease concentration was assumed to be 1%, the protease batch time was assumed to be one hour, and the temperature within the crevice after the batch process was assumed to be 35°C . Twenty-five degrees Celsius would be a more appropriate temperature to use, but the kill time data has not been determined for this temperature. Since Fig. 2.7 is for the killing of HPV-2 for 0.1% protease, the sample calculation was done for a back wall enzyme concentration of 0.1% protease. The example disinfection time calculation can be broken into two parts:

- The time for the protease concentration to reach 0.1% at the back wall during the post-batch diffusion process.

- The time needed to kill the HPV-2 after the 0.1% protease concentration was reached.

The sum of these two times yields the time to disinfect the needle after the batch process was completed.

According to Fig. 2.6, the concentration at the back wall reached 0.1% concentration after approximately 20 hours during the post-batch diffusion process. From Fig. 2.7 the number of HPV-2 was reduced from 10^6 per ml to 10^2 per ml in three hours at a temperature of 35° C. If this information was extrapolated, then it would have taken an additional hour and a half to have a 10^6 reduction in the HPV-2. A six log reduction in pathogens was described in Section 2.3.5 as the definition of disinfection. Therefore, for a protease concentration of 0.1% at 35° C, it would have taken 4.5 hours for the needle to be disinfected. Now, for a conservative estimate of disinfection time, the 20 hour diffusion time for the back wall of the crevice to reach 0.1% enzyme concentration and the 4.5 hours needed to kill the pathogens were added, resulting in a total disinfection time of 24.5 hours or approximately one day for a 1.27 centimeter open-ended hypodermic needle. So by using this simple conservative method, the disinfection time for any one-dimensional crevice after the batch process can be evaluated using equation (2.17) along with an updated form of Fig. 2.7.

This calculation was a conservative estimate due to the observation that the "germ" killing capability of enzyme concentrations lower than 0.1% at the back wall had not been considered. Once data for these lower concentrations becomes available more accurate disinfection times can be evaluated. These more accurate and shorter disinfection times will be determined by taking into account the integral effect that lower protease concentrations have on kill rates of pathogens.

3

Re-entrant Crevice Diffusion Models

Aside from the one-dimensional crevices within the waste, there was the possibility of other types of materials containing what would be classified as re-entrant cavities. These are crevices whose interior dimensions are larger than their openings. The restriction presented by the small openings could possibly result in slow diffusion of enzyme into these cavities. Since there were an infinite number of possible re-entrant crevice shapes within the waste stream, it would be ideal to develop one simple model based on dimensionless groups which characterized the diffusion of enzyme through these voids. This goal was accomplished in the following procedure:

1. Characterize re-entrant crevices within the waste stream.

2. Analyze a re-entrant crevice for which an exact solution existed.

3. Define several simple rectangular re-entrant crevice shapes and solve the mass diffusion equation using a finite difference technique.

4. Determine dimensionless groups which allow these rectangular shapes to be compared with the exact solution from step 2.

5. Compare the enzyme concentration of the exact solution with the enzyme concentration of the rectangular shapes using the dimensionless groups and determine the exact solution's accuracy in predicting the enzyme concentration at any instant in time for most rectangular crevices.

6. Determine theoretical disinfection time of these crevices.

The assumptions for the re-entrant crevice model were the same as in the one-dimensional model.

- The crevice which needed to be disinfected was filled with a liquid and this solvent had similar properties to water.

- The enzyme/water-like solution was at the appropriate pH and temperature for optimum enzyme activity.

- The concentration of enzyme at the opening of the crevice was constant and equivalent to the enzyme concentration in the slurry.

3.1 Re-entrant Crevice Characterization

As previously discussed, there were a variety of materials in the waste stream considered to be two-dimensional crevices. In order to determine the types of re-entrant cavities which are present in infectious medical waste, samples of non-infectious waste were characterized. Non-infectious waste has the same make-up as infectious waste, but it has not been used in areas which risk exposure to pathogens. The most commonly occurring crevice-containing items or diffusion media in these samples were plastics tubes, pipettes, sponges, and gauze. Therefore, the two-dimensional diffusion media was separated into two categories:

- Porous media (gauze, sponges)
- Re-entrant crevices

3.1.1 Porous media

Porous media such as sponges must be considered separately from other types of crevices due to their permeable structure. Also, the diffusion coefficient for these types of materials is difficult to measure. There are actually two diffusion coefficients associated with porous media: the diffusion coefficient of the solute through the material and diffusion coefficient of the solute through the open area. These two coefficients combine to give an apparent diffusion coefficient for the particular media.

It was determined through this crevice characterization that most porous media within the waste stream were cellulose derivative. Therefore, a few qualitative experiments were conducted using cellulose sponges in an agitated cellulase enzyme/water solution at proper temperature and pH. These types of porous materials were hydrolyzed by the cellulase in

less than an hour. For this reason the porous media diffusion model was not analyzed since these materials will no longer be present during the protease treatment time and the focus of Chapter 3 was dedicated to the re-entrant crevice case.

3.1.2 Re-entrant Crevices

The other types of crevices, which were found in the sample waste, were those of the re-entrant type. Some examples of re-entrant crevices isolated within the sample waste were tubes and pipettes. These materials might contain infected blood or other contaminated fluid and therefore, needed to be disinfected. These objects were approximated as a sector-shaped cavity. This shape was chosen because it closely matched the geometry of these objects and an exact solution existed for the mass diffusion representation of this shape. By varying the angle and inner radius of the sector-shaped cavity different re-entrant crevices could be simulated. This crevice shape is described in the next section.

3.2 Development of Fundamental Two-Dimensional Model

The type of crevice which was analyzed can be envisioned as a piece of pie with a bite taken from the tip. The tip end was open to the slurry containing the enzyme with the rest of the sector allowing no mass transfer to occur across its boundaries. This crevice shape was chosen due to its similarity to a variety of crevices and most importantly because the exact solution could be obtained with minimal effort.

Due to the geometry of this crevice shape, the mass diffusion equation was considered in cylindrical coordinates given in Özisik [31].

$$\frac{1}{r}\frac{\partial}{\partial r}\left(r\frac{\partial C_e}{\partial r}\right)+\frac{1}{r^2}\frac{\partial^2 C_e}{\partial \Phi^2}+\frac{\partial^2 C_e}{\partial z^2}=\frac{1}{D}\frac{\partial C_e}{\partial t} \tag{3.1}$$

This equation was simplified to the following governing equation,

$$\frac{1}{r}\frac{\partial}{\partial r}\left(r\frac{\partial C_e}{\partial r}\right)+\frac{1}{r^2}\frac{\partial^2 C_e}{\partial \Phi^2}=\frac{1}{D}\frac{\partial C_e}{\partial t} \tag{3.2}$$

boundary conditions,

$$\frac{\partial C_e}{\partial r}=0 \text{ for } r=b \tag{3.3}$$

$$C_e=C_\infty \text{ for } r=a \tag{3.4}$$

$$\frac{\partial C_e}{\partial \Phi}=0 \text{ for } \Phi=0 \tag{3.5}$$

$$\frac{\partial C_e}{\partial \Phi}=0 \text{ for } \Phi=\Phi_o \tag{3.6}$$

and initial condition.

$$C_e=0 \text{ for } t=0 \tag{3.7}$$

where Φ is the angular position of the sector, Φ_o angle of the sector, r is the radial position, a is the inside radius of the sector, and b is the outer radius of the sector. The assumptions of no turbulence within the crevice and inifinite turbulence outside the crevice were satisfied by equations (3.2) and (3.4), respectively. Figure 3.1 shows the sector crevice problem with the approximate boundary and initial conditions.

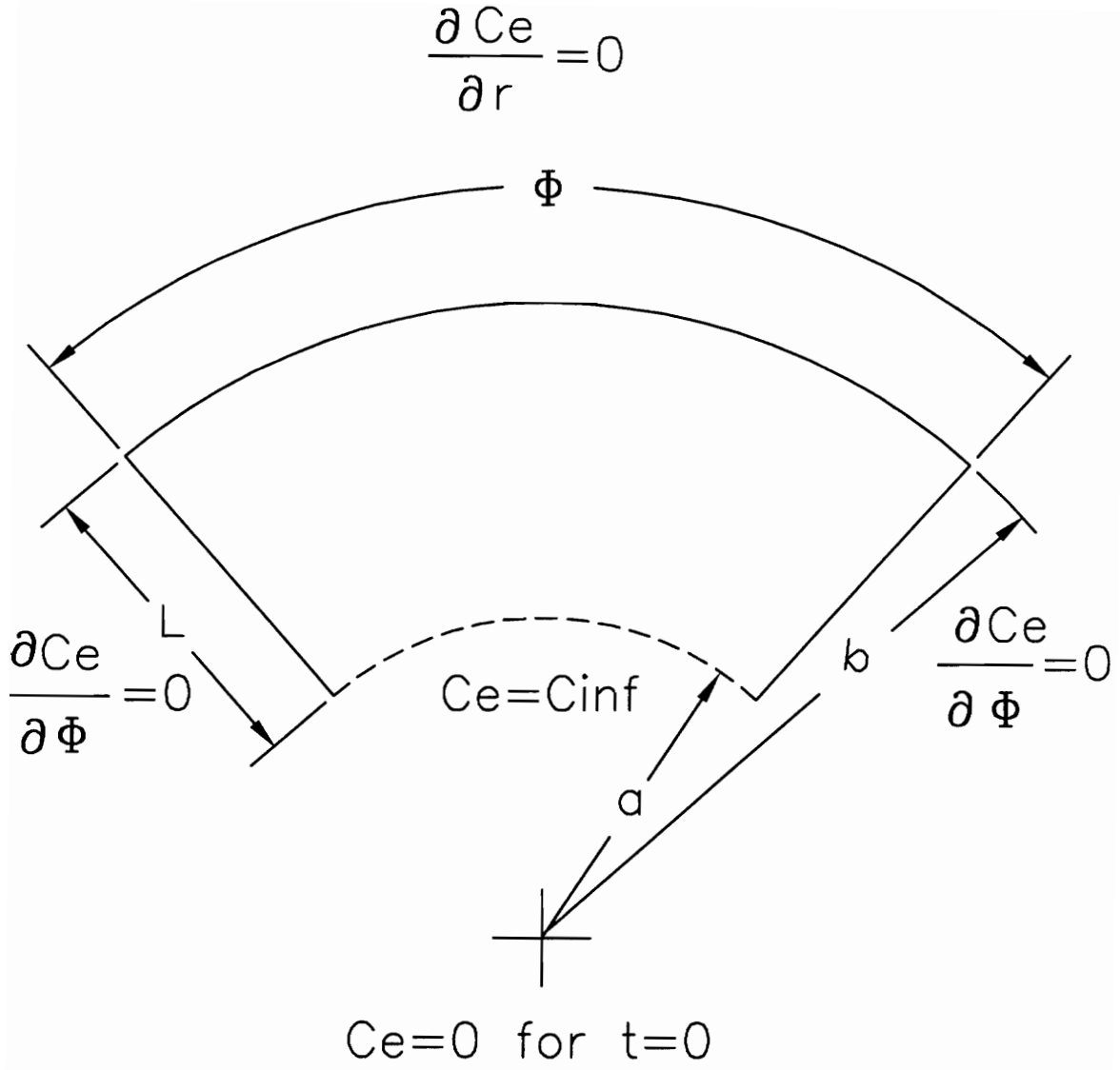

Figure 3.1 - Sector Crevice Problem Definition

3.3 Exact Solution for Sector Crevice

Once the governing equation and boundary conditions were specified, the exact solution for the enzyme concentration at any position and time was solved using separation of variables. For this two-dimensional case, a number of solution methods could have been employed, however the rigorous solution using separation of variables is shown in Appendix A. The solution is

$$\theta(R,\tau) = 1 - \sum_{m=1}^{\infty} \frac{1}{N(\beta_m)} e^{-\beta_m \tau} R_o R_1 \tag{3.8}$$

where

$$\theta(R,\tau) = \frac{C_e(R,\tau)}{C_\infty} \qquad \tau = \frac{Dt}{(b-a)^2}$$

$$N(\beta_m) = \frac{2}{\pi^2} \frac{(J_o^2(\beta_m \frac{a}{b-a}) - J_1^2(\beta_m \frac{b}{b-a})}{\beta_m^2 J_o^2(\beta_m \frac{a}{b-a})}$$

$$R_o = J_1(\beta_m \tfrac{b}{b-a}) Y_o(\beta_m R) - J_o(\beta_m R) Y_1(\beta_m \tfrac{b}{b-a})$$

$$R_1 = \frac{1}{\beta_m} \frac{a}{b-a} \left[J_1(\beta_m \tfrac{a}{b-a}) Y_1(\beta_m \tfrac{b}{b-a}) - J_1(\beta_m \tfrac{b}{b-a}) Y_1(\beta_m \tfrac{a}{b-a}) \right]$$

$$R = \frac{r}{b-a}$$

and $\beta_m's$ are the positive roots of the following transcendental equation:

$$J_1(\beta_m \tfrac{b}{b-a}) Y_o(\beta_m \tfrac{a}{b-a}) - J_o(\beta_m \tfrac{a}{b-a}) Y_1(\beta_m \tfrac{b}{b-a}) = 0 \tag{3.9}$$

The most critical position in the crevice was the outer radius so the dimensionless back wall length was defined as:

$$B = \frac{b}{b-a} \tag{3.10}$$

and the dimensionless inner radius $\frac{a}{b-a}$ can be written as:

$$\frac{a}{b-a} = B - 1 \tag{3.11}$$

Now, equations (3.8 and 3.9) can be written in terms of the dimensionless back wall length using equations (3.10 and 3.11) resulting in

$$\theta(B,\tau) = 1 - \sum_{m=1}^{\infty} \frac{1}{N(\beta_m)} e^{-\beta_m \tau} R_o R_1 \tag{3.12}$$

where

$$\theta(B,\tau) = \frac{C_e(B,\tau)}{C_\infty}$$

$$N(\beta_m) = \frac{2}{\pi^2} \frac{(J_o^2(\beta_m(B-1)) - J_1^2(\beta_m B))}{\beta_m^2 J_o^2(\beta_m(B-1))}$$

$$R_o = J_1(\beta_m B) Y_o(\beta_m B) - J_o(\beta_m B) Y_1(\beta_m B)$$

$$R_1 = \frac{B-1}{\beta_m} [J_1(\beta_m(B-1)) Y_1(\beta_m B) - J_1(\beta_m B) Y_1(\beta_m(B-1))]$$

and $\beta_m's$ are the positive roots of the following transcendental equation:

$$J_1(\beta_m B) Y_o(\beta_m(B-1)) - J_o(\beta_m(B-1)) Y_1(\beta_m B) = 0 \tag{3.13}$$

The results to this solution were determined by the computer program listed in Appendix B. The results to this sector crevice problem are shown in Fig. 3.2. Figure 3.2 plots the dimensionless concentration, $\theta(B,\tau)$, versus dimensionless time, τ, for various values of the dimensionless back wall length, $B = \frac{b}{b-a}$. It will be shown later that Fig. 3.2 can be used to predict the molecular diffusion field for most simple rectangular-shaped crevices.

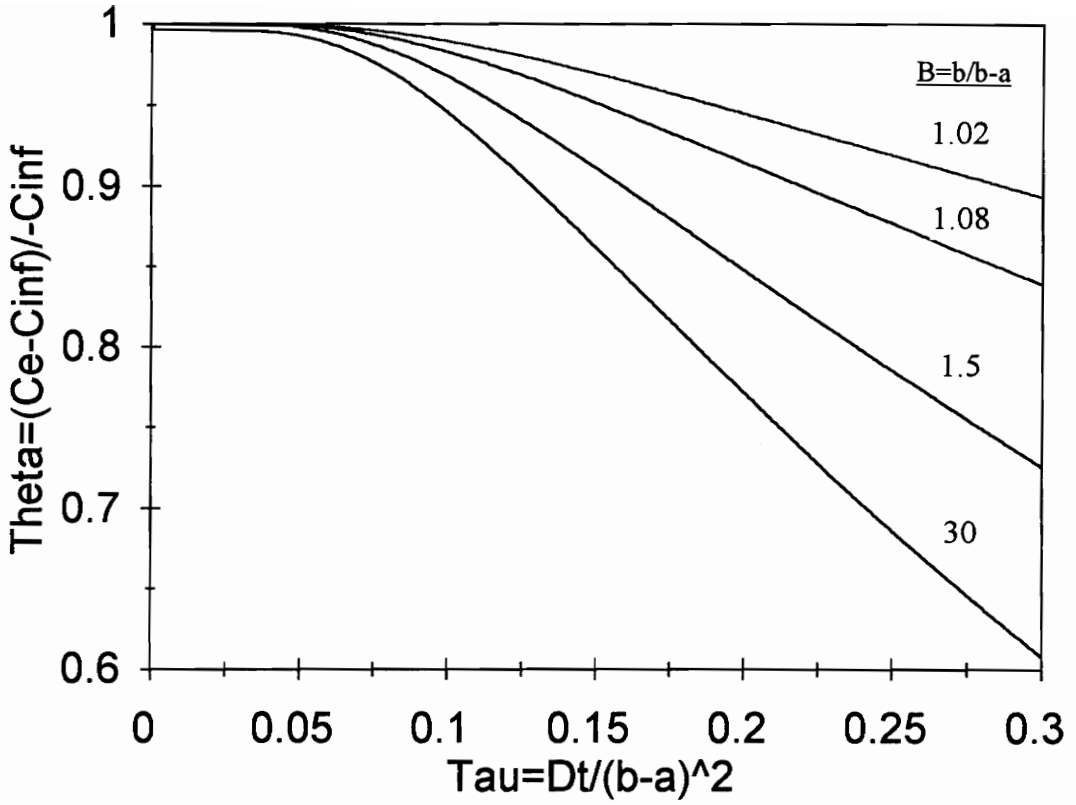

Figure 3.2 - Concentration Versus Time for a Sector Crevice.

3.4 Rectangular Crevice Models

It was impossible to imagine the number of re-entrant crevice shapes which could be present in the waste stream due to the shredding process. However, if a few simple rectangular shapes were modeled using a finite difference technique and then somehow related to the sector crevice exact solution, the exact solution could be used as a quick estimate for the enzyme penetration into these voids. This method would eliminate the need to use the finite difference code every time the dimensions of the crevice were changed. The next two sections show the rectangular shapes which were analyzed and describe the numerical technique employed to determine the transient enzyme concentration within these shapes.

3.4.1 Rectangular Crevice Notation

Figure 3.3 and Figure 3.4 illustrate the two rectangular geometries (Shape 1 and Shape 2) which were analyzed. The dimensions of the crevice opening were allowed to change as well as the width and length of the crevice. As shown in the Fig. 3.3, i designates the nodal position of m total nodes in the x-direction and h designates the nodal position of n total nodes in the y-direction. Also, k denotes the total number of nodes for the crevice opening. By using k for the bottom row, the crevice opening size can be controlled such that the crevice opening size is equal to $k\Delta x$. The width of the crevice is $m\Delta x$ and the length of the crevice is $n\Delta y$.

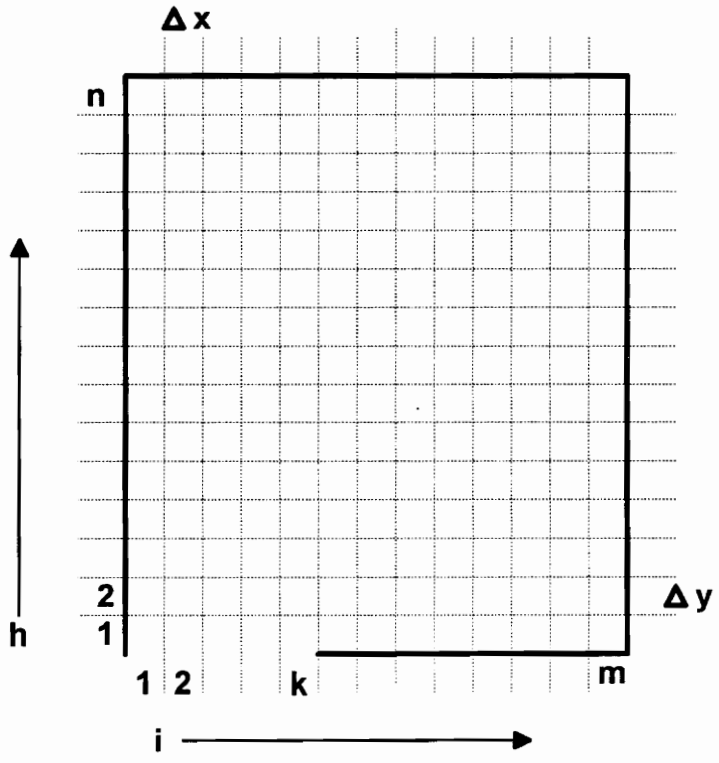

Figure 3.3 - Rectangular Crevice Notation (Shape 1).

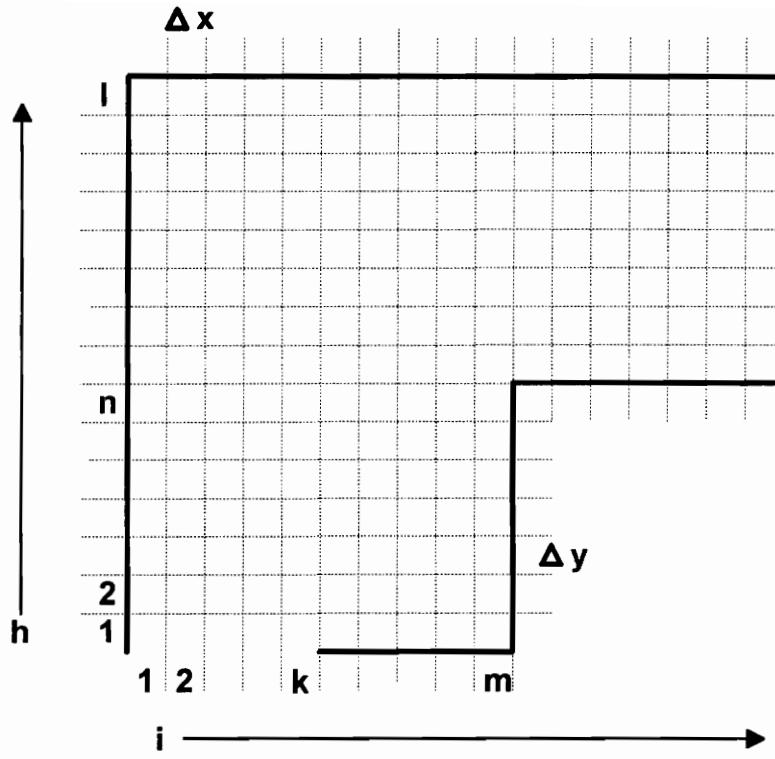

Figure 3.4 - Rectangular Crevice Notation (Shape 2).

In Fig. 3.4 the indices were modified in order accommodate the more complex geometry of Shape 2. i designates the position of j total nodes in the x-direction with m nodes in the x-direction for the bottom rectangle and h designates the position of l total nodes in the y-direction with n nodes in the y-direction for the bottom rectangle. Again k denotes the total number of nodes for the crevice opening. By using k for the bottom row, the crevice opening size can be controlled such that the crevice opening size is equal to $k\Delta x$. Also as m approaches j or as n approaches l, Shape 2 becomes Shape 1. This was the notation used in the finite difference computer codes listed in Appendix B which incorporated the alternating-direction implicit method explained in the next section.

3.4.2 Alternating Direction Implicit Method

The alternating-direction implicit (A.D.I.) method introduced by Peaceman and Rachford [32], provided an efficient method for solving problems involving large number of nodes. This method allowed for less computational time and involved solving a tridiagonal matrix line by line instead of having to solve the entire diffusion field simultaneously. To illustrate the procedure, the following two-dimensional, time-dependent mass diffusion equation was considered

$$\frac{\partial^2 C_e}{\partial x^2} + \frac{\partial^2 C_e}{\partial y^2} = \frac{1}{D}\frac{\partial C_e}{\partial t} \tag{3.14}$$

A rectangular network of mesh size Δx, Δy over the region was constructed with time steps of size Δt. Then, the coordinates x, y, and t were denoted by

$$x = i\Delta x,\ y = h\Delta y,\ \text{and}\ t = p\Delta t \tag{3.15}$$

and the concentration $C_e(x,y,t)$ at the location (x, y), at time t was

$$C_e(x,y,t) = C_e(i\Delta x, h\Delta y, p\Delta t) \equiv C_{ih}^{p} \tag{3.16}$$

where i, h, and p were integers.

The method involved representing the space derivatives in finite differences using an implicit and explicit difference approximation alternatively for $\frac{\partial^2 C_e}{\partial x^2}$ and $\frac{\partial^2 C_e}{\partial y^2}$. For example, if $\frac{\partial^2 C_e}{\partial x^2}$ was represented in the implicit form in terms of the unknown values of $C_{e\,m,n}^{p+1}$ from the (p+1)th time level, the derivative $\frac{\partial^2 C_e}{\partial y^2}$ was represented by an explicit approximation. That is, the finite difference form of various derivatives in terms of the unknown values of concentration for the (p+1)th time level became

$$\left(\frac{\partial^2 C_e}{\partial x^2}\right)^{p+1} = \frac{C_{i-1,j}^{p+1} - 2C_{i,j}^{p+1} + C_{i+1,j}^{p+1}}{\Delta x^2} \tag{3.17}$$

$$\left(\frac{\partial^2 C_e}{\partial y^2}\right)^{p+1} = \frac{C_{i,j-1}^{p} - 2C_{i,j}^{p} + C_{i,j+1}^{p}}{\Delta y^2} \tag{3.18}$$

$$\left(\frac{\partial C_e}{\partial t}\right)^{p+1} = \frac{C_{i,j}^{p+1} - C_{i,j}^{p}}{\Delta t} \tag{3.19}$$

To proceed the solution from the (p+1)th step to the (p+2)th step, the finite difference form of the equation (3.14) was written using an explicit form for $\frac{\partial^2 C_e}{\partial x^2}$ and implicit form for $\frac{\partial^2 C_e}{\partial y^2}$:

$$\left(\frac{\partial^2 C_e}{\partial x^2}\right)^{p+2} = \frac{C_{i-1,j}^{p+1} - 2C_{i,j}^{p+1} + C_{i+1,j}^{p+1}}{\Delta x^2} \tag{3.20}$$

$$\left(\frac{\partial^2 C_e}{\partial y^2}\right)^{p+2} = \frac{C_{i,j-1}^{p+2} - 2C_{i,j}^{p+2} + C_{i,j+1}^{p+2}}{\Delta y^2} \tag{3.21}$$

This alternation was repeated in each subsequent pair of time steps.

Once the discretized finite difference equation was determined, the concentration distribution was obtained for Shape 1 and Shape 2 using the computer codes listed in Appendix B. In this particular computer code, the concentration of enzyme was determined for the upper right corner of the rectangular shape (node $h = n$, $i = m$ for Shape 1 and node $h = l$, $i = j$ for Shape 2) described in Fig. 3.3 and Fig. 3.4.

3.5 Rectangular Crevice Comparison to Sector Crevice

In Section 3.3 the concentration at the outer radius for a sector-shaped crevice was determined using the dimensionless groups, θ, τ, and B, such that this concentration can be obtained easily for any combination of inner and outer radius. Therefore, by using one concise figure (Fig. 3.2) the degree of enzyme penetration can be determined quickly for

an infinite number of sector dimensions. This could not be done with the rectangular crevices since these rectangular shapes do not have the appropriate dimensionless groups associated with them. The diffusion of enzymes into the rectangular shapes needed to be compared to the diffusion of enzymes into the sector shapes. Therefore θ, τ, and B from the sector crevice needed to be related to the rectangular opening area, Ao, the rectangular volume, V, the characteristic length, L, and the time, t. The relationship between these parameters was developed in the following manner:

1. Define the characteristic length for the rectangular shapes.

2. Use the volume and area of the opening of the shapes to compare the rectangular shapes to the sector shapes.

3. Define the dimensionless volume, Vo, and relate it to the dimensionless back wall length, B.

Through this analysis it was determined that the dimensionless volume Vo was a more appropriate parameter to compare the diffusion into the sector and rectangular shapes than the dimensionless back wall length B.

3.5.1 Characteristic Length

In the analysis of these rectangular shapes, the most important position to determine the enzyme concentration within the crevice was the point furthest away from the crevice opening. This point will most surely need the longest time to obtain a significant concentration of enzyme in for disinfection. Therefore, if this area has been disinfected by the protease, then it can be assumed that the rest of the crevice has been disinfected as well. Now, since there was a specific point within the crevice for which the enzyme concentration was needed, a characteristic length (L) was defined from the crevice opening to this particular point as shown in Fig. 3.5 for Shape 1 and Shape 2. This

characteristic length (L) was equivalent to the outer radius minus the inner radius (b-a). From the figure the crevice opening dimension was defined as Ao.

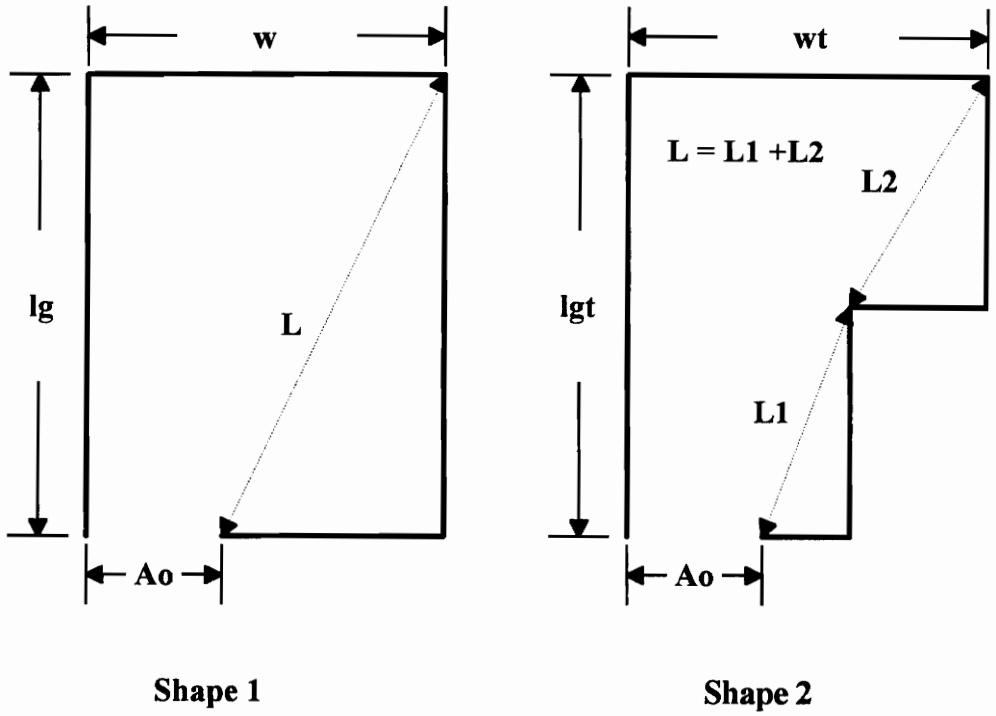

Figure 3.5 - Rectangular Crevices with Characteristic Length.

3.5.2 Sector - Rectangular Volume Analysis

This analysis allows a rectangular geometry to be compared to a sector geometry through the manipulation of the following parameters: volume, area of opening to the crevice, and the characteristic length. The inner and outer radius of a sector is defined by these various parameters in this analysis.

Define the following variables: volume of sector (V_{sector}), area of sector opening (Ao_{sector}), inner radius (a), outer radius (b), depth of crevice (d), angular dimension of sector (Φ),

characteristic length (L), volume of rectangle (V), area of crevice opening for the rectangle (Ao).

$$V_{\text{sector}} = d\pi(b^2 - a^2)\frac{\Phi}{2\pi} \tag{3.22}$$

$$Ao_{\text{sector}} = 2d\pi a\frac{\Phi}{2\pi} \tag{3.23}$$

$$L = b - a \tag{3.24}$$

Now, divide the sector volume by the area of the sector opening yielding:

$$\frac{V_{\text{sector}}}{Ao_{\text{sector}}} = \frac{b^2 - a^2}{2a} = \frac{(b+a)(b-a)}{2a} \tag{3.25}$$

Solve equation (3.24) for the inner radius a and substitute this result for a in equation (3.25)

$$\frac{V_{\text{sector}}}{Ao_{\text{sector}}} = \frac{(2b-L)L}{2b-2L} \tag{3.26}$$

Now, replace the sector volume and area of the opening in equation (3.26) with the rectangular volume and area of the opening to the rectangular crevice. This can be done if the assumption is made that the rectangular crevice's volume divided by the rectangular crevice's opening area is equivalent to the sector's volume divided by the sector's opening area.

$$\frac{V}{Ao} = \frac{(2b-L)L}{2b-2L} \tag{3.27}$$

Solving equation (3.27) for the outer radius b results in

$$b = \frac{\frac{V}{Ao} - \frac{L}{2}}{\frac{V}{AoL} - 1} \tag{3.28}$$

Substituting equation (3.24) into equation (3.28) and solving for the inner radius a results in

$$a = -\frac{V}{Ao} \pm \sqrt{\left(\frac{V}{Ao}\right)^2 + b^2} \tag{3.29}$$

The volume, characteristic length, and area of the opening to the rectangular crevices shown in Fig. 3.5 was used in equation (3.28) and equation (3.29) to determine an apparent sector-shaped crevice with an inner and outer radius of a and b, respectively. This "transformation" is illustrated in Fig. 3.6 with the rectangular crevice (Shape 1) shown by the solid line and the apparent sector crevice shown by the dotted line.

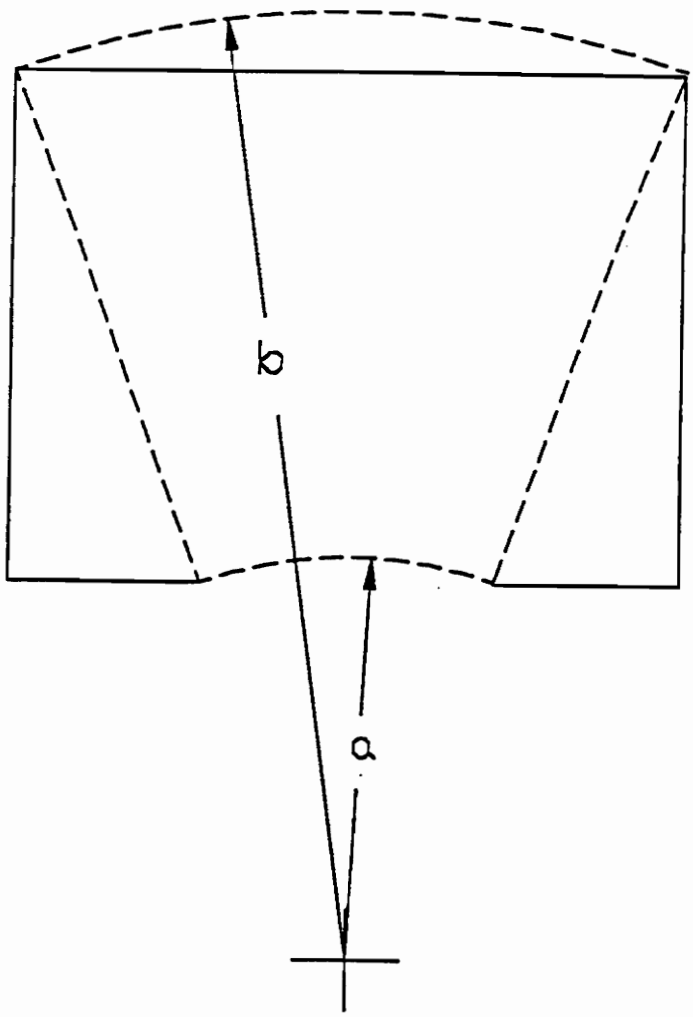

Figure 3.6 - Rectangular-Sector Transformation.

The finite difference computer code was now used to determine the transient enzyme concentration at the far corner for a number of different rectangular volumes and crevice opening areas by varying the length, width, and opening size. The enzyme concentration at the outer radius of the sector and the far corner of the rectangle was then compared by determining the apparent inner and outer radius of the rectangular shape and using these two dimensions in the sector crevice computer code listed in Appendix B. A series of curves was then generated comparing the diffusion of enzyme into these two shapes.

3.5.3 Dimensionless Volume

In the sector exact solution analysis in Section 3.3, the dimensionless back wall, B, was the parameter used to illustrate the various sector geometries. Through the analysis in Section 3.5.2 and through much computer time, it was seen that the dimensionless volume $Vo = \frac{Volume}{AoL}$ was a better parameter to compare the various geometries than B. By using Vo the comparison of the sector and rectangular geometries could be presented in a much cleaner form. B and Vo are related by the following

$$B = \frac{Vo - \frac{1}{2}}{Vo - 1} \tag{3.30}$$

By using the analysis in Section 3.5.2, it can be shown that Vo for the rectangular crevice and Vo for its apparent sector crevice are equivalent. By using the dimensionless volume, the enzyme concentration as a function of time at the back wall of the sector as given by the exact solution was compared to the concentration at the far corner of the rectangular shapes given by the numerical solution. This comparison is detailed in Section 3.6.

It will be shown that one group of curves (Figure 3.7) can be used to determine the approximate diffusion time or concentration at the characteristic length defined by $L=b-a$ or as L is defined by Fig. 3.5 for these two simple rectangular shape. For Shapes 1 and 2, $b-a$ was equal to L for all of the cases which were analyzed. However, it could not be shown algebraically that $L=b-a$ as defined in equations (3.28) and (3.29) for all re-entrant crevices.

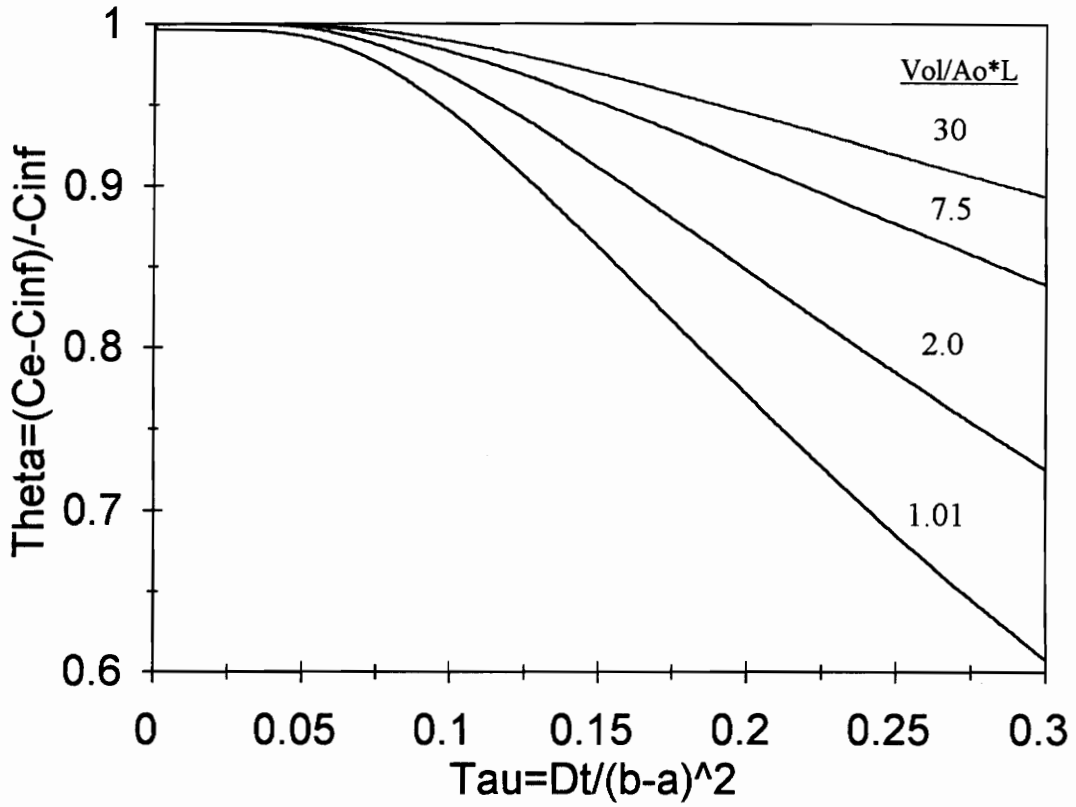

Figure 3.7 - Sector Crevice Concentration for Various Dimensionless Volumes.

3.6 Rectangular-Sector Comparison

In order to determine the accuracy of the comparison method discussed in Section 3.5, a series of simple rectangular crevices were analyzed. The A.D.I. computer code was used

to determine the transient enzyme concentration at the distance L for these shapes. The length, width, and size of the opening of both Shapes 1 and 2 were varied in order to attain a variety of dimensionless volumes (Vo) which could range from one to infinity. Equations (3.28 and 3.29) were used to determine each rectangular crevice's corresponding inner and outer radius, a and b. Now these dimensions were used in the sector crevice problem to determine the transient enzyme concentration at the outer radius. Remember that Vo for the rectangle and its corresponding sector are equivalent. Thus, the rectangular and sector geometries were compared using this dimensionless group. The analysis of Shape 1 required only three dimensionless parameters: $\theta(B,\tau)$, τ, and Vo which is a function of B shown in equation (3.30). The analysis of Shape 2 was not as straight forward as Shape 1. In order to compare Shape 2 with the sector crevice solution, two additional dimensionless parameters had to be defined. These were the width ratio $\frac{m}{j}$ and the height ratio $\frac{n}{l}$.

First, the transient enzyme concentration for each value of Vo for the sector and both rectangular shapes was compared. As Vo approached unity, the crevice (Shapes 1 and 2) corresponded to a rectangle with the width dimension open entirely to the slurry enzyme concentration. The crevice geometry for $Vo = 1$ for both Shapes 1 and 2 was identical to the one-dimensional crevice problem discussed in Chapter 2 and thus the transient concentration was identical as well. As Vo increased, the transient enzyme concentration for Shapes 1 and 2 began to deviated from the transient concentration for the sector crevice.

Figure 3.8 is given to compare the transient enzyme concentration for the two geometries (sector and Shape 1) for a specific value of *Vo* equal to 30. It also shows the upper limit of the transient enzyme concentration for Shape 2 for *Vo* equal to 30. The upper limit is shown because there are an infinite number of configurations of Shape 2 depending on $\frac{m}{j}$ and $\frac{n}{l}$ and therefore only the worst case is plotted. The width and length ratio for this worst case curve is listed on Fig. 3.8. If the error between Shape 1 and the sector curves is analyzed for τ greater than 0.1, it remains relatively constant at 24 percent with error defined by

$$Error(const.\ \tau) = \left| \frac{\text{rectangular crevice conc. - sector crevice conc.}}{\text{rectangular crevice conc.}} \right| \times 100 \qquad (3.31)$$

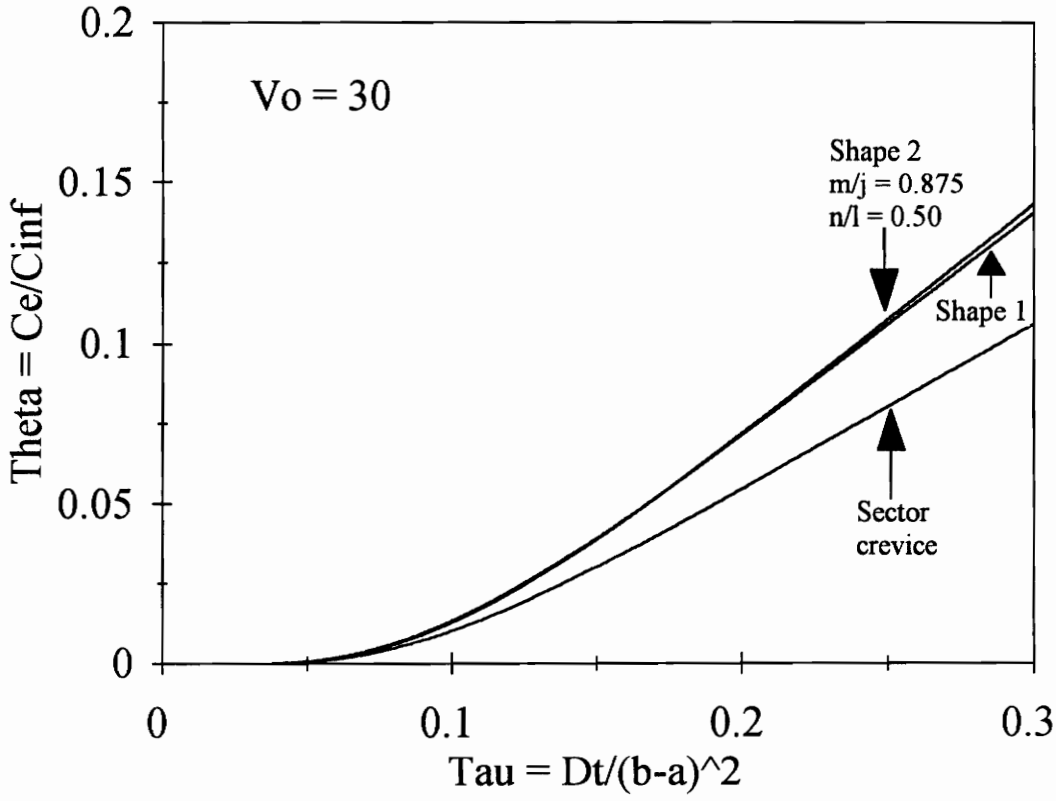

Figure 3.8 - Transient Concentration for *Vo* = 30 Corresponding to Shape 1 and the Worst Case for Shape 2.

The error of 24 percent is relatively high, but if the sector crevice model is used for a quick estimate for these rectangular geometries this will provide an additional factor of safety to insure that these types of voids are disinfected. This error decreases to zero as *Vo* approaches one.

For comparison the dimensionless time, τ, was compared with the dimensionless volume, *Vo*, for a specified dimensionless enzyme concentration, $\theta(B,\tau) = \frac{C_e(B,\tau)}{C_\infty}$, of 0.1 at the back wall. This comparison for Shape 1 is shown in Fig. 3.9.

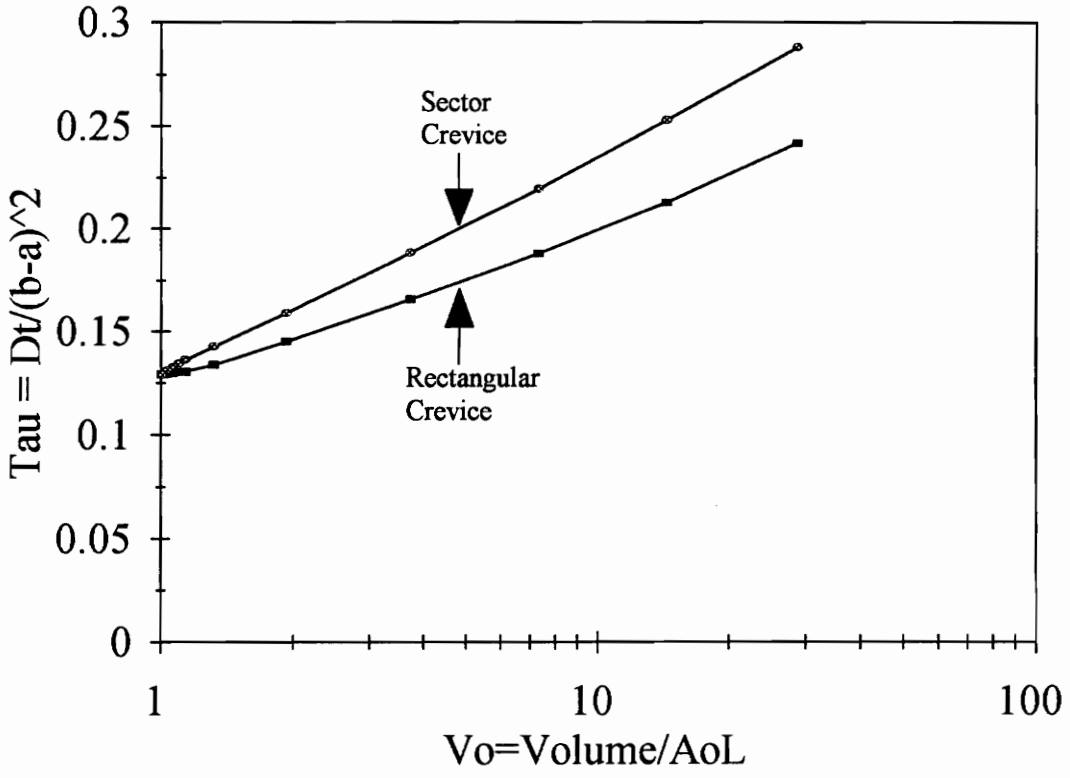

Figure 3.9- Time versus Volume Comparison for θ = 0.1 (Shape 1).

As shown, the sector and rectangular crevice had the same value of τ for *Vo* equal to one. This indicated that the sector crevice exact solution (Fig. 3.7) was equivalent to the

diffusion into rectangular crevice (Shape 1 and 2) when the crevice opening was equivalent in size to the crevice width. As the dimensionless volume increased, the error also increased. This error increased as *Vo* approaches infinity. When the crevice opening was small compared to the width dimension, the sector crevice exact solution did not approximate the rectangular crevice very well.

For example, for *Vo* of 5 or less, the sector exact solution approximated the diffusion time conservatively with an error of 10 percent or less and for *Vo* of 30, the diffusion time was approximated conservatively with an error of 20 percent. The error was defined by

$$Error(const\ V_o) = \frac{\text{Sector crevice } \tau \text{ - Shape 1 } \tau}{\text{Sector crevice } \tau} \times 100 \qquad (3.32)$$

This error associated with the comparison was actually important because it provided a factor of safety in diffusion estimates. This allows Fig. 3.7 to be used with confidence when analyzing rectangular shapes similar to Shape 1 because the conservative approximation corresponded to higher enzyme concentrations in the rectangular crevices and therefore, guaranteed pathogen disinfection.

For Shape 2 the dimensionless time τ was compared with *Vo* for θ=0.1 at the back wall similarly to Fig. 3.9. Since Shape 2 incorporated two additional parameters, the width and length ratios, there was a series of curves instead of only one curve for the rectangular case. This resulted in three figures shown in Appendix D. Each figure is for a specific length ratio $\frac{n}{l}$ and on each figure a series of curves is shown for specific values of width ratio $\frac{m}{j}$.

4

Diffusion Conclusions

4.1 One-Dimensional Model Conclusions

The one-dimensional problem will be the most frequently occurring phenomena within the waste stream due to the use of hypodermic needles in many infectious waste applications. Therefore, it was essential to determine if the majority of these needles will be disinfected during the process or at least be exposed to the protease enzyme in order for complete disinfection to occur shortly thereafter. This work can only serve as an initial guideline to determine disinfection time once various parameters on the entire system have been set.

Due to the uncertainty of these various parameters such as protease enzyme concentration, batch time, pathogen kill time, etc., actual conclusions regarding complete disinfection cannot be drawn to date. This uncertainty does not allow for quantitative values to be placed on the time to reach a 10^6 per ml reduction in pathogens. However, this research can be used to determine approximate disinfection times once the various parameters for the bioremediation process have been determined. Based on the one-dimensional diffusion only models detailed in Chapter 2 of this paper, a few conclusions concerning the disinfection of a 1.27 cm open-ended crevice were made.

1. During the protease treatment time tentatively ranging from 1 to 3 hours, the entire one-dimensional crevice will not be disinfected entirely. However, substantial numbers of enzymes should be present within the initial segment of the crevice (the first 0.2 cm section of the crevice) depending on the slurry protease concentration.

2. Based upon the tentative protease concentration of 1% and a hypothetical ambient temperature of 35° C, the entire crevice will be disinfected in less than a day after protease treatment. For a batch time of 1 hour, disinfection will occur in 1 day after treatment; for a batch time of 3 hours disinfection will occur in approximately 14 hours after treatment.

3. These approximate disinfection times were given based upon tentative process parameters. However, these approximate times given as examples are conservative estimates and actual disinfection of the crevices should be completed sooner than indicated in conclusion 2 for several reasons:

    - Possible enhancement of enzyme penetration due to capillary action or convection.

    - Faster kill times due the integral effect of enzyme concentrations lower than 0.1%. In other words more microbe disinfection data needs to be taken at lower concentrations and then the log reduction of "bugs" can be integrated with respect to time to determine these more accurate disinfection times.

    - Some lab tests have shown that the cellulase enzyme used in the initial stage of the process has some effect on bacteria inoculation. These results have not been considered.

    - Temperature of 50°C inoculates some stains of virus and bacteria; this temperature conducts through the needle wall.

4.2 Re-entrant Model Conclusions

As previously mentioned, re-entrant crevices will also be present in the infectious waste stream. Re-entrant models were developed based on an exact solution and finite difference solutions. The transient, dimensionless concentration of enzyme at either the outer radius or the far corner was determined for each shape. Unfortunately, not enough information was known to predict disinfection times for such objects for reasons previously discussed. However, these models should be able to be used to predict disinfection times for most re-entrant geometries once the various process parameters have been set. Along with this information, additional conclusions were drawn in reference to the rectangular - sector comparison. The conclusions were as followed:

1. The sector-shaped crevice was used to approximate diffusion times or solute concentration in rectangular shapes with an error which ranged from zero to 20 percent.

2. The comparison was exact for crevices with openings equivalent to the width of the rectangle. This case was also equivalent to the one-dimensional case.

3. The error increased as the crevice opening approached zero and the width dimension was kept constant. This case was equivalent to a dimensionless volume of infinity. This error will serve as a factor of safety when disinfection times are estimated for these types of crevices.

4.3 Future Work

Although most of the ground work has been covered on enzyme diffusion in small one-dimensional and re-entrant crevices, there is some work that needs to be completed. The following list summarizes the future work which needs to be performed in order to understand enzyme diffusion and disinfection of small crevices in infectious medical waste.

1. The size of all particles within the waste stream has been assumed to be less than 0.5" in their largest dimension. This particles size was suggested by the shredder manufacturer. Now that the shedder of the first system is in place, the particle size of the shredded waste should be better understood.

2. Perform experimental capillary tube tests described in Appendix C using experimental method 2. From these tests determine if the diffusion only assumption was valid.

3. Once the protease process parameters have been set, determine degree of enzyme penetration during the process for both the one-dimensional and re-entrant cases.

4. Generate disinfection time curves for both one-dimensional and re-entrant crevices from updated viral and bacterial inoculation data provide by the Department of Veterinary Medicine. A series of curves should be generated incorporating all possible process parameters as well as pathogen log reduction data. The curves also should account for the lower enzyme concentrations by integrating the log reduction of microbes

with respect to time to yield more accurate results. The series of curves will provide a quick and easy guideline to estimate cavity disinfection.

Part II

Cellulose Breakdown within the Batch Reactor

5

Overview of Cellulose

Cellulose is probably the most abundant biological compound on earth, in the form of lignified cellulose (wood) and as , more or less, pure cellulose in paper, fibers, and textiles [27, Boyce]. Since cellulose is one of the most abundant and widely used resources, it also is one of the main waste products, either natural or man-made. As a result, cellulose-containing substances compose the majority of material in infectious medical waste and it would be advantageous to degrade this material prior to disposal. The bioremediation process utilizes cellulases to degrade cellulose (paper) to a reduced form. The cellulases also hydrolyze paper to a varying degree depending on the origin of the paper (e.g. Was the paper derived from cotton, hardwood, softwood? Was the paper produced from mechanically treated pulp or both mechanically and chemically treated pulp?). Therefore, three areas of background information needed to be covered in this chapter:

- Molecular structure of cellulose
- Basics of cellulose hydrolysis by cellulases.
- Composition of various papers in medical waste.

5.1 Molecular Structure of Cellulose

The fundamental building block of cellulose is glucose ($C_6 H_{12} O_6$). These molecules of glucose are coupled together by β(1-4) bonds as shown in Fig. 5.1. The length of cellulose molecules in a fiber varies from less than 15 glucose units to as many as 14,000 glucose units, depending on the origin of the cellulose [33, Cowling and Brown].

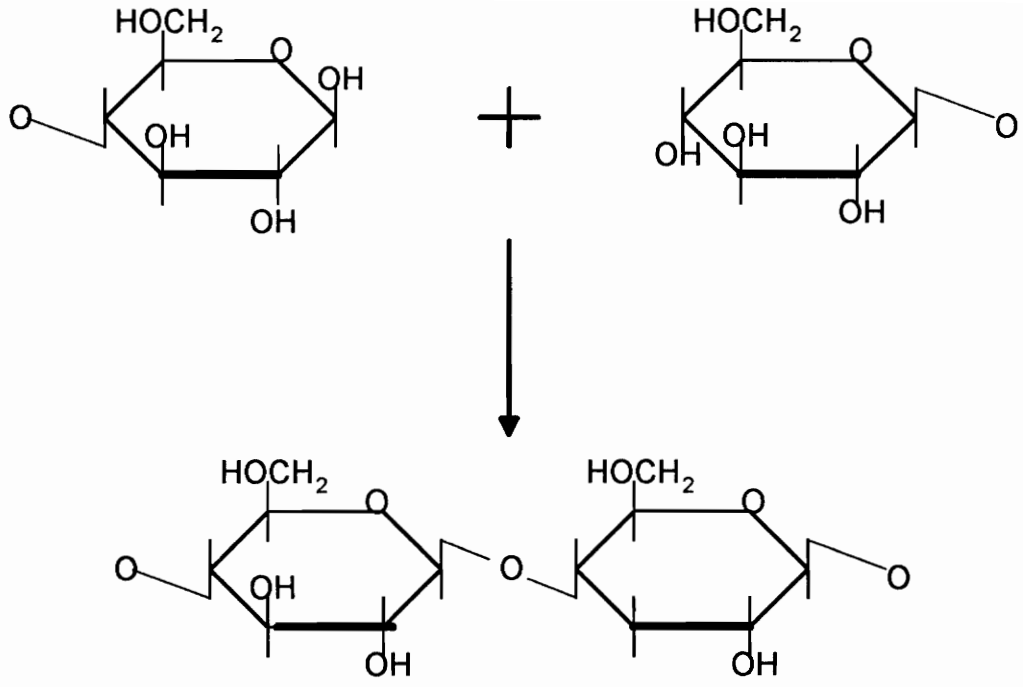

Figure 5.1 - Beta Configuration Found in Cellulose.

These long strands of cellulose are usually linked together by hydrogen bonds to form even larger units. There is no set pattern to these bond sites, but it is thought that one cellulose molecule has areas with an orderly configuration of hydrogen bonds and other areas with very few or no hydrogen bonds. The areas with the orderly configuration of hydrogen bonds are known as crystalline cellulose due to their rigid structure while the flexible regions with few or no hydrogen bonds are known as amorphous cellulose [27, Boyce]. This type of structure is visualized in Fig. 5.2.

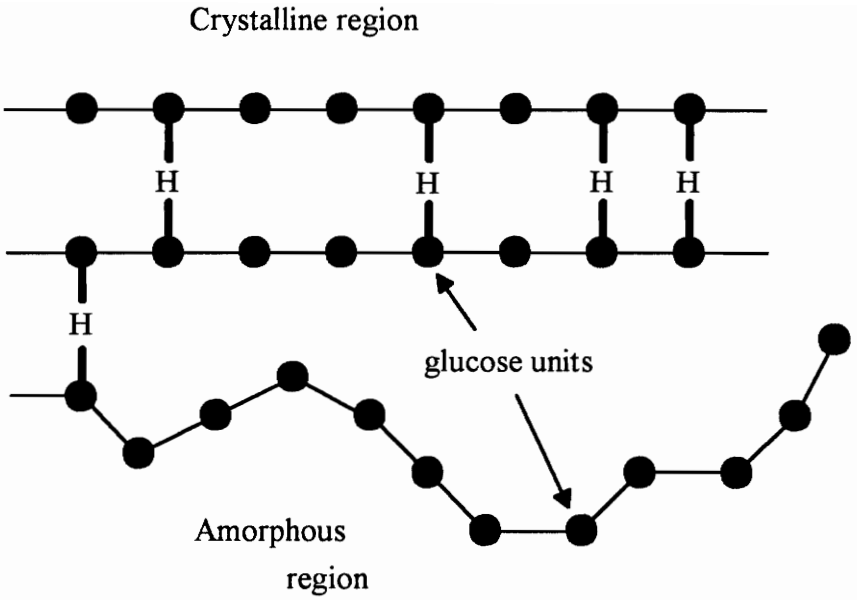

Figure 5.2 - Cellulose Structure.

At the end of the cellulose molecule, there is non-reducing segment. This segment has the same basic structure as Fig. 5.1 except that the oxygen bond on one end has been replaced by a hydroxyl group (OH). This small difference in composition becomes important when considering enzymes which degrade cellulose because there is a specific enzyme which targets the ends of the cellulose fiber.

5.2 Basics of Cellulose Hydrolysis by Cellulases

Now that a basic understanding of the cellulose fiber has been developed, an overview of enzymatic hydrolysis can be covered. When it is said that cellulose hydrolyzes, the following reaction takes place:

$$C_{6(n+m)}H_{10(n+m)+2}O_{5(n+m)+1} + H_2O \rightarrow C_{6n}H_{10n+2}O_{5n+1} + C_{6m}H_{10m+2}O_{5m+1} \quad (5.1)$$

Equation (5.1) is written for a cellulose fiber with $n+m$ glucose groups and the reaction occurs and divides the fiber between n^{th} and $n+1^{th}$ unit. This type of reaction occurs in the presence of many reagents (acids, etc.), but in the bioremediation process this reaction occurs due to the activity of cellulase enzymes.

Cellulase enzymes are typical of all enzymes in that they are proteins and are composed of L-amino acids. These amino acids are linked together by the formation of amide or peptide linkages (Figure 5.3) [34, Malcolm]. The R is a chemical group which is characteristic of each L-amino acid and the superscript designates the many amino acids which compose a particular enzyme.

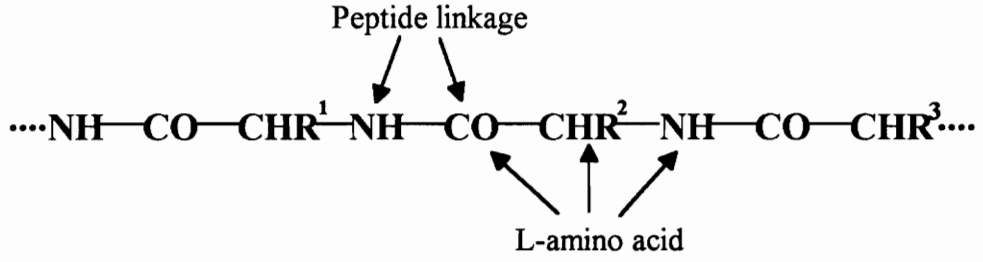

Figure 5.3 - Linkage of L-amino acids in the Formation of an Enzyme.

Cellulase enzymes are large with a molecular weight range from 25,000 to over 100,000. The properties of these enzymes arise from the way in which the chain shown in Fig. 5.3 folds. These chains can fold on either side of the CHR groups only and usually form an α helix structure due to this freedom of rotation about these two bonds. Cellulases which are derived from the fungal strain *Trichoderma viride* have been shown to predominantly exhibit the α helix formation described by Malcolm and by King and Vessal [35]. The cellulases descibed by King and Vessal have been studied extensively and the amino acid composition has been determined according to Table 5.1. These amino acids can be substituted into Fig. 5.3 to give the entire structure of cellulases derived from *Trichoderma viride* which are typical of most cellulases.

Table 5.1 - Amino Acid Composition of the Endo and Exo-glucanases of *Trichoderma viride*.

Amino Acid	Endo-glucanase	Exo-glucanase
	(*Moles/mole of Protein*)	
Lysine	12	14
Histidine	9	7
Arginine	15	16
Aspartic Acid	74	65
Threonine	44	38
Serine	40	46
Glutamic Acid	46	35
Proline	21	34
Glycine	62	55
Alanine	46	50
Cystine	1	3
Valine	30	25
Methionine	2	5
Isoleucine	30	21
Leucine	36	32
Tyrosine	17	18
Phenylalanine	18	19
Ammonia	93	130

In the ideal system, there would be just one type of cellulase enzymes and only one set type of cellulose with a known length and degree of crystallinity. These enzymes would randomly hydrolyze the cellulose fiber moving from one glucose unit to another until the entire fiber was reduced to nothing more than sugar dissolved in water. However, there are no ideal systems and therefore, no one form of cellulose and not only one type of cellulase enzymes. There are three groups of cellulase listed by Emert et al. [16].

- Group 1 - Endo-glucanase and Exo-glucanase
- Group 2 - Cellobiase
- Group 3 - Hydrocellulase and Cellobiohydrolase

Group 1 is the workhorse in cellulose hydrolysis when it comes to bond cleavage. Endo-glucanases randomly cleave interior $\beta(1\text{-}4)$ bonds along the cellulose chain. These enzymes have an affinity for cellulose with a high degree of polymerization. They would rather attack a cellulose fiber of 1000 glucose units than attack a cellulose fiber of 100

glucose units. However, these enzymes exhibits no set pattern for hydrolysis. They also break the hydrogen bonds which form crystalline cellulose but at a reduced rate compared to $\beta(1\text{-}4)$ bond cleavage. Therefore, for efficient hydrolysis of cellulose by these enzymes, amorphous cellulose is required.

Exo-glucanases systematically cleave glucose from the end of the cellulose chain. These enzymes would seem to be of little importance when considering a long cellulose chain, but it has been found that enzyme preparations containing only endo-glucanases have had little effect on native cellulose. However, when a mixture of both endo-glucanases and exo-glucanases were used, a significant degree of hydrolysis occurred. Wood and McCrae [36] have proposed that these two enzyme types work in a synergistic manner on long strands of cellulose fiber.

Group 2 is the category of enzymes (cellobiase) which hydrolyze the short disaccharides into two glucose molecules. These disaccharides, known as cellobiose, result from endo and exo-glucanase activity. Wood and McCrae discovered that as cellobiose in the system increases, the activity of exo-glucanase was reduced and therefore, production of glucose was slowed considerably. Therefore, to enhance the production of glucose, cellobiase needs to be present in the reacting mixture.

Group 3 is the main category of enzymes which reduces crystalline cellulose to amorphous cellulose. However, this reduction to the amorphous form is at a slower rate when compared to the activities of enzymes in Group 1 and Group 2. Wood and McCrae also reported that the activity of cellobiohydrolases on crystalline cellulose was increased in the presence of endo and exo-glucanases. This group of enzymes has an additional function to cleave the non-reducing ends from the cellulose chain which produces cellobiose.

Figure 5.4 [27, Boyce] illustrates the cleavage of bonds by the representative cellulases. Each of the three groups is shown with its appropriate bond cleavage site on the cellulose fiber.

From each group there is a synergistic effect when all three groups of enzymes are present in a solution. No pure form of one group has the ability to degrade native cellulose to any appreciable degree. Therefore, for maximum hydrolyzation of cellulose, a mixture of all three groups is the most effective. Fortunately, the microorganisms (*Trichoderma viride and Trichoderma reesei*), which yield cellulases, produce all three categories of cellulases simultaneously, and most commercially available cellulases are produced from these microorganisms due to their high enzyme yield. These crude mixtures containing all three categories are the type of enzymes used in the bioremediation process.

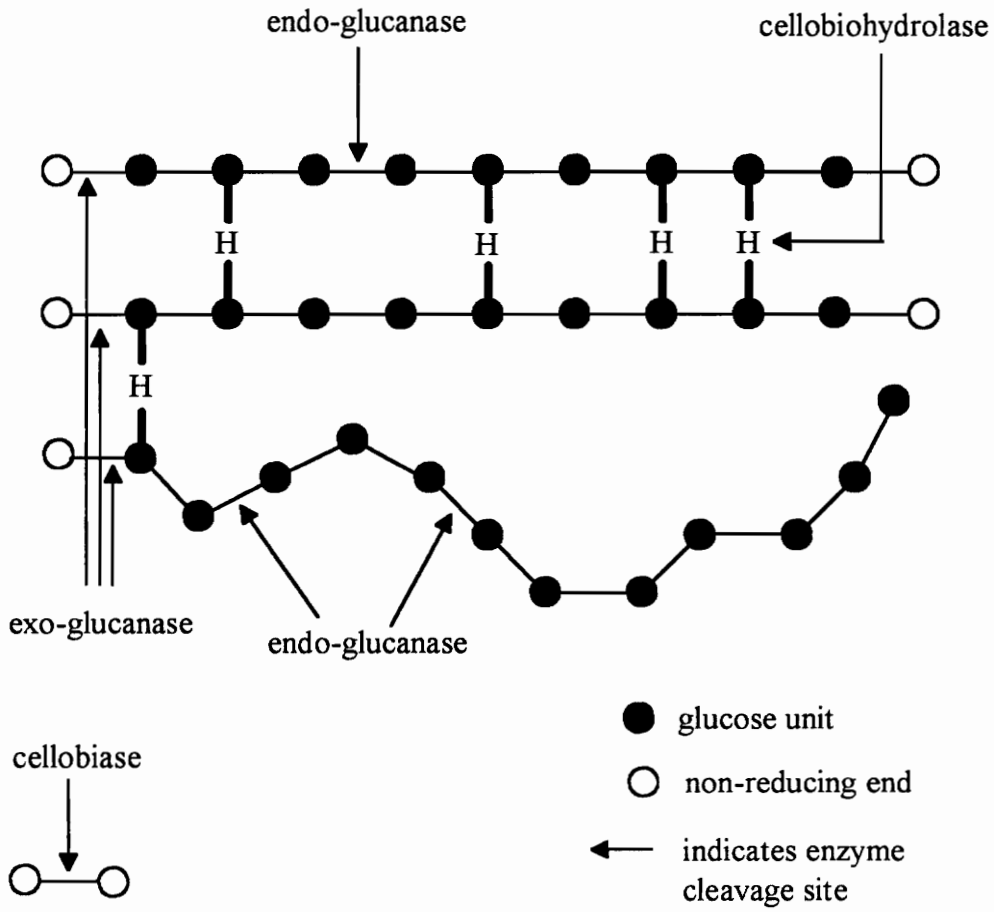

Figure 5.4 - Cellulose Degradation by Cellulases.

5.3 Composition of Various Paper Types in Medical Waste

Studies have shown that as much as 60 percent of medical waste is composed of paper [3, Carpenter]. This number does not include other cellulose-derived materials such as cotton gauze and cellulose sponge material. Within this 60 percent, there is a variety of paper types which include mostly absorbent papers, but might include others such as newspaper or writing papers. Each of these paper types has a different composition depending on the origin of paper and the pulping process and therefore, hydrolyze differently in the presence of cellulases.

5.3.1 Composition of Wood

In order to understand the degree of hydrolysis of paper due cellulase activity, the amount of cellulose within the paper must be taken into consideration. Since wood is the major raw material of paper, the make-up of wood should be examined more closely. The average composition of wood is given in Table 5.2.

Table 5.2 - Average Composition of Wood.

Cellulose	40% - 47%
Hemicellulose	25% - 30%
Lignin	16% - 31%
Extractives	1% - 8%

From Table 5.2 wood contains less than 50 percent cellulose with the remaining composed of mostly hemicellulose and lignin.

Hemicelluloses are similar to cellulose in that they are large molecules made up of sugars [37, Nissan]. However, they differ from cellulose in several respects:

1. They are made not only of glucose but of other sugars as well.

2. They are usually branched, not straight-chained.

3. They have active groups, such as COOH, beside the OH groups found in cellulose.

Ligin is an amorphous substance that is partly aromatic in nature; it contains methoxyl groups, and aliphatic and phenolic hydroxyl groups. Lignin is not a compound, but is a system and varies in composition with method of isolation and with species, age, growing conditions, etc., of the tree or lignified material. It has been called a "cementing material" which holds the fibrous structure intact. It is insoluble in water and in common organic solvents. It is readily attacked and solubilized by oxidizing agents [38, Britt].

Extractives are a diverse group of substances. Some are involved in growth of the cells or result from metabolic processes. Examples are the pectic substances and proteins, volatile oils such as turpentine, fatty acids, and alcohols. Most of these substances are soluble in water or in neutral organic solvents and therefore, are collectively known as extractives [38, Britt].

5.3.2 Basics of Wood Pulp

Since the basic composition of wood is known, the types of wood pulps which produce such papers as absorbents, newspapers, etc. can be discussed. In general there are two types of wood pulp:

- Mechanical pulp
- Chemical pulp

with other pulps lying somewhere between these two. Mechanical pulp has the highest yield (mass of pulp from the pulping process divided by the initial mass of wood into the pulping process) because the wood is simply ground or refined. Therefore, almost none of the cellulose, hemicellulose, and lignin is lost. These pulps are used in papers such as newsprint and magazine papers. Chemical pulps have a yield of only about 45% - 50%.

At this yield, almost all the lignin is removed and the pulp consists of mostly pure cellulose and some hemicellulose. These pulps produce more permanent papers used for writing and bond papers. There are also some other pulps which fall between these extreme categories which use some form of mild chemical treatment.

The papers produced from chemical pulps are stronger due to the high number of cellulose fibers. These fiber surfaces have many hydroxyl groups which attract water molecules and bond with them through hydrogen bonds [37, Nissan]. In paper making, as the water evaporates the hydroxyl groups on the cellulose are joined through a single layer of water molecules, again by hydrogen bonding. Finally, as the water is completely dried off, the hydroxyl groups of the cellulose molecules join directly, making firmly bonded paper. The importance of these hydrogen bonds will become clear in this research because these bonds play a major role in holding paper together, thus resulting in a higher apparent viscosity in the batch reactor. These bonds need to be broken along with the hydrolysis of cellulose in order to achieve maximum viscosity reduction and maximize the solids concentration in the tank.

5.3.3 Activity of Cellulases on Paper in the Batch Reactor

As discussed, paper is more than just cellulose. Most papers in medical waste are produced from the pulps which fall between mechanical and fully chemical treated pulps. Therefore, there is lignin and hemicellulose present in these papers. At this point the bioremediation process includes cellulose degrading enzymes only. Therefore, the lignin and hemicellulose remains in the waste material.

The type of paper which contains the least amount of cellulose material is newsprint and therefore, results in less overall hydrolysis of paper during the cellulase process time. Since the average composition of medical waste papers is unknown, newsprint was used as the paper type in agitator power tests and the simulated medical waste tests in this research. This provided "a worst case", conservative estimate for these tests.

6

Cellulose Hydrolysis Experimentation

The use of cellulase in the batch reactor enhances the performance of the bioremediation process because the enzymes hydrolyze the paper which is present in infectious medical waste. This hydrolysis allows more waste to be processed per batch and also reduces the viscosity of the slurry. However, the extent of both of these benefits was unknown and needed to be determined. In the initial testing of this process, small-scale batch tests were conducted in order to determine the value of cellulase addition. This chapter describes these small-scale experiments which cover two areas of interest:

- The Increase in Maximum Mixable Solids Concentration Due to Cellulase Activity
- The Influence of Cellulose Hydrolyzation on Agitator Power

6.1 Maximum Mixable Solids Concentration Experiments

In the initial research in the batch reactor process, the amount of material which could be disinfected in one batch was unknown. This information was essential in understanding the feasibility of this technology because it was necessary to assess the cost of enzymes, acid, base, hot water, and electricity. The more waste which is processed in one batch, the more cost effective this technology becomes. Therefore, the small-scale tests needed to be conducted in order to determine the maximum solids concentration which could be agitated with and without cellulase.

This section describes the small-scale simulated waste experiments as follows:

1. Simulated medical waste sample
2. Experimental apparatus and setup
3. Experimental procedure
4. Simulated medical waste results

6.1.1 Simulated Medical Waste Sample

Before testing began, the composition of the waste stream needed to be known. A congressional report on the material breakdown of infectious hospital waste suggests that an average redbag contains (by weight) about 60% paper, 30% polymers/synthetics, and 2% metal with the remaining 8% composed of glass, cloth, human tissue, chemicals, etc. [3, Carpenter]. Therefore, the simulated medical waste used in these experiments was structured similarly to these numbers excluding the cloth, human tissue, and chemicals. The composition of the simulated waste (Table 6.1) was as follows:

Table 6.1 - Simulated Medical Waste Composition.

Material	Weight Percentage
paper	60%
plastic	30%
diapers	4%
glass	4%
metal	2%

Referring to Table 6.1, the paper was newsprint, the plastic was from polyethylene plastic cups, the diapers were the disposable type, and the metal was from aluminum cans. The plastic, diaper, glass, and metal particles' largest dimension was 1.27 cm (0.5 in) or smaller with a few paper pieces exceeding 2.54 cm (1 in). The newsprint had been processed through the shedder while the rest of the material was cut by hand. For this reason the newsprint particle size was not as uniform as the rest of the waste sample.

6.1.2 Experimental Apparatus and Setup

The components in the experiments were as follows:

Agitator:	Lightnin Labmaster II Mixer
Impeller Type:	2 - Four-blade Turbine with 45° pitch (2 in dia, 3/8 in width)
Test Beaker:	Polypropylene, 6 in dia by 9 in height

Thermocouple:	Type T
Transmitter:	For Type T, 4-20 mA output
pH Electrode:	Cole-Parmer Self-Cleaning Flat Electrode
Transmitter:	0-14 pH range, 4-20 mA output

The agitator was a variable speed mixer which displayed time and shaft power. Two turbine impellers were used with a diameter of 2 in. These were spaced such that one blade was 0.5 in off the bottom of the beaker and the other was positioned 1 in below the unagitated liquid level. The pH electrode and the thermocouple were mounted in the beaker to measure pH and temperature at all time. The beaker was placed in a water bath which was heated by an electric hot plate. This water bath kept the slurry at constant temperature (50°C) for optimum cellulase activity.

A total volume of 2 liters was used for all tests. The solids concentration was set at 15% by weight. Tests were conducted with and without enzyme. When cellulase was used, the enzyme concentration was 2% by total weight of the slurry. Three different commercially available cellulases were tested which were supplied by Novo-Nordisk Industries and Genencor International.

6.1.3 Experimental Procedure

The experimental procedure for the simulated waste tests were as follows:

1. The proper amount of water, acid, and enzyme was mixed in the beaker at a low speed of 200 rpm. The acid was added until the pH was 4.3 and the solution temperature was 50°C. These were the conditions for optimum cellulase activity according to the enzyme suppliers.

2. 28.4 grams of waste was added 11 times at 10 minute intervals to simulate the suggested 800 lb/hr feed rate of the shedder and a tank volume of 1200 gallons for the large-scale system. After the eleventh addition, the batch contained 15% waste by weight. Shaft power was monitored and recorded throughout the entire test.

3. Once the first batch of waste was added the agitator speed was increased to 800 rpm because in some preliminary testing, this speed agitated the samples vigorously without splashing the slurry out of the beaker.

4. Small amounts of acid were to added throughout the test because paper is a weak base and with each addition of waste the pH increased slightly.

5. The slurry temperature was kept constant at 50°C by adjusting the water bath temperature.

6. As the solids concentration increased over time, the degree of agitation was monitored visually. When the particles in the waste failed to mix in the beaker (or in other words when the waste began to move as a solid body), the solids concentration at that instant was taken to be the maximum mixable solids concentration for the particular test.

7. Once the 15% solids concentration was attained, the test was allowed to continue for an additional 50 minutes. The shaft power was monitored and recorded during this additional time as well.

8. After the test was completed, the slurry was then poured over a 15 wire per inch screen. The samples were squeezed over the screen and then dried at 50°C in an oven over night or until completely dry. The resulting sample was weighed and the dry mass reduction was determined.

9. Each test was performed three times and the shaft power from these three trials was averaged for each time interval and plotted versus time.

6.1.4 Simulated Medical Waste Results

In the initial stages of these experiments, very little was known about the topic of cellulose breakdown in the batch reactor. The range of such parameters as solids concentration, enzyme concentration, feed rate, etc. were unknown and therefore, were determined more or less through trial and error. The procedure which was described in the previous section evolved from a number of tests which for various reasons were failures, but provided a better understanding of the cellulase process. This section describes very briefly the results from these "learning" experiments and then discusses the results from the series of tests described in Section 6.1.3.

Some of the "learning" experiments were as follows:

- The initial solids concentration which was tested was 25% at a feed rate scaled down from 800 lbs/hr. This concentration was not feasible to mix. Poor mixing occurred before the 15% solids concentration mark was achieved. Therefore, the solids concentration was reduced to 15% for the experiments which are described in this report.

- The initial feed rate for the shedder was listed at 1100 lbs/hr. In the scaled down version of this feed rate, it was observed that this did not allow enough time for the cellulase to hydrolyze the substrate effectively. For this reason the feed rate was reduced to 800 lbs/hr, which after consulting the manufacturer of the shedder, is a more accurate throughput for this shredding application.

- Initial tests used 1%, 2%, and 4% cellulase concentration by total weight of the slurry. Two percent enzyme was chosen for the simulated waste tests due to the slow observed breakdown of the 1% when compared to 2% and the high cost of 4% cellulase as compared to 2% cellulase.

- A few tests were run which replaced 5% of the newsprint with 5% cotton. The cotton caused problems due to wrapping on the agitator shaft and the agitator power was extremely high. This should not be a problem in the large scale system because the size of the cotton pieces compared to the size of the agitator shaft and impeller will be small.

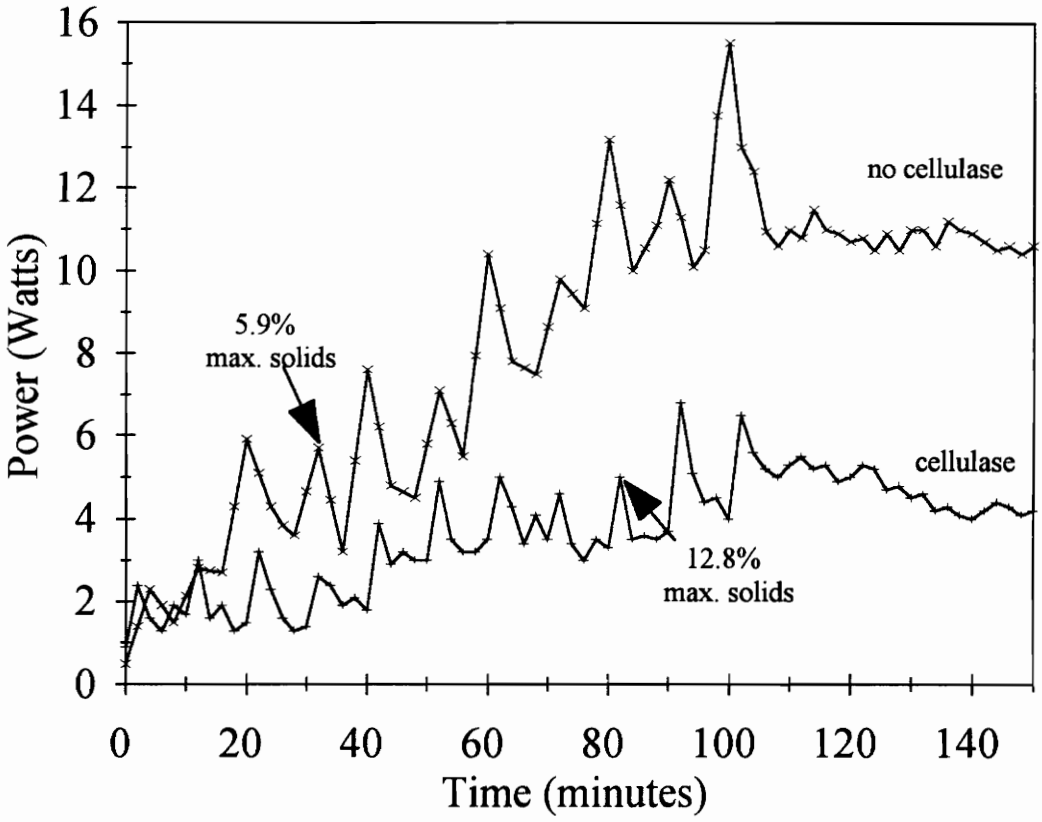

Figure 6.1 - Shaft Power Versus Time for Simulated Medical Waste with and without Cellulase.

Based upon these "learning" experiments, the 15% solids concentration, 2% enzyme tests were conducted as described in Section 6.1.3. Figure 6.1 illustrates the ensemble averaged shaft power versus time for both the enzyme and the no enzyme conditions. As previously mentioned, the experiments were run with three different commercially available cellulases. For simplicity Fig. 6.1 contains the data for the cellulase which

degraded the paper most effectively. This particular cellulase gave the lowest shaft power measurements and therefore, reduced the viscosity the most out of the three cellulases used.

The most important information from Fig. 6.1 was the maximum mixable solids concentration. For the slurry with no enzyme, the maximum solids concentration which could be agitated was only 5.9% by total weight. However, with the addition of 2% cellulase enzyme, the maximum mixable solids concentration more than doubled to 12.8% by total weight.

Each of the waste additions resulted in a power spike which can be seen in Fig. 6.1 at each 10 minute interval up to 100 minutes. The data shows a dramatic difference in agitator power between the slurry with cellulase and the slurry without cellulase. This difference was observed in the less dramatic "spiking" affect as well as the reduced final agitator power after 150 minutes for the slurry with cellulase when compared to the slurry without enzyme. These curves illustrate the viscosity reducing capabilities of cellulase enzyme in a medical waste slurry with high paper content.

In these experiments there was some problem with paper wrapping around the agitator shaft. This was attributed to the large size of the paper when compared to the size of the agitator shaft. This should not occur in the large scale reactor due to the larger size of the agitator shaft and impellers. Care was taken not to record the shaft power when a large amount of paper was wrapped on the shaft and impellers. This problem could be heard by the vibration of the beaker and agitator and was observed by the large increase in shaft power. In most cases this happened for only a few seconds and the power was recorded shortly after the problem corrected itself. As expected, this problem occurred most frequently at the beginning of each test and for the slurries containing no cellulase.

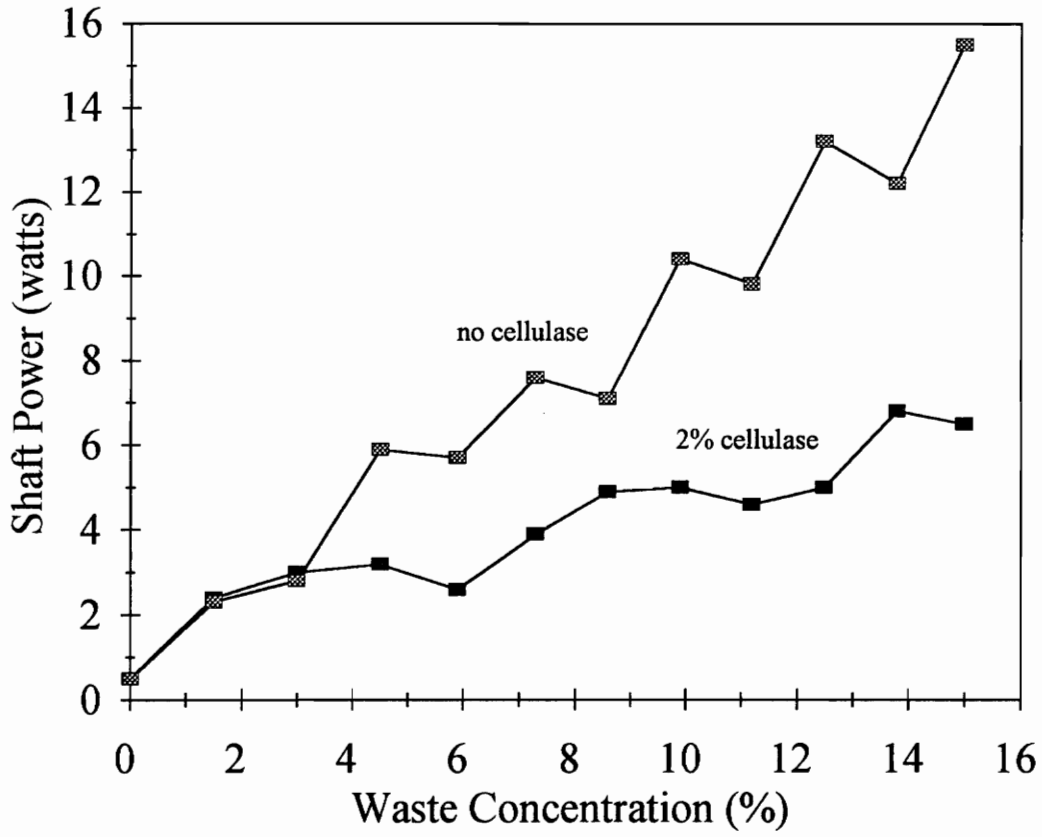

Figure 6.2 - Shaft Power Versus Waste Concentration with and without Cellulase.

Figure 6.2 illustrates the agitator shaft power versus waste concentration (by total weight) for slurries with and without cellulase. This figure resulted from plotting the power spikes after each addition versus the simulated waste concentration. The viscosity reducing value of cellulase is seen by the reduction in shaft power after the waste concentration reached 3% when compared to the no cellulase slurry.

After the 2 1/2 hour cellulase reaction time, the slurry was dewatered and the resulting waste was dried. The dry waste was weighed and the waste mass reduction was determined with the results listed in Table 6.2. The mass reduction listed was the average of three tests for both the no cellulase and cellulase slurries. It was assumed that the reduction in mass occurred solely due to the hydrolyzation of the paper and that no other

material (plastic, glass, metal, etc.) was lost through the small separating screen. This corresponds to a mass reduction of 23.4% knowing that the simulated waste sample contained 60% paper. This assumption seems to be validated by the large difference in mass reduction between the no enzyme samples and the enzyme sample.

Table 6.2 - Mass Reduction of Simulated Waste Samples.

	Initial Mass (g)	Final Mass (g)	Mass Reduction (%)
No Cellulase	311.4	307.8	1.2
Cellulase	311.4	267.6	14.1

The small reduction in mass observed in the no cellulase sample was probably a loss in paper as well. This reduction resulted from the mechanical breakdown of paper into smaller pieces from the agitation. Some of these paper pieces were reduced such that they passed through the separating screen.

The mass reduction in other papers especially absorbent types and papers produced from chemical pulps (Section 5.3.2) is expected to be much greater than that of newsprint, since newsprint is only about 50% cellulose. One might expect that the mass reduction of papers produced from chemical pulps would be twice as much as the mass reduction of newsprint. This is because papers produced from chemical pulps have twice as much cellulose as papers produced from mechanical pulps (newsprint).

From this series of tests, a better understanding of cellulase activity on medical waste in the batch reactor was developed. In summary the value of cellulase was quantified in three areas:

- 2% cellulase more than doubled the waste concentration which could be agitated.

- 2% cellulase reduced the shaft power by as much as 50% when compared to the no cellulase tests.
- The slurries with 2% cellulase had a mass reduction of 14.1% compared to a mass reduction of 1.2% for slurries without cellulase.

6.2 Influence of Cellulose Hydrolyzation on Agitator Power

Up until now in this chapter, the focus has been on processing medical waste in the batch reactor. However, in order to develop a fundamental understanding of the breakdown of paper and the resulting reduction in viscosity in the batch reactor, experimentation must be done with paper only in the test vessel. This section describes the test procedure as well as the results from the hydrolyzation of paper and the influence this breakdown has on reducing the shaft agitator power.

6.2.1 Experimental Procedure

Experiments were conducted with and without cellulase enzyme. Only one commercially available enzyme was used in order to reduce the number of test cases. This enzyme sample was chosen based on preliminary results of its viscosity reducing capabilities. This cellulase sample contains all three groups of enzymes discussed in Chapter 5 which are needed for maximum hydrolysis of cellulose. A total volume of 2 liters was used for all tests based upon the density of each component in the slurry. Newsprint concentrations of 1%, 2%, and 4% by weight were tested. When cellulase was used, the enzyme concentration was 2% by total weight of the slurry. The components and the setup in these experiments remained the same as in Section 6.1.1.

The procedure for experiments was as follows:

For tests without cellulase

1. Initially, 2 liters of water was placed in the beaker at 50°C and the agitator power was recorded at 800 rpm. This value was the power needed to agitate water only and was subtracted from the power readings taken for the slurries containing paper.

2. The proper mass of paper was weighed and volume of water was measured depending on the concentration of paper for the specific test. The density of the newsprint (1.35 g/ml) and was determined experimentally. This was done by adding a known mass of newsprint to a known volume of water. This mixture was agitated to allow all the air to leave the internal voids in the paper. The final volume of the mixture was measured and the density was determined from the mass of the paper and the volume change from the addition of the paper.

3. The agitator shaft was positioned in the beaker as described in experimental setup in Section 6.1.2 and the paper sample was distributed evenly around the shaft and impellers. The proper amount of water was added to increase the volume in the beaker to 2 liters based upon the density of paper and was allowed to sit for 30 seconds.

4. The mixing was begun and the first power reading was taken after 10 seconds which allowed the mixer to reach the 800 rpm speed. Temperature was kept constant at 50°C and the pH was not monitored.

5. Power was recorded every 10 seconds for the first two minutes and then every minute up to the 10 minute mark. After 10 minutes readings were taken every 2

minutes up to the 20 minute mark and then every 5 minutes thereafter. The experiment was concluded after the agitator power reached a minimum.

6. The slurry was separated through a 15 wire per inch screen and the sample was dried at 50°C and weighed. The apparent mass reduction was calculated from these results.

7. Each test was repeated three times and the three power readings at each sample time were averaged and recorded.

For tests with cellulase

1. The proper amount of paper, water, and enzyme was weighed depending on the concentration of paper for the specific test. The specific gravity of the enzyme was 1.1.

2. The agitator shaft was positioned in the beaker as described in Section 6.1.1 and the paper sample was distributed evenly around the shaft and impellers.

3. The water at 50°C and enzyme were mixed together in a separate beaker and then enough glacial acetic acid was added to lower the pH to 4.0. (This mixing cannot be done in the test beaker because due to the absorption of the paper, the enzyme and acid will not be mixed uniformly at the beginning of the test, especially with higher paper concentrations.)

4. The water/enzyme solution was poured into the test beaker and allowed to soak for 30 seconds. Mixing then began at 800 rpm and the first power reading was taken after 10 seconds. Power readings were taken at the same time intervals listed in Step 5 of the no cellulase procedure. The pH increased to 4.3 or higher due to the basic nature of the paper. Additional acid was added to lower the pH to 4.3 if the pH rose above 4.3.

5. Steps 5, 6, and 7 for the no cellulase case were followed.

6.2.2 Paper Breakdown Results

This section discusses the results in two areas of the newsprint hydrolysis tests:

- cellulase activity's influence on agitator power.
- mass reduction due to cellulase activity.

In a paper/water slurry which is subjected to agitation, the power as well as the apparent viscosity will reduce over time with or without cellulase. Without cellulase the agitator power will reduce from the mechanical shearing of the paper as well as the breaking of hydrogen bonds which were formed when the paper was made. With cellulase the agitator power will be reduced further due to the breakdown of cellulose by cellulase into reduced sugars. The results from the agitation experiments illustrate all of these mechanisms of power reduction. The 1%, 2%, and 4% paper concentration tests show the power reduction due mechanical breakdown for the no cellulase tests and the cellulase tests exhibit the further reduction in agitator power from $\beta(1\text{-}4)$ bonds being cleaved by cellulase enzyme.

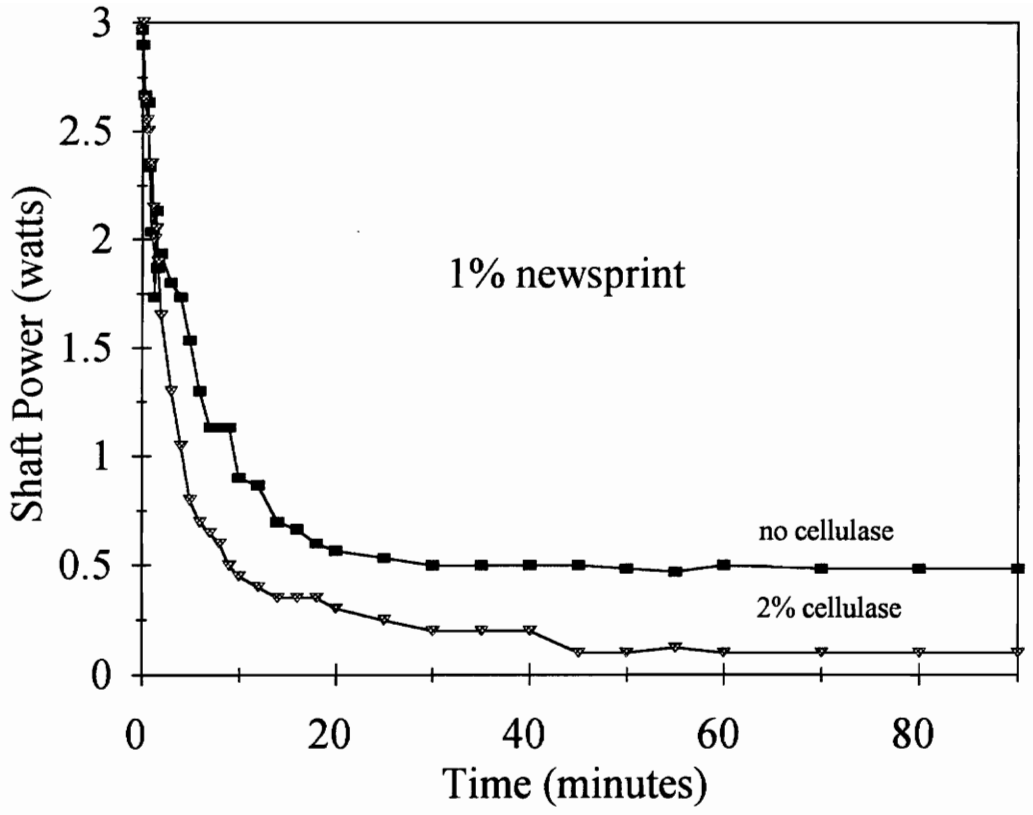

Figure 6.3 - Shaft power versus time for 1% newsprint with and without cellulase.

Figure 6.3 illustrates the reduction in agitator shaft power (ensemble averaged) over time for a slurry containing 1% newsprint with and without cellulase. For both sets of data the initial power was approximately the same at 3 watts which was expected since no enzymatic or mechanical breakdown had occurred at time zero. Initially, for the no cellulase tests, there was a large variation in the agitator power due largely to the nonuniformity of the paper size and small amounts of paper wrapping around the agitator shaft. This was not as much of a problem in the tests with cellulase because the activity of the enzymes quickly begin to breakdown the paper yielding a more uniform slurry.

As time proceeded further, the enhanced power reducing capabilities of cellulase enzyme was observed by the increased rate of breakdown of paper as well as the lower final

power required to agitate the slurry when compared to the no cellulase tests. The minimum power of 0.6 watts for the no cellulase case was reached after 30 minutes. Where as with the addition of 2% cellulase, 0.6 watts was reached after only 9 minutes. Also, the minimum power required to agitate the slurry was reduced from 0.6 watts to 0.1 watts with the addition of cellulase.

Figures 6.4 and 6.5 illustrate the ensembled averaged shaft power versus time with and without cellulase for 2% and 4% paper concentration, respectively. The results from these tests exhibit similar trends to Fig. 6.3 and provide additional support for the use of cellulase to reduce the viscosity of paper slurries.

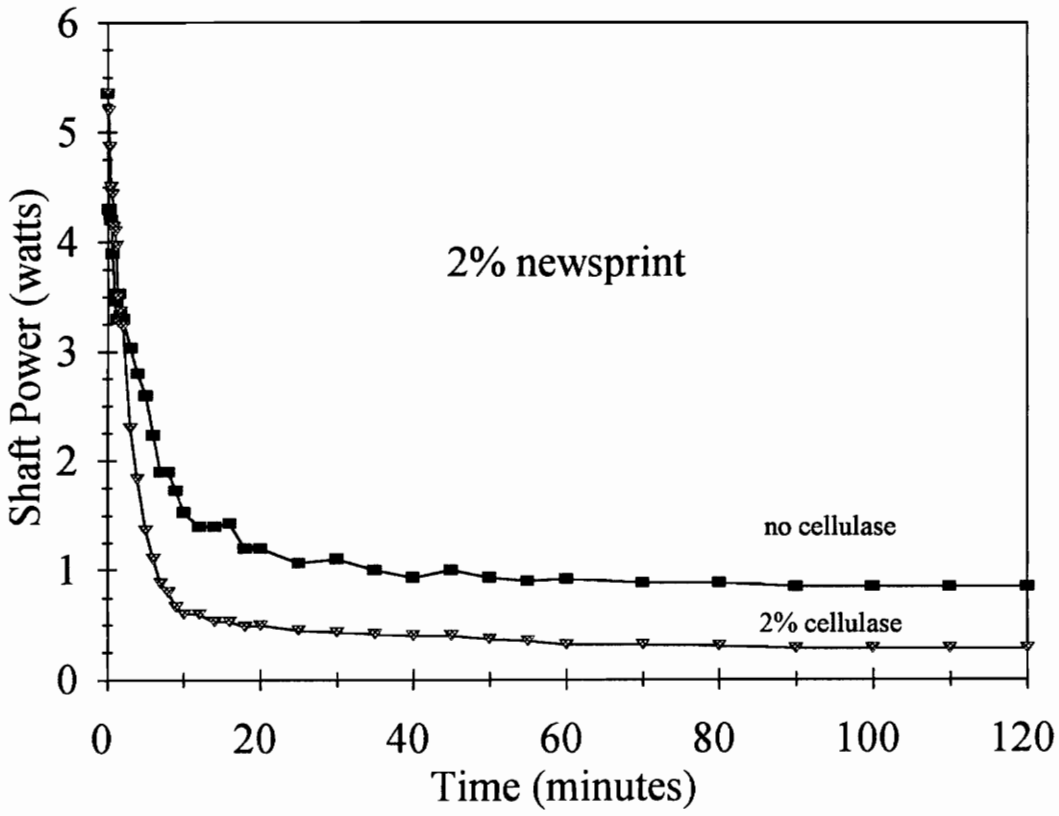

Figure 6.4 - Shaft power versus time for 2% newsprint with and without cellulase.

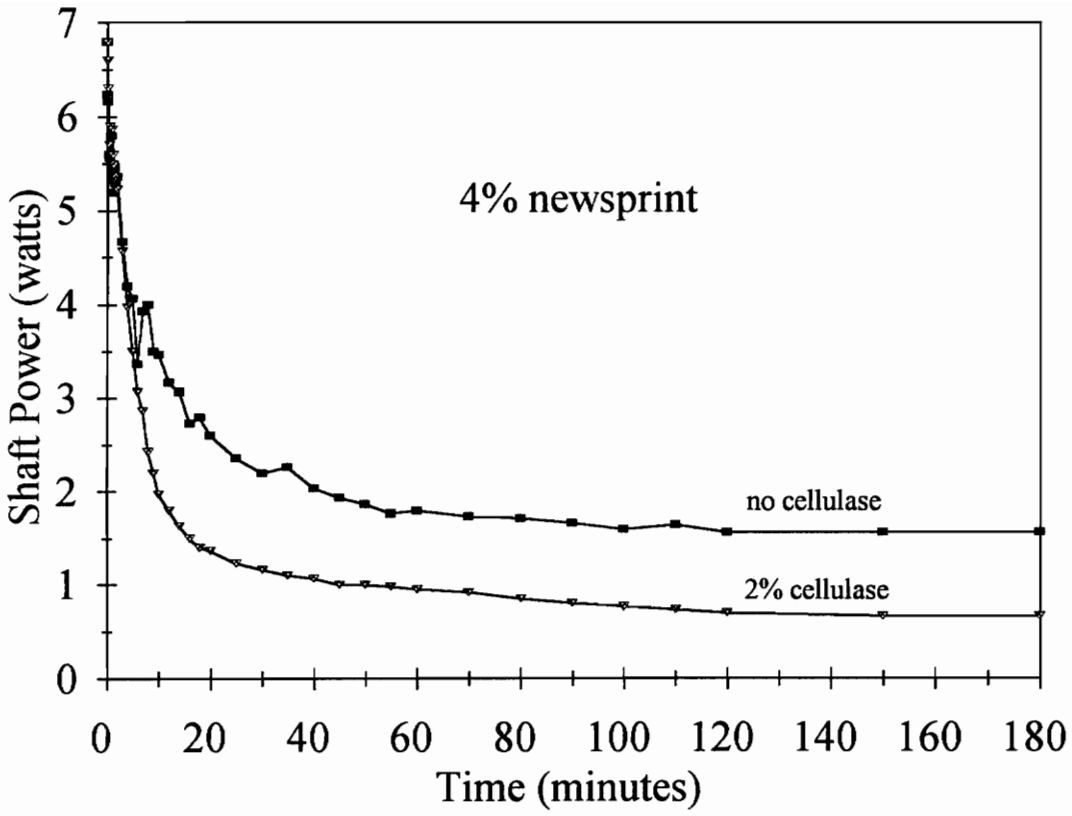

Figure 6.5 - Shaft power versus time for 4% newsprint with and without cellulase.

Table 6.3 - Mass reduction of paper samples.

	Initial Mass (g)	Final Mass (g)	Mass Reduction (%)
No Cellulase			
1% paper	19.8	16.1	18.2
2% paper	39.7	35.2	11.3
4% paper	79.9	76.6	4.1
Cellulase			
1% paper	19.8	0.0	100.0
2% paper	39.7	3.9	90.2
4% paper	79.9	20.4	74.5

The mass reduction of the paper was also measured to determine the degree of breakdown of the paper samples. The mass reduction results are listed in Table 6.3. It was apparent from the data that the addition of cellulase enhanced the degradation of paper. In the no cellulase tests, some paper was lost due to mechanical breakdown from agitation. This loss required that some of the particles be mechanically sheared small enough to pass through the 15 wire per inch screen. With the addition of cellulase, the mass reduction increased dramatically. For the 1% paper with cellulase tests, the slurry passed through the screen during separation without leaving any "cake". This does not mean that all of the paper was hydrolyzed to glucose, but that the paper was degraded to the degree that all of the newsprint mainly glucose, cellulose, hemicellulose, and lignin passed through the holes in the screen. This slurry after hydrolysis had the appearance of dirty water.

The 2% and 4% paper with cellulase samples also experienced increased mass reduction when compared to their identical no cellulase cases. Theoretically, if the 2% and 4% samples were allowed to hydrolyze for a longer period of time, these slurries would exhibit 100% reduction in mass as well. However, the tests were stopped when the agitator power reached a minimum.

Now, the mass reduction from the simulated waste experiments and the mass reduction from the newsprint experiments can be compared. The mass reduction in paper for the simulated waste experiments was 23.4% compared to the mass reduction of 74.5% for a slurry containing 4% newsprint. This large difference can be explained for two reasons. First, in the simulated waste experiments the newsprint concentration in the slurry was 9%. This higher concentration would take longer to hydrolyze completely when compared to the 4% newsprint test and therefore, more time was needed to achieve maximum cellulose degradation. Second, the pieces of plastic, glass, and metal in the simulated waste act as a filter to trap some of the paper particles which were small enough to pass through the screen from doing so. Thus, the apparent mass reduction was lowered.

From this series of tests, a better understanding of the degradation of newsprint by cellulase activity was developed in two areas: cellulase activity's influence on agitator power and the loss of mass due to cellulase activity. In summary, with the addition of 2% cellulase the shaft power was greatly reduced in all paper concentrations (1%, 2%, and 4%). This was most noticeable in the minimum power needed to agitate the slurry where in all tests the minimum power was reduced by at least 50% with the addition of cellulase. The loss of mass due to cellulase activity ranged from 74.5% for 4% newsprint to 100% for 1% newsprint. This data reinforces the capability of cellulase to breakdown paper to a reduced form.

7

Cellulose Hydrolysis Model

The cellulose degradation experiments displayed the phenomena of the breakdown of paper due mechanical agitation and cellulase activity by reduction in agitator power. Now, from these data a fundamental understanding of the breakdown could be developed through modeling the power results. The power results were modeled by looking at the different components which make-up paper and each components influence on shaft agitator power. The shaft power associated with two of these components was best fit with an equation of exponential form. Therefore, the total agitator power at any instant in time could be predicted by summing each component's influence on agitator power. In order to fully understand this hydrolysis model, the following topics will be covered:

- Theory of power to agitate the various components of paper
- Procedure and method for determining coefficients and time constants
- Model Results

7.1 Model Theory

In order to understand the breakdown of paper and its influence on agitator power, the different components within paper which can cause an increase in viscosity were analyzed. It was determined from the data that three components within paper influence the slurry viscosity. These three components were:

- The cellulose and non-cellulose mass held together by hydrogen bonds.
- The cellulose fibers held together by $\beta(1\text{-}4)$ bonds.
- The non-cellulose components of paper (hemicellulose, lignin, etc.)

It was assumed that the three components had an additive (linear) relationship. Each of these components has a shaft power associated with it when being mixed in a slurry. The power associated with each component was defined as followed:

- $\mathbf{P_h}$ = The power to agitate the cellulose and non-cellulose mass held together by hydrogen bonds.
- $\mathbf{P_b}$ = The power to agitate the cellulose fibers held together by β(1-4) bonds.
- $\mathbf{P_n}$ = The power to agitate the non-cellulose components of the paper

As discussed in Chapter 5, the pulp which make-up paper is held together by hydrogen bonds. These bonds were formed as the water was evaporated from the sheet during papermaking. When paper is reintroduced into a water environment, many processes occur. The most significant of which is the breaking of these hydrogen bonds by the absorption of water into the structure of paper. This phenomena is enhanced by the mechanical agitation provided by the mixer. As the number of bonds reduce, the paper structure weakens and deteriorates with time. This process can be observed by the reduction in agitator power, P_h , as a function of time and can be observed in both the cellulase and the no cellulase experiments.

In the presence of cellulase, the structure of paper is deteriorated even further. The cellulase attacks the cellulose fibers, reducing these chains to smaller and smaller lengths. There is a certain agitator power, P_b , needed to mix these long strands of cellulose initially and this power reduces with time as the cellulose fibers are hydrolyzed further and further to their raw form (glucose). One would expect that if a certain type of paper contained longer cellulose fibers and/or a higher concentration of cellulose, the power, P_b, needed to agitate this component would be greater than the P_b for other paper types containing shorter cellulose fibers and/or a lower concentration of cellulose.

The last component which is present in the paper is the non-cellulose component. This component contains mostly lignin and hemicellulose. This material contributes a constant power, P_n , required to agitate it because it does not breakdown in the batch reactor whether cellulase is present or not. After the paper has been degraded by the water and mechanical agitation and after the reaction of cellulase hydrolyzing the cellulose has reached equilibrium, the power required to agitate the slurry is due solely to the non-cellulose components and the water.

Based upon this theory of power contributions, from each individual component, the sum of these components yields the shaft power at any instant in time:

$$P_{total} = P_h + P_b + P_n \tag{7.1}$$

For the no cellulase tests, the only component in equation 7.1 which degrades with time is P_h. This is because there is no cellulase present to reduces the power associated with the cellulose fibers which are formed by the β(1-4) bonds. P_h has an exponential degradation associated with it and this power approaches zero with time. With no cellulase in the slurry, the minimum power which is achieved is actually $P_b + P_n$ and in order to determine each of these values a test with cellulase needs to be conducted as well. Therefore, the no cellulase model has the form:

$$P_{total}(\text{no cellulase}) = P_h e^{-\frac{t}{\tau_h}} + P_b + P_n \tag{7.2}$$

where τ_h is the time constant for the breakdown due to mechanical agitation and the reduction of hydrogen bonds in paper.

For the tests with the cellulase, the power, P_h , is kept the same as in equation 7.2 and the power to mix the cellulose strands exhibits an exponential decay as well. Therefore, the P_b contribution to total power is fit with an exponential term resulting in the following power equation for slurries with cellulase:

$$P_{total}(\text{cellulase}) = P_h e^{-\frac{t}{\tau_h}} + P_b e^{-\frac{t}{\tau_b}} + P_n \tag{7.3}$$

where τ_b is the time constant for the reduction of β(1-4) bonds.

Each of these power coefficients as well as the time constants needed to be determined from the experimental data. One would expect that each of the power coefficients increase with paper concentration reaching some limit once the slurry becomes to viscous to agitate. The time constant, τ_h , was also expected to increase with concentration, since it would take longer for the increased mass of paper with more hydrogen bonds to be degraded. The time constant, τ_b, was also expected to increase if the enzyme concentration was kept constant and the paper concentration was increased for the similar reason of a higher β(1-4) bond to enzyme ratio than for lower paper concentration. Therefore, all coefficients and time constants in this model should increase with paper concentration given that the same paper type is used.

7.2 Method for Determining Coefficients and Time Constants

Based upon the theory of the model described, a method for determining these coefficients and time constants from the data was developed. The method entailed determining each of the power coefficients from the data and then fitting the exponential form of the data by choosing values for each time constant until the data and the curve closely matched. P_h, P_b, and P_n could be determined from the power at time equal zero and as time approached infinity. This required a lot of trial and error to determine the τ_h which most closely matched both the cellulase and no cellulase data for each paper concentration. Once τ_h was set then τ_b could be determined. This method of "eyeballing" the time constant values was the only effective method due to the large degree of noise in the data from the initial non-uniformities (large paper pieces compared to impeller diameter) in the slurry.

In order to systematically determine each of the coefficients and time constants the following procedure was followed for each paper concentration:

1. $P_{\max} = P_{total} = P_h + P_b + P_n$ at $t = 0$. This is the ensembled average including both the cellulase and no cellulase case.

2. $P_h = (P_{total}$ at $t = 0) - (P_{total}$ (no cellulase) as $t \rightarrow \infty)$.

3. $P_b = (P_{total}$ (no cellulase) as $t \rightarrow \infty) - (P_{total}$(cellulase) as $t \rightarrow \infty)$. This is the reduced power achieved at the end of the no cellulase tests.

4. $P_n = P_{total}$(cellulase) as $t \rightarrow \infty$. This is the reduced power which was achieved at the end of the cellulase tests.

5. τ_h is determined by solving equation (7.2) for τ_h

$$\tau_h = \frac{-t}{\ln\left(\frac{(P_{total}(\text{no cellulase}) \textit{ for } t) - P_n - P_b}{P_h}\right)} \tag{7.4}$$

6. τ_b is determined by solving equation (7.3) for τ_b

$$\tau_b = \frac{-t}{\ln\left(\frac{(P_{total}(\text{cellulase}) \textit{ for } t) - P_n - P_h e^{-\frac{t}{\tau_h}}}{P_b}\right)} \tag{7.5}$$

7. After Steps 5 and 6 were followed, it was determined that the "eyeballing" method previously described for chosing the time constants provided a better curve fit for both the cellulase and no cellulase data. Therefore, the time constants τ_h and τ_b were actually determined from curve fitting the two sets of data as described in Steps 8 and 9.

8. Chose values of τ_h until the model fits the data closely for the no cellulase tests. (This value of τ_h should also closely match the data for the cellulase tests with the exception that the power levels off at a higher value because the exponential decay of P_b has not been added to the no cellulase power model.)

9. Chose values of τ_b until the data for the cellulase tests is closely fit by the cellulase power model.

10. Repeat this procedure for each value of paper concentration and then plot the power coefficients versus concentration to determine if the coefficient/concentration trends which were hypothesized in Section 6.1 were followed. Plot the time constants versus paper concentration in order to determine any trends which might exist for the time constants.

One might suggest that a more complicated model might exist which separates the power contribution into more than three components. However, due to the noise in the data, it was determined that separating the power contribution into more components would not yield a more accurate model. By using this simple procedure which incorporated only three power contributions, the agitator power can be approximated for all values of time.

7.3 Model Results

The procedure in Section 7.2 was followed to determine the various power coefficients and time constants. This section discusses these coefficients and time constants and tries to explain the relation these constants have with paper concentration. These constants are discussed in the following order:

- coefficients and constants for no cellulase curves
- coefficients and constants for cellulase curves
- coefficients and constants versus paper concentration

The coefficients for the no cellulase case were developed initially. This no cellulase case was described in the model theory and had the form:

$$P_{total}(\text{no cellulase}) = P_h e^{-\frac{t}{\tau_h}} + P_b + P_n \qquad (7.2)$$

The sum of the constants P_b and P_n give the minimum power needed to agitate the slurry without cellulase activity. The power coefficients and the mechanical

breakdown/hydrogen bond time constant τ_h for the three paper concentrations are shown in Table 7.1.

Table 7.1 - Power Coefficients and Constants for Various Paper Concentration.

Paper Conc. (%)	P_h (watts)	P_b (watts)	P_n (watts)	τ_h (minutes)	τ_b (minutes)
1	2.48	0.38	0.10	4.0	2
2	4.55	0.57	0.28	4.5	2
4	5.23	0.90	0.67	12.0	2

Figure 7.1 illustrates equation 7.2 with the appropriate coefficients and constants from Table 7.1. Figure 7.1 shows the predicted shaft power versus time for the various paper concentrations.

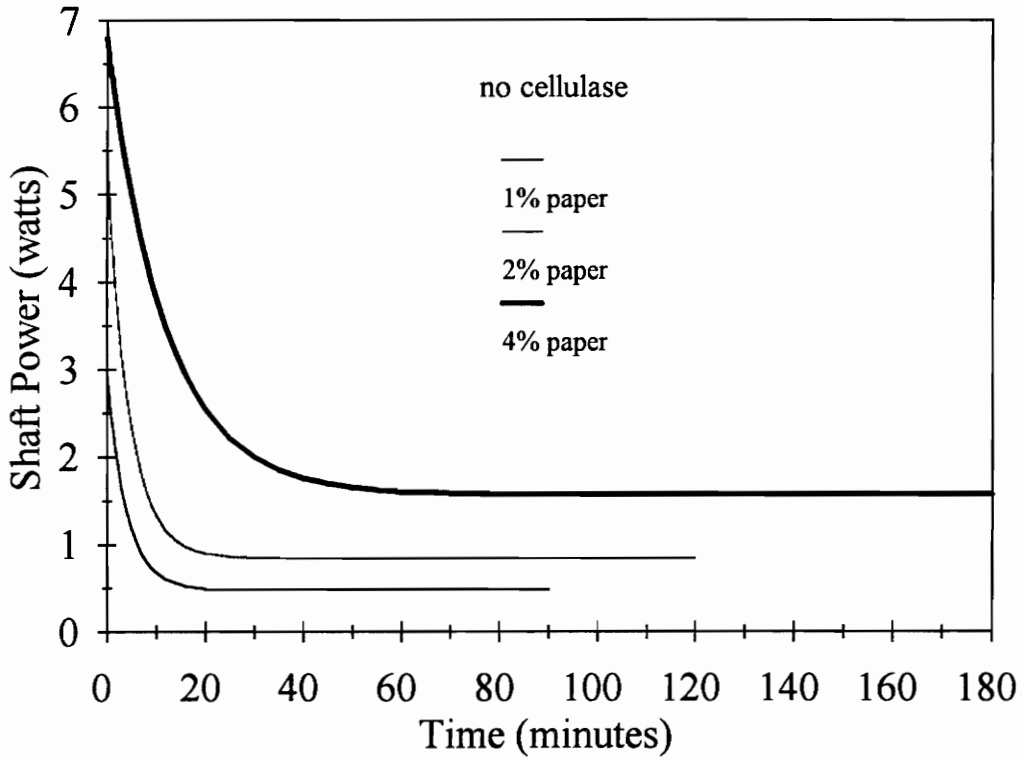

Figure 7.1 - Power Reduction over Time Due to Mechanical Agitation.

For the 2% cellulase case, the model fit an exponential term to the power to agitate the long cellulose fibers, P_b. This form of the model was also discussed in Section 7.1 and had the form:

$$P_{total}(\text{cellulase}) = P_h e^{-\frac{t}{\tau_h}} + P_b e^{-\frac{t}{\tau_b}} + P_n \qquad (7.3)$$

This form of the model utilized the same values listed in Table 7.1 and included an additional time constant τ_b associated with the power needed to agitate the unhydrolyzed cellulose strands. This time constant was evaluated to be a constant (τ_b= 2 minutes) for all paper concentrations constant.

Figure 7.2 illustrates equation 7.3 with the appropriate coefficients and constants from Table 7.1 and the additional exponential term. Figure 7.2 shows the predicted shaft power versus time for the various paper concentrations with the addition of 2% cellulase.

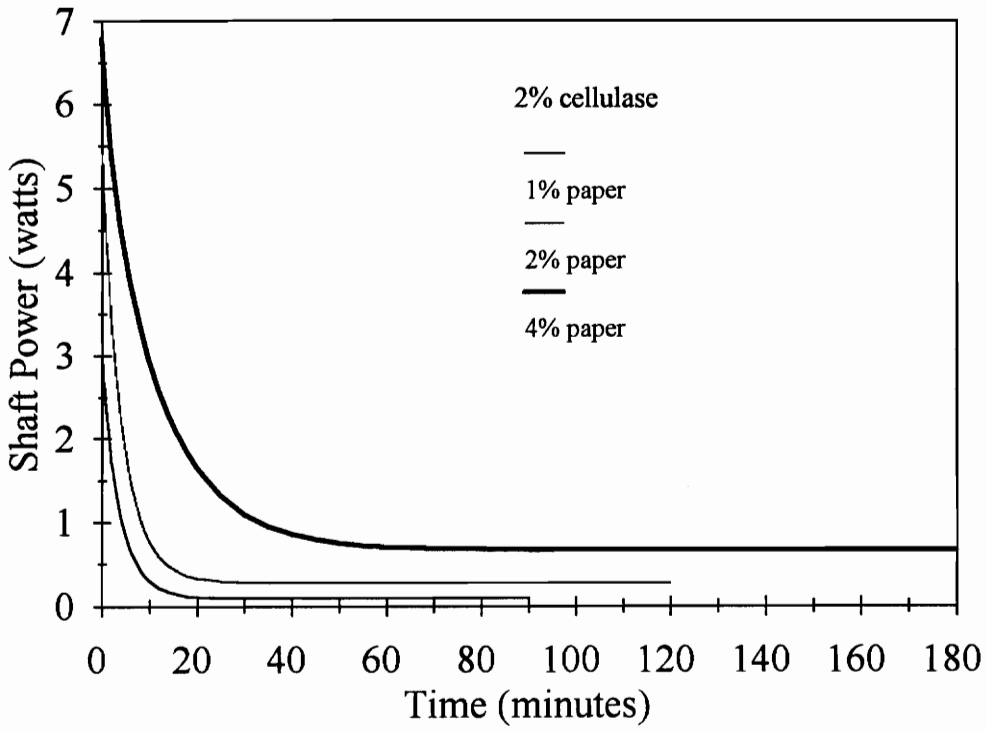

Figure 7.2 - Power Reduction over Time Due to Mechanical Agitation and Cellulase Activity.

Now that the curves which predict the shaft power have been presented, the trends in paper concentration can be discussed. Figure 7.3 illustrates the power and time constants relationship with paper concentration except for the time constant τ_b which was constant in concentration.

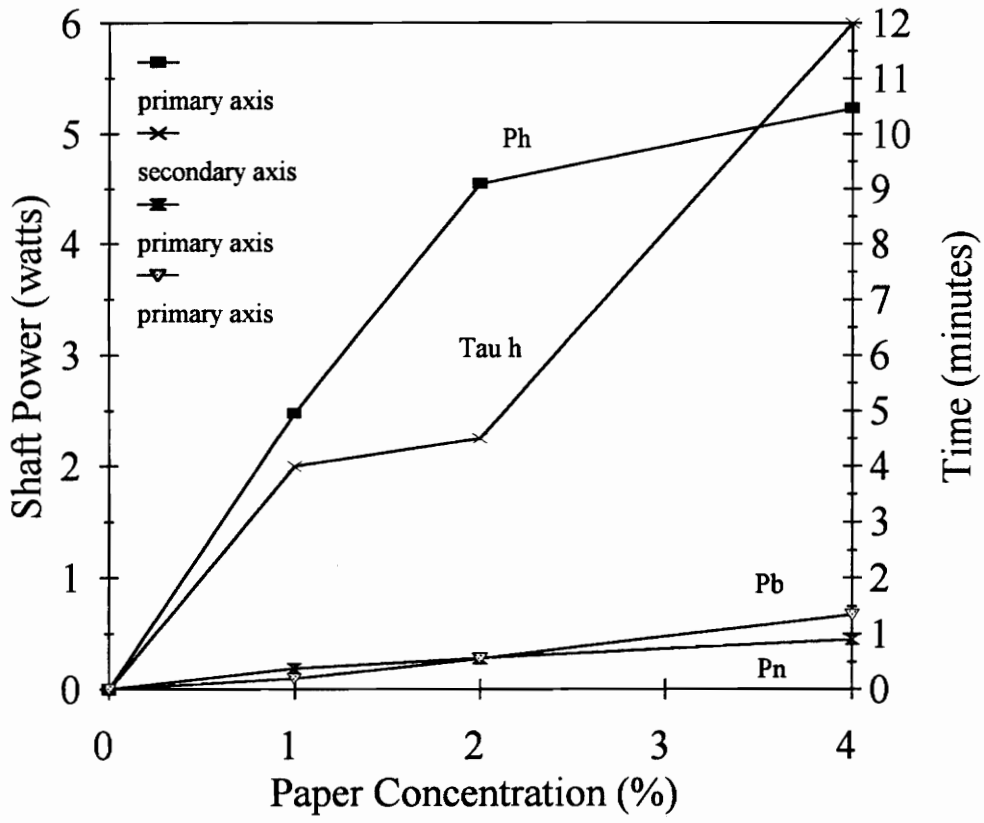

Figure 7.3 - Coefficients and Constants Relationship with Paper Concentration.

P_n and P_b are fairly linear in concentration. However, P_h begins to level and reach a maximum as the paper concentration increases. This could be due to the high viscosity of the 4% solution initially before any breakdown occurred and could indicate that P_h for higher paper concentrations approaches some maximum. This maximum could possibly be due to the impeller generating a low-solids area around the impeller at high concentrations.

The relationship between the time constants τ_h and τ_b is not as easily understood as the power coefficients. τ_h increases with concentration; this is the only trend that is certain. In order to determine if this relationship is first or second order, a greater range of paper concentrations need to be tested. τ_b is constant with concentration. This could possibly be due to the concentration of enzyme used. Two percent cellulase by total weight of the slurry is a large dose of enzyme. In commercial applications cellulase concentrations rarely exceed 2% by weight of the substrate (paper). Therefore, one hypothesis could be that there is not enough cellulose present in the slurry to utilize this high dose of enzyme and for this reason τ_b is constant for these high enzyme to substrate ratios. Once the paper concentration reaches the limit where all of the enzyme is being used at the surface of the paper, τ_b should begin to increase. In other words the cellulase process is not agitator limited (τ_b) while the mechanical breakdown is agitator limited (τ_h).

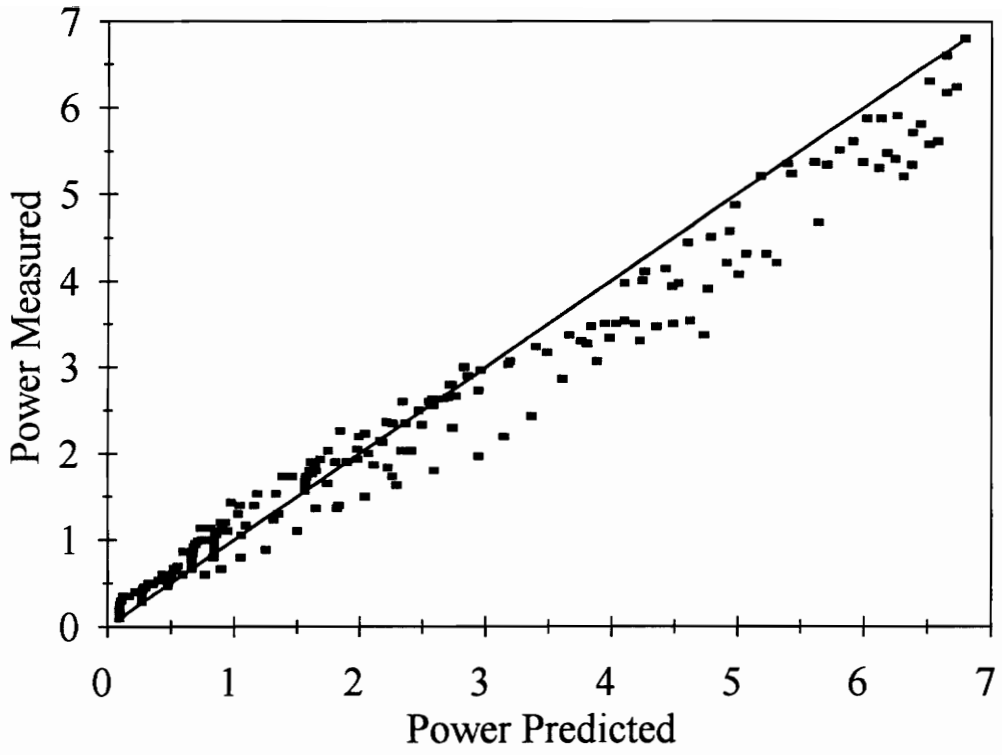

Figure 7.4 - Model Comparison with Experimental.

Figure 7.4 compares the model with the actual data by plotting the measured power versus the predicted power for both the cellulase and no cellulase data. A line with a slope of 1 is plotted to show how closely the model predicts the actual data. From Fig. 7.4 one can see that the model predicts the shaft power most accurately for values of shaft power less than 3 watts. For values greater than 3 watts the model yields values greater than actually were measured.

8

Cellulose Breakdown Conclusions

The addition of cellulase into a slurry containing cellulose-derived material greatly enhances the breakdown of the waste. This was demonstrated by the increase in maximum solids concentration in the simulated medical waste experiments and by the reduction in agitator power in the newsprint experiments. The following sections will discuss the conclusions drawn on the following topics:

- Simulated waste experiments
- Newsprint experiments

8.1 Simulated Waste Experiments

The medical waste experiments were conducted primarily to simulate the actual degradation process which will occur in the large scale bioremediation system and to determine the maximum solids concentration which could be agitated. However, from these experiments data were gathered which helped quantify the added value of cellulase enzyme in the bioremediation process. This value was seen by the increase in agitatable solids concentration and the reduction in agitator shaft power with the addition of cellulase. These conclusions are discussed as well as the future simulated waste tests which need to be conducted in the large scale system and in the small scale experiments.

A few distinct conclusions can be made concerning the addition of cellulase to medical waste samples containing high amounts of paper.

- The addition of 2% cellulase more than doubles the solids concentration which is able to be processed in one batch.
- The cellulase reduces the viscosity of the slurry, thus, reducing the work load of the agitator which is reflected by lower shaft power at

each waste concentration and by a reduced spiking affect at each waste addition.

- The cellulase accelerates the natural breakdown of cellulose. This results in a large mass reduction when compared to waste treated with no cellulase

Aside from these conclusions, there are many areas of future work which need to be explored to develop a better understanding of this hydrolysis process in medical waste. First and foremost is the comparison of this test to the large-scale system. Similar results in the large scale tank are essential in proving the cost and environmental benefits of this bioremediation technology.

Small-scale tests should also be continued. It is impossible to list the number of tests and different combinations of these tests which could be conducted, but here are a few which need further study.

- Test other commercially available enzymes. Hemicellulase enzymes are available from various companies. A mixture of hemicellulase and cellulase might degrade the paper even further. There are also some lignase enzymes being developed. These could be of further assistance.

- Test waste samples with various types of paper. Cellulase degrades types of paper differently as explained in Chapter 5. Medical waste does not only contain newsprint type paper and therefore more paper types need to be included in the simulated waste samples.

- Test waste samples containing various paper concentrations. Medical waste contains on the <u>average</u> 60% paper by weight. This will not always be the case.

- Test the concentration of glucose in the effluent. The product of cellulose breakdown by cellulase is glucose. The concentration of glucose in the effluent should be determined and considered as a renewable resource.

- These cellulase enzymes stay active for as long as 48 hours under the 50°C and 4.3 pH conditions and are expensive. Recycling of these enzymes needs to be investigated.

8.2 Newsprint Experiments

The newsprint experiments were conducted primarily to determine the viscosity reducing capabilities of cellulase by monitoring the agitator power. However, mass reduction of paper was determined to quantify the degree of breakdown of the paper. Also, models from the data needed to be developed to better understand the hydrolysis of cellulose. This section states the conclusions from this work as well as future work which needs to be conducted in the large-scale system and in small-scale experiments.

A few distinct conclusions can be made concerning the breakdown of cellulose in newsprint due to mechanical agitation and cellulase activity.

- Agitator power reduces over time without cellulase due to the shearing of paper from the agitation. The power also reduces due to the cleavage of hydrogen bonds from the reintroduction of water.

- The agitator power rate of reduction is increased and the final power to agitate the slurry is reduced significantly due to the activity of cellulase.

- This breakdown phenomena can be modeled simply by the addition of three contributions to power: P_h, the power needed to agitate the cellulose and non-cellulose material held together by hydrogen bonds, P_b, the power needed to agitate the cellulose fibers linked together by β(1-4) bonds, and P_n, the power needed to agitate the non-cellulose material in the paper.

- Cellulase addition is an effective method in reducing the paper to its simpler form. This is seen in the mass reduction results as well as the power reduction results.

This research has provided a better understanding of the breakdown of cellulose-derived materials although there is still much research which needs to be done. On the large-scale system, similar experiments should be conducted to determine if the cellulose hydrolysis/power model described is valid in a scaled-up version of the test beaker. The power constants will increase, but one could hypothesize that the time constants will remain the same. These models will allow the prediction of agitator power in larger or smaller systems and aid in determining the specifications of the agitator for each new system.

On a small-scale, several series of tests should be performed. Most of these tests are identical to the tests described for the simulated waste experiments.

- Test a wider range of paper concentrations. This would yield a better understanding of the power component time constants dependence on paper concentration.

- Test other commercially available enzymes. Hemicellulase enzymes are available from various companies. A mixture of hemicellulase and cellulase might degrade the paper even further. There are also some lignase enzymes being developed An enzyme mixture of all three of these enzyme types would in theory reduce P_n to zero.

- Test a variety of different paper types. This would yield a series of curves to predict agitator power for all paper types.

- Test glucose concentration. This would help quantify the hydrolysis of the cellulose to reduced sugars for each paper type and enzyme type.

- Compare breakdown results with solutions of known viscosity to determine the apparent viscosity of the cellulose slurries.

9

Review and Summary

The work described in the preceding eight chapters focused on the two mechanisms of enzyme diffusion and cellulose breakdown within the tank of the bioremediation process. Little has been said within this report to tie this research together with the whole bioremediation project. This chapter will describe to the reader how to use this information to benefit the project for licensing of the system and new designs for future systems. It will also restate most of the conclusions drawn in Chapters 4 and 8. These topics will be discussed in the following manner:

1. Summary of Diffusion Conclusions

2. Guidelines for Determining Disinfection of Crevices

3. Summary of Cellulose Breakdown Conclusions

9.1 Enzyme Diffusion Review and Summary

Once again, the one-dimensional and re-entrant crevice diffusion work can only serve as an initial guideline to determine disinfection time once various parameters on the entire system have been set. Due to the uncertainty of these various parameters such as protease enzyme concentration, batch time, pathogen kill time, etc., actual conclusions regarding complete disinfection cannot be drawn to date. This uncertainty does not allow for quantitative values to be placed on the time to reach a 10^6 per ml reduction in pathogens. However, this research can be used to determine approximate disinfection times once the various parameters for the bioremediation process have been determined.

Based on the one-dimensional diffusion only models detailed in Chapter 2 of this paper, the following conclusions concerning the disinfection of a 1.27 cm open-ended crevice were made:

1. During the protease treatment time tentatively ranging from 1 to 3 hours, the entire one-dimensional crevice will not be disinfected entirely. However, substantial numbers of enzymes should be present within the initial segment of the crevice (the first 0.2 cm section of the crevice) depending on the slurry protease concentration.

2. Based upon the tentative protease concentration of 1% and a hypothetical ambient temperature of 35° C, the entire crevice will be disinfected in less than a day after protease treatment. For a batch time of 1 hour, disinfection will occur in 1 day after treatment; for a batch time of 3 hours disinfection will occur in approximately 14 hours after treatment.

3. These approximate disinfection times were given based upon tentative process parameters. However, these approximate times given as examples are conservative estimates and actual disinfection of the crevices should be completed sooner than indicated in conclusion 2 for several reasons:

    - Possible enhancement of enzyme penetration due to capillary action or convection.

    - Faster kill times due the integral effect of enzyme concentrations lower than 0.1%. In other words more microbe disinfection data needs to be taken at lower concentrations and then the log reduction of "bugs" can be integrated with respect to time to determine these more accurate disinfection times.

- Some lab tests have shown that the cellulase enzyme used in the initial stage of the process has some effect on bacteria inoculation. These results have not been considered.

- Temperature of 50°C inoculates some strains of virus and bacteria; this temperature conducts through the needle wall.

As previously mentioned, re-entrant crevices will also be present in the infectious waste stream. Re-entrant models were developed based on an exact solution and finite difference solutions. The transient, dimensionless concentration of enzyme at either the outer radius or the far corner was determined for each shape. Unfortunately, not enough information was known to predict disinfection times for such objects for reasons previously discussed. However, these models should be able to be used to predict disinfection times for most re-entrant geometries once the various process parameters have been set. Along with this information, additional conclusions were drawn in reference to the rectangular - sector comparison. The conclusions were as followed:

1. The sector-shaped crevice was used to approximate diffusion times or solute concentration in rectangular shapes with an error which ranged from zero to 20 percent.

2. The comparison was exact for crevices with openings equivalent to the width of the rectangle. This case was also equivalent to the one-dimensional case.

3. The error increased as the crevice opening approached zero and the width dimension was kept constant. This case was equivalent to a dimensionless volume of infinity. This error will serve as a factor of safety when disinfection times are estimated for these types of crevices.

9.2 Guidelines for Determining Disinfection of Crevices

Most of the ground work for determining crevice penetration and disinfection has been discussed. Using the information discussed in Part I of this report, disinfection times for a one-dimensional crevice and the re-entrant crevices described should be relatively easy to determine. However, what if a re-entrant crevice shape other than a sector or rectangle is discovered in the waste stream. How can the disinfection time of this new re-entrant geometry be approximated? The following steps can be used to determine approximate disinfection time for the new crevice:

1. Measure the opening area *Ao* of the crevice.

2. Determine the point within the crevice which is furthest away from the crevice opening and measure this dimension. This distance will be the characteristic length of the new crevice.

3. Determine the volume of the crevice and calculate the dimensionless volume *Vo*.

4. Now use *Vo* from Step 3 to determine enzyme penetration using the appropriate sector crevice diffusion curve.

5. Determine disinfection time based on updated pathogen inoculation data.

Remember this is only an approximation. However, as long as the parameters such as the volume, the crevice opening area, and the characteristic length of the new crevice are measured carefully, the sector crevice with the same parameters should again give a conservative estimate for penetration times and therefore, provide an additional factor of safety for the inoculation of this particular crevice.

9.3 Summary of Cellulose Breakdown Conclusions

The addition of cellulase into a slurry containing cellulose-derived material greatly enhances the breakdown of the waste. This was demonstrated by the increase in maximum solids concentration in the simulated medical waste experiments and by the reduction in agitator power in the newsprint experiments. Once again, the conclusions from the medical waste experiments as well as the newsprint experiments are restated in the following paragraphs.

The medical waste experiments were conducted primarily to simulate the actual degradation process which will occur in the large scale bioremediation system and to determine the maximum solids concentration which could be agitated. However, from these experiments data were gathered which helped quantify the added value of cellulase enzyme in the bioremediation process. This value was seen by the increase in agitatable solids concentration and the reduction in agitator shaft power with the addition of cellulase.

A few distinct conclusions can be made concerning the addition of cellulase to medical waste samples containing high amounts of paper.

- The addition of 2% cellulase more than doubles the solids concentration which is able to be processed in one batch.
- The cellulase reduces the viscosity of the slurry, thus, reducing the work load of the agitator which is reflected by lower shaft power at each waste concentration and by a reduced spiking affect at each waste addition.
- The cellulase accelerates the natural breakdown of cellulose. This results in a large mass reduction when compared to waste treated with no cellulase

The newsprint experiments were conducted primarily to determine the viscosity reducing capabilities of cellulase by monitoring the agitator power. However, mass reduction of paper was determined to quantify the degree of breakdown of the paper. Also, models from the data needed to be developed to better understand the hydrolysis of cellulose.

A few distinct conclusions can be made concerning the breakdown of cellulose in newsprint due to mechanical agitation and cellulase activity.

- Agitator power reduces over time without cellulase due to the shearing of paper from the agitation. The power also reduces due to the cleavage of hydrogen bonds from the reintroduction of water.
- The agitator power rate of reduction is increased and the final power to agitate the slurry is reduced significantly due to the activity of cellulase.
- This breakdown phenomena can be modeled simply by the addition of three contributions to power: P_h, the power needed to agitate the cellulose and non-cellulose material held together by hydrogen bonds, P_b, the power needed to agitate the cellulose fibers linked together by $\beta(1\text{-}4)$ bonds, and P_n, the power needed to agitate the non-cellulose material in the paper.

Cellulase addition is an effective method in reducing the paper to its simpler form. This is seen in the mass reduction results as well as the power reduction results.

This research has provided a better understanding of the breakdown of cellulose-derived materials although there is still much research which needs to be done. On the large-scale system, similar experiments should be conducted to determine if the cellulose hydrolysis/power model described is valid in a scaled-up version of the test beaker. The power constants will increase, but one could hypothesize that the time constants will remain the same. These models will allow the prediction of agitator power in larger or smaller systems and aid in determining the specifications of the agitator for each new system.

Appendix A

Diffusion Solutions

A.1 One-Dimensional Diffusion Solutions

A.1.1 One-Dimensional Diffusion During Batch Process

This problem has the following governing equation,

$$\frac{\partial C_e(x,t)}{\partial t} = D_{AB}\frac{\partial^2 C_e(x,t)}{\partial x^2} \tag{A.1}$$

boundary conditions,

$$C_e(x,t) = C_\infty \text{ for } x = 0, t > 0 \tag{A.2}$$

$$\frac{\partial C_e(x,t)}{\partial x} = 0 \text{ for } x = L, t > 0 \tag{A.3}$$

and initial condition.

$$C_e(x,t) = F(x) = 0 \text{ for } 0 \le x \le L, t = 0 \tag{A.4}$$

Define $\Phi(x,t)$ as follows

$$\Phi(x,t) = \frac{C_\infty - C_e(x,t)}{C_\infty} \tag{A.5}$$

Substituting equation A.5 into the equations A.1 - A.4 yields

$$\frac{\partial \Phi(x,t)}{\partial t} = D_{AB}\frac{\partial^2 \Phi(x,t)}{\partial x^2} \tag{A.6}$$

$$\Phi(x,t) = 0 \text{ for } x = 0, t > 0 \tag{A.7}$$

$$\frac{\partial \Phi(x,t)}{\partial x} = 0 \text{ for } x = L, t > 0 \tag{A.8}$$

$$\Phi(x,t) = F(x) = 1 \text{ for } 0 \le x \le L, t = 0 \tag{A.9}$$

To solve this problem assume the separation of function $\Phi(x,t)$ into a space- and time-dependent functions in the form

$$\Phi(x,t) = \chi(x)\Gamma(t) \tag{A.10}$$

The substituting of equation (A.10) into equation (A.6) yields

$$\frac{1}{\chi(x)}\frac{d^2\chi(x)}{dx^2} = \frac{1}{D_{AB}\Gamma(t)}\frac{d\Gamma(t)}{dt} \tag{A.11}$$

In equation (A.11), the left-hand side is a function of x, and the right-hand side is a function of t; therefore, both sides are equal to the same constant which we will call $-\beta^2$ resulting in

$$\frac{1}{\chi(x)}\frac{d^2\chi(x)}{dx^2} = \frac{1}{D_{AB}\Gamma(t)}\frac{d\Gamma(t)}{dt} = -\beta^2 \tag{A.12}$$

Then, the function $\Gamma(t)$ satisfies the differential equation

$$\frac{d\Gamma(t)}{dt} + D_{AB}\beta^2\Gamma(t) = 0 \tag{A.13}$$

which has a solution in the form

$$\Gamma(t) = e^{-D_{AB}\beta^2 t} \tag{A.14}$$

The space-variable function $\chi(x)$ satisfies the differential equation

$$\frac{d^2\chi(x)}{dx^2} + \beta^2\chi(x) = 0 \text{ for } 0 < x < L \tag{A.15}$$

If the separated solution (A.10) is introduced to the boundary conditions (A.7) and (A.8) we obtain

$$\chi = 0 \text{ for } x = 0 \tag{A.16}$$

$$\frac{d\chi}{dx} = 0 \text{ for } x = L \tag{A.17}$$

The problem defined by equations (A.15 - A.17) is an eigenvalue problem, because it has solutions only for certain values of the separation parameter $\beta = \beta_m$, $m = 1, 2, 3, \ldots$, which are called the eigenvalues; the corresponding solution $\chi(\beta_m, x)$ are called the eigenfunctions of the problem. Assuming these eigenvalues and eigenfunctions are known, the complete solution for $\Phi(x, t)$ is constructed by a linear superposition of the above separated elementary solutions in the form

$$\Phi(x,t) = \sum_{m=1}^{\infty} c_m \chi(\beta_m, x) e^{-D_{AB}\beta_m^2} \tag{A.18}$$

This solution satisfies both the differential equation (A.1) and the boundary conditions (A.2 - A.3) of the mass diffusion problem, but it does not satisfy the initial condition (A.4). Therefore, the application of the initial condition to equation (A.18) yields

$$F(x) = 1 = \sum_{m=1}^{\infty} c_m \chi(\beta_m, x) \tag{A.19}$$

The unknown coefficients c_m's can be determined by making use of the orthogonality of the eigenfunctions given as

$$\int_o^L \chi(\beta_m, x)\chi(\beta_n, x)dx = 0 \text{ for } m \neq n \tag{A.20}$$

$$\int_o^L \chi(\beta_m, x)\chi(\beta_n, x)dx = N(\beta_m) \text{ for } m = n \tag{A.21}$$

where, the normalization integral or the norm, $N(\beta_m)$, is defined as

$$N(\beta_m) = \int_0^L [\chi(\beta_m, x)]^2 dx \tag{A.22}$$

To determine the coefficients c_m we operate on both sides of equation (A.19) by the operator

$$\int_0^L \chi(\beta_n, x)dx \tag{A.23}$$

and utilize the orthogonality property given by equations (A.20 and A.21); this results in

$$c_m = \frac{1}{N(\beta_m)} \int_0^L \chi(\beta_m, x) F(x) dx \tag{A.24}$$

The substitution of equation (A.24) into equation (A.18) yields the solution for the dimensionless concentration as

$$\Phi(x,t) = \sum_{m=1}^{\infty} e^{-D_{AB}\beta_m^2 t} \frac{1}{N(\beta_m)} \chi(\beta_m, x) \int_0^L \chi(\beta_m, x') F(x') dx \tag{A.25}$$

This separation of variables method is developed in Özisik [26] and should be referred to for a more in-depth explanation. The eigenfunction $\chi(\beta_m, x)$, the norm $N(\beta_m)$, and eigenvalues β_m are listed in Özisik for the boundary conditions of this problem and are as follows:

$$\chi(\beta_m, x) = \sin \beta_m x \tag{A.26}$$

$$N(\beta_m) = \frac{L}{2} \tag{A.27}$$

with the eigenvalues $\beta_m' s$ being positive roots of

$$\cos \beta_m L = 0 \tag{A.28}$$

which results in

$$\beta_m = \frac{(2m-1)\pi}{2L} \tag{A.29}$$

Substituting equations (A.26 and A.27) into equation (A.25) and then integrating yields the solution to this problem

$$\frac{C_e(x,t)}{C_\infty} = \theta(x,t) = 1 + \frac{2}{L} \sum_{m \to 1}^{\infty} -\frac{1}{\beta_m} \sin(\beta_m x) e^{-D_{AB}\beta_m^2 t} \tag{A.30}$$

A.1.2 One-Dimensional Diffusion (Post-Batch)

This problem has the following governing equation,

$$\frac{\partial C_e(x,t)}{\partial t} = D_2 \frac{\partial^2 C_e(x,t)}{\partial x^2} \tag{A.31}$$

boundary conditions,

$$\frac{\partial C_e(x,t)}{\partial x} = 0 \text{ for } x = 0, t > 0 \tag{A.32}$$

$$\frac{\partial C_e(x,t)}{\partial x} = 0 \text{ for } x = L, t > 0 \tag{A.33}$$

and initial condition.

$$C_e(x,T) = F(x) = C_\infty - \frac{2C_\infty}{L} \sum_{n=1}^{\infty} \frac{1}{\gamma_n} \sin(\gamma_n x) e^{-D_1 \gamma_n^2 T} \tag{A.34}$$

where

$$\gamma_n = \frac{(2n-1)\pi}{2L} \tag{A.35}$$

Define $\Phi(x,t)$ as follows

$$\Phi(x,t) = \frac{C_\infty - C_e(x,t)}{C_\infty} \tag{A.36}$$

Substituting equation (A.34) into equations (A.31 - A.33) yields this governing equation,

$$\frac{\partial \Phi(x,t)}{\partial t} = D_2 \frac{\partial^2 \Phi(x,t)}{\partial x^2} \tag{A.37}$$

boundary conditions,

$$\frac{\partial \Phi(x,t)}{\partial x} = 0 \text{ for } x = 0, t > 0 \tag{A.38}$$

$$\frac{\partial \Phi(x,t)}{\partial x} = 0 \text{ for } x = L, t > 0 \tag{A.39}$$

and initial condition.

$$\Phi(x,T) = F(x) = -\frac{2}{L}\sum_{n=1}^{\infty}\frac{1}{\gamma_n}\sin(\gamma_n x)e^{-D_1\gamma_n^2 T} \tag{A.40}$$

Following the same procedure for separation of variables listed by equations (A10 - A.24) yields the form of the solution

$$\Phi(x,t) = \sum_{m=1}^{\infty} e^{-D_2\beta_m^2 t}\frac{1}{N(\beta_m)}\chi(\beta_m,x)\int_0^L \chi(\beta_m,x')F(x')dx \tag{A.41}$$

where β_m is the new separation parameter for $m = 1,2,3\ldots$

The eigenfunction $\chi(\beta_m,x)$, the norm $N(\beta_m)$, and eigenvalues β_m are listed in Özişik [26] for the boundary conditions of this problem and are as follows:

$$\chi(\beta_m,x) = \cos\beta_m x \tag{A.42}$$

$$N(\beta_m) = \frac{L}{2} \tag{A.43}$$

with the eigenvalues $\beta_m' s$ being positive roots of

$$\sin\beta_m L = 0 \tag{A.44}$$

which results in

$$\beta_m = \frac{m\pi}{L} \tag{A.45}$$

For this particular set of boundary condtions, there is an additional eigenvalue $\beta_0 = 0$ which has a corresponding $N(\beta_0) = L$ and eigenfunction $\chi(\beta_0,x) = 1$.

Now the integral in equation (A.41) can be evaluated. For simplicity this integral was evaluated separately for β_0 and β_m and then the results were added to yield the solution.

For $\beta_0 = 0$ substituting the norm $N(\beta_0)$ and the eigenfunction $\chi(\beta_0,x)$ into equation (A.41) yields

$$-\frac{2}{L^2}\int_0^L\sum_{n=1}^{\infty}\frac{1}{\gamma_n}\sin(\gamma_n x)e^{-D_1\gamma_n^2 T}dx \tag{A.46}$$

Evaluating equation (A.46) results in

$$-\frac{2}{L^2}\sum_{n=1}^{\infty}\frac{1}{\gamma_n^2}e^{-D_1\gamma_n^2 T} \tag{A.47}$$

For β_m substituting the norm $N(\beta_m)$ and the eigenfunction $\chi(\beta_m, x)$ into equation (A.41) yields

$$\frac{2}{L}\sum_{m=1}^{\infty} e^{-D_2\beta_m^2 t}\cos(\beta_m x)\int_0^L \cos(\beta_m x)\left(-\frac{2}{L}\sum_{n=1}^{\infty}\frac{1}{\gamma_n}\sin(\gamma_n x)e^{-D_1\gamma_n^2 T}\right)dx \tag{A.48}$$

In order to evaluate the integral in equation (A.48), the following product-to-sum identity was used

$$\sin(mx)\cos(nx) = \frac{1}{2}(\sin[(m-n)x] + \sin[(m+n)x]) \tag{A.49}$$

Evaluating equation (A.48) given equation (A.49) yields

$$\frac{2}{L}\sum_{m=1}^{\infty} e^{-D_2\beta_m^2 t}\cos(\beta_m x)\left[-\frac{2}{L}\sum_{n=1}^{\infty}\frac{e^{-D_1\gamma_n^2 T}}{\gamma_n^2-\beta_m^2}\right] \tag{A.50}$$

Combining equations (A.47 and A.50) yields the solution

$$\Phi(x,t) = -\frac{2}{L^2}\left[2\sum_{m=1}^{\infty}\sum_{n=1}^{\infty} e^{-D_2\beta_m^2 t}\cos(\beta_m x)\frac{e^{-D_1\gamma_n^2 T}}{\gamma_n^2-\beta_m^2} + \sum_{n=1}^{\infty}\frac{e^{-D_1\gamma_n^2 T}}{\gamma_n^2}\right] \tag{A.51}$$

Substituting the definition of $\Phi(x,t)$ and defining $\theta(x,t) = \dfrac{C_e(x,t)}{C_\infty}$ yields

$$\theta(x,t) = 1 - \frac{2}{L^2}\left[2\sum_{m=1}^{\infty}\sum_{n=1}^{\infty} e^{-D_2\beta_m^2 t}\cos(\beta_m x)\frac{e^{-D_1\gamma_n^2 T}}{\gamma_n^2-\beta_m^2} + \sum_{n=1}^{\infty}\frac{e^{-D_1\gamma_n^2 T}}{\gamma_n^2}\right] \tag{A.52}$$

A.2 Re-entrant Sector Exact Solution

This problem has the following governing equation,

$$\frac{1}{r}\frac{\partial}{\partial r}\left(r\frac{\partial C_e(r,\Phi,t)}{\partial r}\right)+\frac{1}{r^2}\frac{\partial^2 C_e(r,\Phi,t)}{\partial \Phi^2}=\frac{1}{D}\frac{\partial C_e(r,\Phi,t)}{\partial t} \tag{A.53}$$

boundary conditions,

$$\frac{\partial C_e(r,\Phi,t)}{\partial r}=0 \text{ for } r=b \tag{A.54}$$

$$C_e(r,\Phi,t)=C_\infty \text{ for } r=a \tag{A.55}$$

$$\frac{\partial C_e(r,\Phi,t)}{\partial \Phi}=0 \text{ for } \Phi=0 \tag{A.56}$$

$$\frac{\partial C_e(r,\Phi,t)}{\partial \Phi}=0 \text{ for } \Phi=\Phi_0 \tag{A.57}$$

and initial condition.

$$C_e(r,\Phi,t)=0 \text{ for } t=0 \tag{A.58}$$

Due to the geometry of this problem, the concentration gradient in the angular direction is always zero. Therefore, the Φ term drops out of the governing equation.

Also, define the following dimensionless groups

$$\Psi(r,t)=\frac{C_e(r,t)-C_\infty}{-C_\infty} \tag{A.59}$$

$$\tau=\frac{Dt}{(b-a)^2} \tag{A.60}$$

$$R=\frac{r}{b-a} \tag{A.61}$$

Substituting equations (A.59 - A.61) into equations (A.53 - A.55 and A.58) yields the dimensionless form of the governing equation,

$$\frac{1}{R}\frac{\partial}{\partial R}\left(R\frac{\partial \Psi(R,\tau)}{\partial R}\right) = \frac{\partial \Psi(R,\tau)}{\partial \tau} \tag{A.61}$$

boundary conditions,

$$\frac{\partial \Psi(R,\tau)}{\partial R} = 0 \text{ for } R = \frac{b}{b-a} \tag{A.62}$$

$$\Psi(R,\tau) = 0 \text{ for } R = \frac{a}{b-a} \tag{A.63}$$

and initial condition.

$$\Psi(R,\tau) = 1 \text{ for } \tau = 0 \tag{A.64}$$

By following a separation of variables method similar to equations (A.10 - A.24) and listed in Özişik [26] yields the following form of the solution

$$\Psi(R,\tau) = \sum_{m=1}^{\infty} \frac{1}{N(\beta_m)} e^{-\beta_m^2 \tau} R_o(\beta_m R) \int_{\xi=\frac{a}{b-a}}^{\frac{b}{b-a}} \xi R_o(\beta_m, \xi) d\xi \tag{A.65}$$

where β_m is the new separation parameter for $m = 1, 2, 3, \ldots$ and ξ is a dummy variable for R.

The eigenfunction $R_o(\beta_m R)$, the norm $N(\beta_m)$, and eigenvalues β_m are listed in Özişik for the boundary conditions of this problem and are as follows

$$R_o(\beta_m R) = J_1(\beta_m \tfrac{b}{b-a}) Y_o(\beta_m R) - J_o(\beta_m R) Y_1(\beta_m \tfrac{b}{b-a}) \tag{A.66}$$

$$N(\beta_m) = \frac{2}{\pi^2} \frac{(J_o^2(\beta_m \frac{a}{b-a}) - J_1^2(\beta_m \frac{b}{b-a})}{\beta_m^2 J_o^2(\beta_m \frac{a}{b-a})} \tag{A.67}$$

and the eigenvalues β_m are the positive roots of the following transcendental equation.

$$J_1(\beta_m \tfrac{b}{b-a}) Y_o(\beta_m \tfrac{a}{b-a}) - J_o(\beta_m \tfrac{a}{b-a}) Y_1(\beta_m \tfrac{b}{b-a}) = 0 \tag{A.68}$$

The eigenvalues in equation (A.68) were solved numerically. The eigenvalues were determined in the subroutine (recrev) in the sector crevice computer code in Appendix B.

Let's look at only the integral part of equation (A.65) and call it R_1

$$R_1 = \int_{\xi=\frac{a}{b-a}}^{\frac{b}{b-a}} \xi R_o(\beta_m, \xi) d\xi \tag{A.69}$$

Substituting equation (A.66) for $R_o(\beta_m, \xi)$ into equation (A.69) gives

$$R_1 = \int_{\xi=\frac{a}{b-a}}^{\frac{b}{b-a}} \left[J_1\left(\beta_m \frac{b}{b-a}\right) \xi Y_o(\beta_m \xi) - Y_1\left(\beta_m \frac{b}{b-a}\right) \xi J_o(\beta_m \xi) \right] d\xi \tag{A.70}$$

Integrating equation (A.70) and applying the limits of integration results in

$$R_1 = \frac{1}{\beta_m} \frac{a}{b-a} \left[J_1(\beta_m \tfrac{a}{b-a}) Y_1(\beta_m \tfrac{b}{b-a}) - J_1(\beta_m \tfrac{b}{b-a}) Y_1(\beta_m \tfrac{a}{b-a}) \right] \tag{A.71}$$

Equation (A.71) can now be substituted into equation (A.65) to give the solution to the differential equation (A.61).

$$\Psi(R, \tau) = \sum_{m=1}^{\infty} \frac{1}{N(\beta_m)} e^{-\beta_m^2 \tau} R_o R_1 \tag{A.71}$$

Define

$$\theta(R, \tau) = \frac{C_e(R, \tau)}{C_\infty} \tag{A.72}$$

and the solution becomes

$$\theta(R, \tau) = 1 - \sum_{m=1}^{\infty} \frac{1}{N(\beta_m)} e^{-\beta_m \tau} R_o R_1 \tag{A.73}$$

with R_o, R_1, $N(\beta_m)$, and β_m defined in equations (A.66, A.71, A.67, and A.68), respectively.

Appendix B

Diffusion Computer Codes

B.1 One-Dimensional Diffusion Computer Codes

B.1.1 Code Listing for Batch Process

```
c234567
c
c this program calculates the molecular diffusion of protease enzyme
c through a one-dimensional crevice which could be taken as a
c hypodermic needle closed at one end or a needle twice as long with
c both ends open.
c
c
c input the diffusion coefficient of the specified enzyme through a
c particular media, the length of the crevice with one end closed, and
c the point or distance within the crevice (needle) which the time
c or the concentration of enzyme is needed.
c
      write(*,*) 'input diffusion coefficient for enzyme, length of crevice,
     #and point of interest within the crevice'
c
c open data file to store results
c
     open(2,file='1d.dat')
     read(*,*) d,a,z
     write(2,*)'  Diffusion coefficient (cm^2/s)'
     write(2,*) d
     write(2,*) 'crevice size (cm)      time (hrs)      fraction of
    #cinf'
c
c input numerical value for Pi
c
     pi=3.14159265
c
c begin to calculate the concentration of enzyme due to diffusion
c progressing forward in time
c
     do 20 k = 1,20
     i=k*3600
```

```
c
c calculate the concentration by summing up the inifinite series
c
      do 10 j=1,100,1
      b=(2*j-1)*pi/(2.*a)
      theta = (2./a)*sin(b*z)*(-1/b)*exp(-d*((b)**2)*i)
      theta2= theta + theta2
 10   continue
      conc = theta2 +1.0
      write(2,15) z,k,conc
 15   format(f10.2,i18,f20.3)
c
c reset the concentration to zero in order to progress in time
c
      theta2=0
 20   continue
      stop
      end
```

B.1.2 Code Listing for Post-Batch Diffusion

```
c234567
      double precision d,a,t,x,i,g,old,small,small1,b,big,big1,old1,
     $conc,dn
c
c this program calculates the concentration of protease enzyme
c at any position in a one dimensional crevice given an initial
c concentration distribution.  This initial concentration
c distribution was taken from the results of the initial
c one-dimensional crevice model.
c
c
c input the diffusion coefficient of the specified enzyme through a
c particular media in cm^2/s, the length of the crevice with one end
c closed in centimenters, the batch time in seconds for the
c initial condition, and the x-position within the crevice in
c centimeters
c
      write(*,*) 'input batch diffusion coefficient in cm^2/s, length of
     #crevice in cm, batch time in seconds, and x-position in cm,'
c
c open data file to store results
c
      open(2,file='kill.dat')
      read(*,*) d,a,t,x
      write(*,*) 'input new diffusion coefficient'
      read(*,*) dn
      write(2,*)'  Batch Diffusion coefficient (cm^2/s)'
      write(2,8) d
      write(2,*)'  New Diffusion coefficient (cm^2/s)'
      write(2,8) dn
      write(2,*)'  Batch time (hours)'
      write(2,7)t/3600.0d0
      write(2,*) 'crevice size (cm)     time (hrs)     fraction of
     #cinf'
  8   format(e10.3)
  7   format(f10.2)
c
c input numerical value for Pi
c
      pi=3.14159265d0
c
```

```
c begin to calculate the concentration of enzyme due to diffusion
c progressing forward in time
c
      do 20 k = 1,30
      i=k*3600.0d0
c
c calculate the concentration by summing up the infinite series
c
      do 9 m=1,200
      g=(2.0d0*m-1)*pi/(2.0d0*a)
      old=exp(-d*(g**2)*t)
      small=old/(g**2)
      small1= small + small1
 9    continue
      do 10 j=1,500
      do 11 m=1,500
      b=j*pi/a
      g=(2.0d0*m-1)*pi/(2.0d0*a)
      old1=exp(-d*(g**2)*t)
      big=(2.0d0*cos(b*x)*exp(-dn*(b**2)*i)*old1)/((g**2)-(b**2))
      big1= big + big1
 11   continue
 10   continue
      conc = ((-2.0d0/(a**2))*(big1 + small1)) +1.0d0
      write(2,15) x,k,conc
 15   format(f10.2,i18,f20.3)
c
c reset the concentration to zero in order to progress in time
c
      small1=0.0d0
      big1=0.0d0
 20   continue
      stop
      end
```

B.2 Two-Dimensional Diffusion Computer Codes

The bessel function subroutines were listed by Press [39].

B.2.1 Code Listing for Sector Crevice

```
      double precision dt,dx,a,b,pi,r,f,besjo,besj1,beta,bbsj1,besy1
     $,bbsy1,bbsyo,bbsjo,theta,theta2
c
c           this program calulates the concentration at the
c           back wall of a cylindrical crevice due to diffusion
c           only (exact solution).
c
      real nm
c
c           input time step, x-direction increment for calculating
c           bessel functions, inner radius of crevice, a, and
c           outer radius of crevice, b.
c
      open (4,file='rein4.dat')
      write(*,*) 'input dt, dx, a, and b'
      read(4,*) dt,dx,a,b
      pi=3.141592653589793d0
      r=b/(b-a)
c
c           open data files to store bessel function values and
c           diffusion results.
c
      open (2,file='beta4.dat')
      open (3,file='recrv4.dat')
      write(3,*)'  time     a      b      r      theta'
c
c           call subroutine to calculate eigenvalues from
c           a transcendental equation based on both inner
c           radius, a, and outer radius, b.
c
      call recrev (besjo,besj1,beta,bbsj1,besy1,bbsy1,bbsyo,bbsjo)
c
c           return to the top of the data file.
c
      rewind 2
c
```

```
c            iterate in time and sum the series.
c
     do 20 k = 0,300
     do 10 j = 1,800
     f=k*dt
c
c            reads in the eigenvalues.
c
     read(2,17) besjo,besj1,beta,bbsj1,besy1,bbsy1,bbsyo,bbsjo
 17  format(8f13.8)
     nm= 2.d0*(besjo**2-besj1**2)/((pi**2)*(beta**2)*(besjo**2))
c
c            calculates the contribution to concentration for
c            each eigenvalue.
c
     theta = (a/((b-a)*beta*nm))*exp(-(beta**2)*f)*((bbsj1*besy1)-(bes
    #j1*bbsy1))*((besj1*bbsyo)-(besy1*bbsjo))
c
c            sums the contribution to concentration from each
c            eigenvalue.
c
     theta2 = theta + theta2
 10  continue
c
c            returns to the top of the eigenvalue data file
c            so that time can be stepped forward.
c
     rewind 2
c
c            writes inner radius, outer radius, time, and
c            concentration at the outer radius to the recrv.dat
c            file.
c
     write(3,22) f,a,b,r,theta2
 22  format(4f9.4,f14.8)
     theta2 = 0.d0
c
c            returns so that time can be incremented.
c
 20  continue
     end
c
c            subroutine which calculates bessel functions and
```

```
c             solves the transcendental equation for the eigenvalues
c             the transcendental equation is as follows:
c
c                jo(Bm*b)*y1(Bm*a) - j1(Bm*a)*yo(Bm*b) = 0
c
c             this equation is solved for the eigenvalue Bm.
c
c
c
      subroutine recrev (besjo,besj1,beta,bbsj1,besy1,bbsy1,bbsyo,bbsjo)
      dimension root(4), bm(4), bessjo(4), bessj1(4), bessyo(4),
     #bessy1(4), bbj1(4), bby1(4), bbyo(4), bbjo(4)
c
c             everything is input and calculated in double
c             precision.
c
      real*8 y,p1,p2,p3,p4,p5,q1,q2,q3,q4,q5,r1,r2,r3,r4,r5,r6,s1,s2,s3,
     $s4,s5,s6,t1,t2,t3,t4,t5,t6,v1,v2,v3,v4,v5,v6,a1,a2,a3,a4,a5,b1,b2,
     $b3,b4,b5,c1,c2,c3,c4,c5,c6,e1,e2,e3,e4,e5,e6,f1,f2,f3,f4,f5,f6,g1,
     $g2,g3,g4,g5,g6,bm,dx,a,b,x1,x2,ax,z,z1,xx1,xx,xx2,xx3,bessjo,bessy
     $o,bbj1,bby1,bessj1,bessy1,bbjo,bbyo,root,beta,besjo,besy1,besj1,bb
     $sy1,bbsj1,bbsjo,bbsyo
c
c             input radial increment, inner radius, and
c             outer radius to solve the transcendental equation.
c
      write(*,*) 'dx,a,b'
      read(4,*) dx,a,b
      write(3,*) dx,a,b
c
c             input constants which are used to estimate
c             the bessel functions.
c
      data p1,p2,p3,p4,p5/1.d0,-.1098628627d-2,.2734510407d-4,-.20733706
     $39d-5,.2093887211d-6/,q1,q2,q3,q4,q5/-.1562499995d-1,.1430488765d
     $-3,.6911147651d-5,.7621095161d-6,-.934945152d-7/
      data r1,r2,r3,r4,r5,r6/57568490574.d0,-13362590354.d0,651619640.7d
     $0,-11214424.18d0,77392.33017d0,-184.9052456d0/,s1,s2,s3,s4,s5,s6/
     $57568490411.d0,1029532985.d0,9494680.718d0,59272.64853d0,267.85327
     $12d0,1.d0/
      data t1,t2,t3,t4,t5,t6/-2957821389.d0,7062834065.d0,-512359803.6d0
     $,10879881.29d0,-86327.92757d0,228.4622733d0/,v1,v2,v3,v4,v5,v6/400
     $76544269.d0,745249964.8d0,7189466.438d0,47447.26470d0,226.1030244d
```

```
     $0,1.d0/
      data c1,c2,c3,c4,c5,c6/72362614232.d0,-7895059235.d0,242396853.1d0
     $,-2972611.439d0,15704.48260d0,-30.16036606d0/,e1,e2,e3,e4,e5,e6/14
     $4725228442.d0,2300535178.d0,18583304.74d0,99447.43394d0,376.999139
     $7d0,1.d0/
      data a1,a2,a3,a4,a5/1.d0,.183105d-2,-.3516396496d-4,.2457520174d-5
     $,-.240337019d-6/,b1,b2,b3,b4,b5/.04687499995d0,-.2002690873d-3,.84
     $49199096d-5,-.88228987d-6,.105787412d-6/
      data f1,f2,f3,f4,f5,f6/-.4900604943d13,.1275274390d13,-.5153438139
     $d11,.7349264551d9,-.4237922726d7,.8511937935d4/,g1,g2,g3,g4,g5,g6/
     $.2499580570d14,.4244419664d12,.3733650367d10,.2245904002d8,.102042
     $6050d6,.3549632885d3,1.d0/
c
c          do loop to increment in radial direction.
c
     do 30 i = 1,1600000
c
c          one-dimensional array which stores current
c          value, eigenvalue or bessel function value,
c          and the previous value.
c
     do 25 l = 1,2,1
     bm(l+1) = dx*(i+l-1)
c
c          x1 and x2 is the product of the radial increment
c          and the non-dimensional inner or outer radius.
c
     x1= dx*(i+l-1)*(a/(b-a))
     x2= dx*(i+l-1)*(b/(b-a))
c
c          if x1 is less than the number 8 then use the
c          following equations for calculating the bessel
c          functions.  these equations estimate the bessel
c          functions accurately for radial distances less
c          than 8.
c
     if(abs(x1).lt.8.) then
     y=x1**2
     bessjo(l+1)=(r1+y*(r2+y*(r3+y*(r4+y*(r5+y*r6))))) / (s1+y*(s2+y*(s
    $3+y*(s4+y*(s5+y*s6)))))
     bessyo(l+1)=(t1+y*(t2+y*(t3+y*(t4+y*(t5+y*t6))))) / (v1+y*(v2+y*(v
    $3+y*(v4+y*(v5+y*v6))))) +.636619772d0*bessjo(l+1)*log(x1)
     bbj1(l+1)=x1*(c1+y*(c2+y*(c3+y*(c4+y*(c5+y*c6))))) / (e1+y*(e2+y
```

```
     $*(e3+y*(e4+y*(e5+y*e6)))))
      bby1(l+1)=x1*(f1+y*(f2+y*(f3+y*(f4+y*(f5+y*f6))))) / (g1+y*(g2+y
     $*(g3+y*(g4+y*(g5+y*g6))))) +.636619772d0*(bbj1(l+1)*log(x1)-1./x1)
c
c               if x1 is greater than or equal to eight then
c               use these equations.
c
      else
      ax=abs(x1)
      z=8.d0/ax
      z1=8.d0/x1
      xx1=x1-.785398164d0
      y=z**2
      xx=ax-.785398164d0
      xx2=ax-2.356194491d0
      xx3=x1-2.356194491d0
      bessjo(l+1)=sqrt(.636619772d0/ax)*(cos(xx)*(p1+y*(p2+y*(p3+y*(p4+y
     $*p5))))-z*sin(xx)*(q1+y*(q2+y*(q3+y*(q4+y*q5)))))
      bessyo(l+1)=sqrt(.636619772d0/x1)*(sin(xx1)*(p1+y*(p2+y*(p3+y*(p4+
     $y*p5))))+z1*cos(xx1)*(q1+y*(q2+y*(q3+y*(q4+y*q5)))))
      bbj1(l+1)=sqrt(.636619772d0/ax)*(cos(xx2)*(a1+y*(a2+y*(a3+y*(a4+y*
     $a5))))-z*sin(xx2)*(b1+y*(b2+y*(b3+y*(b4+y*b5))))*sign(1.d0,x1)
      bby1(l+1)=sqrt(.636619772d0/x1)*(sin(xx3)*(a1+y*(a2+y*(a3+y*(a4+y*
     $a5))))+z1*cos(xx3)*(b1+y*(b2+y*(b3+y*(b4+y*b5)))))
      end if
c

c               if x2 is less than the number 8 then use the
c               following equations for calculating the bessel
c               functions.  these equations estimate the bessel
c               functions accurately for radial distances less
c               than 8.
c
      if(abs(x2).lt.8.) then
      y=x2**2
      bessj1(l+1)=x2*(c1+y*(c2+y*(c3+y*(c4+y*(c5+y*c6))))) / (e1+y*(e2+y
     $*(e3+y*(e4+y*(e5+y*e6)))))
      bessy1(l+1)=x2*(f1+y*(f2+y*(f3+y*(f4+y*(f5+y*f6))))) / (g1+y*(g2+y
     $*(g3+y*(g4+y*(g5+y*g6))))) +.636619772d0*(bessj1(l+1)*log(x2)-1./x
     $2)
      bbjo(l+1)=(r1+y*(r2+y*(r3+y*(r4+y*(r5+y*r6))))) / (s1+y*(s2+y*(s
     $3+y*(s4+y*(s5+y*s6)))))
      bbyo(l+1)=(t1+y*(t2+y*(t3+y*(t4+y*(t5+y*t6))))) / (v1+y*(v2+y*(v
```

```
     $3+y*(v4+y*(v5+y*v6))))) +.636619772d0*bbjo(l+1)*log(x2)
c
c              if x1 is greater than or equal to eight then
c              use these equations.
c
      else
      ax=abs(x2)
      z=8.d0/ax
      z1=8.d0/x2
      xx=ax-.785398164d0
      xx1=x2-.785398164d0
      y=z**2
      xx2=ax-2.356194491d0
      xx3=x2-2.356194491d0
      bessj1(l+1)=sqrt(.636619772d0/ax)*(cos(xx2)*(a1+y*(a2+y*(a3+y*(a4*
     $y*a5))))-z*sin(xx2)*(b1+y*(b2+y*(b3+y*(b4+y*b5)))))*sign(1.d0,x2)
      bessy1(l+1)=sqrt(.636619772d0/x2)*(sin(xx3)*(a1+y*(a2+y*(a3+y*(a4+
     $y*a5))))+z1*cos(xx3)*(b1+y*(b2+y*(b3+y*(b4+y*b5)))))
      bbjo(l+1)=sqrt(.636619772d0/ax)*(cos(xx)*(p1+y*(p2+y*(p3+y*(p4+y*p
     $5))))-z*sin(xx)*(q1+y*(q2+y*(q3+y*(q4+y*q5)))))
      bbyo(l+1)=sqrt(.636619772d0/x2)*(sin(xx1)*(p1+y*(p2+y*(p3+y*(p4+y*
     $p5))))+z1*cos(xx1)*(q1+y*(q2+y*(q3+y*(q4+y*q5)))))
      end if
c
c              solve the transcendental equation using the
c              calculated bessel functions.
c
      root(l+1)=-bessyo(l+1)*bessj1(l+1) + bessy1(l+1)*bessjo(l+1)
c
c              pick out the eigenvalue when root(l+1) is
c              equal to zero by interpolation.
c
      if (root(l+1).gt.0.and.root(l).lt.0.) then
      beta=(((bm(l+1)-bm(l))*(0.d0-root(l)))/(root(l+1)-root(l))) + bm(l
     $)
      besjo=(((bessjo(l+1)-bessjo(l))*(0.d0-root(l)))/(root(l+1)-root(l)
     #)) + bessjo(l)
      besy1=(((bessy1(l+1)-bessy1(l))*(0.d0-root(l)))/(root(l+1)-root(l)
     #)) + bessy1(l)
      besj1=(((bessj1(l+1)-bessj1(l))*(0.d0-root(l)))/(root(l+1)-root(l)
     #)) + bessj1(l)
      bbsy1=(((bby1(l+1)-bby1(l))*(0.d0-root(l)))/(root(l+1)-root(l))
     #) + bby1(l)
```

```
      bbsj1=(((bbj1(l+1)-bbj1(l))*(0.d0-root(l)))/(root(l+1)-root(l))
     #) + bbj1(l)
      bbsjo=(((bbjo(l+1)-bbjo(l))*(0.d0-root(l)))/(root(l+1)-root(l))
     #) + bbjo(l)
      bbsyo=(((bbyo(l+1)-bbyo(l))*(0.d0-root(l)))/(root(l+1)-root(l))
     #) + bbyo(l)
c
c               write the eigenvalues to the data file.
c
      write(2,15) besjo,besj1,beta,bbsj1,besy1,bbsy1,bbsyo,bbsjo
      else
      endif
c
c               pick out the eigenvalue when root(l+1) is
c               equal to zero by interpolation.
c
      if (root(l+1).lt.0.and.root(l).gt.0.) then
      beta=(((bm(l+1)-bm(l))*(0.-root(l)))/(root(l+1)-root(l))) + bm(l)
      besjo=(((bessjo(l+1)-bessjo(l))*(0.d0-root(l)))/(root(l+1)-root(l)
     #)) + bessjo(l)
      besj1=(((bessj1(l+1)-bessj1(l))*(0.d0-root(l)))/(root(l+1)-root(l)
     #)) + bessj1(l)
      besy1=(((bessy1(l+1)-bessy1(l))*(0.d0-root(l)))/(root(l+1)-root(l)
     #)) + bessy1(l)
      bbsy1=(((bby1(l+1)-bby1(l))*(0.d0-root(l)))/(root(l+1)-root(l))
     #) + bby1(l)
      bbsj1=(((bbj1(l+1)-bbj1(l))*(0.d0-root(l)))/(root(l+1)-root(l))
     #) + bbj1(l)
      bbsjo=(((bbjo(l+1)-bbjo(l))*(0.d0-root(l)))/(root(l+1)-root(l))
     #) + bbjo(l)
      bbsyo=(((bbyo(l+1)-bbyo(l))*(0.d0-root(l)))/(root(l+1)-root(l))
     #) + bbyo(l)
c
c               write the eigenvalues to the data file.
c
      write(2,15) besjo,besj1,beta,bbsj1,besy1,bbsy1,bbsyo,bbsjo
      else
      endif
   15  format(8f13.8)
   25  continue
   30  continue
      return
      end
```

B.2.2 Code Listing For Shape 1

```
c
c This program calculates the concentration of enzyme in any rectangular
c shaped crevice at any instant in time using the alternating direction
c implicit method.
c
c234567
      double precision c,r1,r2,f1,f2,e1,e2,g1,g2,r3,r4,f3,f4,e3,e4,g3,g4
     $,d,t,dt,dx,cinf,fo,ao,w,k,m,n,a,a2,b,b2,r,rtwo,val,val2,vol,l1,l2,
     $vol2
      integer s
      real lg
c
c dimension arrays for data input and output
c
      dimension c(200,200), r1(200,200),r2(200,200),f1(200),f2(200,200),
     $e1(200),e2(200),g1(200),g2(200),r3(200,200),r4(200,200),f3(200),
     $f4(200,200),e3(200),e4(200),g3(200),g4(200)
      write(*,*)' input diffusion coefficient, number of time steps, ti
     $me step, step size, and outside concentration of enzyme'
c
c input values for molecular diffusivity, number of time steps, time
c step, step size, and enzyme concentration on the outside of the
c crevice
c
      open(4,file='input1.dat')
      read(4,*) d,t,dt,dx,cinf
c
c open data file to store enzyme concentration output
c
c234567
      open(2,file='sq.dat')
c
c calculate Fiot number for molecular diffusivity
c
      fo=d*dt/(dx**2)
      write(*,*) ' input crevice opening size, crevice width, and crev
     $length'
c
c input size of opening in the crevice, width of the crevice (opening
c in the crevice is along its width), and length of the crevice
```

```
c
      read(4,*) ao,w,lg
c
c calculate the number of nodes needed in both the x and y direction
c
      k=ao/dx
      m=((w-ao)/dx)+k
      n=lg/dx
      vol = lg*w
      write(2,*)'   vol    ao     w     lg     m      n      k'
      write(2,80) vol,ao,w,lg,m,n,k
 80   format(7f8.3,/)
c
c
c calculate two different characteristic lengths which will be
c equivalent to b-a for the cylindrical case
c
      l1=sqrt((lg**2)+((w-ao)**2))
      l2=sqrt(lg**2+w**2)
c
c calculate the volume of the crevice
c
      vol2=lg*w
c
c calculate the dimensionless number using the volume, area of the
c opening, and the characteristic length
c
      val=vol2/(ao*l1)
      val2=vol2/(ao*l2)
c
c calculate the apparent outer radius of the rectangular crevice
c using the two different characteristic lengths
c
      b= ((vol2/ao)-(l1/2.))/((vol2/(ao*l1))-1.)
      b2=((vol2/ao)-(l2/2.))/((vol2/(ao*l2))-1.)
c
c depending on the conditions specified on the outer radius calculate
c the apparent inner radius of the rectangular crevice using the two
c different characteristic lengths
c
      if (b.ge.0) then
      a= -vol2/ao + sqrt((vol2/ao)**2 + b**2)
      a2= -vol2/ao + sqrt((vol2/ao)**2 + b2**2)
```

```
      r=b/(b-a)
      rtwo=b2/(b2-a2)
      else
      a= -vol2/ao - sqrt((vol2/ao)**2 + b**2)
      a2= -vol2/ao - sqrt((vol2/ao)**2+b2**2)
      r=b/(b-a)
      rtwo=b2/(b2-a2)
      endif
      write(2,*)'     l1        a         b         r
     $val       vol'
      write(2,81)l1,a,b,r,val,vol2
 81   format(6f12.5,/)
c
c assign values to coefficients in the A matrix in order to solve by
c tridiagonal method for the first time step
c
      write(2,*)'       fo              k         m         n'
      do 10 i=2,m
       e1(i)=-fo
       f1(i)=1+(2*fo)
       g1(i-1)=-fo
 10    continue
       f1(1)=1+fo
       f1(m)=1+fo
       write(2,64) fo,k,m,n
 64    format(f15.6,5x,3f12.3,/)
c      do 60 i=1,m
c      write(2,65) e1(i),f1(i),g1(i)
c60    continue
c65    format(3f20.10)
c
c assign values to coefficients in the A matrix in order to solve by
c tridiagonal method for the second time step
c
      do 11 j=2,n
       e2(j)=-fo
        do 17 i=1,k
         f2(i,j-1)=1+(2*fo)
         f2(i,n)=1+fo
 17      continue
        do 18 i=k+1,m
         f2(i,j)=1+(2*fo)
         f2(i,1)=1+fo
```

```
      f2(i,n)=1+fo
 18    continue
      g2(j-1)=-fo
 11   continue
      f2(m,n)=1+fo
c     do 61 i=1,m
c     do 62 j=1,n
c     write(2,63)e2(j),f2(i,j),g2(j)
c62   continue
c61   continue
c63   format(3f18.10)
c
c assign values to coefficients in the B matrix in order to solve by
c tridiagonal method for the first time step
c
     write(2,*)'  l  time  concentration   tau     r'
     do 26 l=1,t
      time=l*dt
     tau=d*time/((b-a)**2)
     tau2=d*time/((b2-a2)**2)
     s=mod(l,2)
     if (s.ne.0) then
     do 12 i=1,k
      r1(i,1)=((cinf+c(i,2))*fo) + (1-(2*fo))*c(i,1)
 12   continue
     do 13 i=k+1,m
      r1(i,1)=c(i,2)*fo + ((1-fo)*c(i,1))
 13   continue
     do 14 i=1,m
      do 15 j=2,n-1
       r1(i,j)=(c(i,j-1)+c(i,j+1))*fo + (1-2*fo)*c(i,j)
 15    continue
 14   continue
     do 16 i=1,m
      r1(i,n)=fo*c(i,n-1)+((1-fo)*c(i,n))
 16   continue
c     do 67 j=1,n
c     write(2,68) r1(1,j),r1(2,j),r1(3,j),r1(4,j),r1(5,j)
c68   format(5f14.9)
c67   continue
c
c assign values to coefficients in the B matrix in order to solve by
c tridiagonal method for the first time step
```

```
c
      else
      r2(1,1)=fo*(c(2,1)+cinf) + (1-fo)*c(1,1)
      do 19 i=2,k
       r2(i,1)= fo*(c(i-1,1)+c(i+1,1)+cinf) + (1-(2*fo))*c(i,1)
 19   continue
      do 20 i=k+1,m-1
       r2(i,1)= fo*(c(i-1,1)+c(i+1,1)) + (1-(2*fo))*c(i,1)
 20   continue
      r2(m,1)=fo*c(m-1,1) + (1-fo)*c(m,1)
      do 21 j=2,n
       r2(1,j)=(fo*c(2,j))+((1-fo)*c(1,j))
 21   continue
      do 22 i=2,m-1
      do 23 j=2,n
       r2(i,j)=fo*(c(i-1,j)+c(i+1,j)) + ((1-(2*fo))*c(i,j))
 23   continue
 22   continue
      do 25 j=2,n
       r2(m,j)=fo*c(m-1,j)+((1-fo)*c(m,j))
 25   continue
c     do 70 j=1,n
c     write(2,71) r2(1,j),r2(2,j),r2(3,j),r2(4,j),r2(5,j)
c71   format(5f13.9)
c70   continue
      endif
c
c begin calculating enzyme concentration in time
c
      s=mod(l,2)
      if(s.ne.0) then
c
c reinitialize the coefficients in the A matrix in order to proceed
c in time
c
       do 40 i=1,n
        do 27 o=1,m
         e3(o)=e1(o)
         f3(o)=f1(o)
         g3(o)=g1(o)
 27      continue
c
c reinitialize the coefficients in the B matrix in order to proceed
```

```
c in time
c
      do 28 q=1,m
       do 29 j=1,n
        r3(q,j)=r1(q,j)
 29     continue
 28    continue
c
c solve entire concentration field using tridiagonal matrix solver for
c every odd time step
c
     do 30 q=2,m
      e3(q)=e3(q)/f3(q-1)
      f3(q)=f3(q)-e3(q)*g3(q-1)
 30   continue
     do 31 q=2,m
      r3(q,i)=r3(q,i)-(e3(q)*r3(q-1,i))
 31   continue
     c(m,i)=r3(m,i)/f3(m)
      do 32 q=m-1,1,-1
       c(q,i)=(r3(q,i)-g3(q)*c(q+1,i))/f3(q)
 32    continue
 40   continue
     write(2,3) l,time,c(m,n),tau,r
 3    format(i6,f8.0,f11.6,2f10.4)
     else
c
c reinitialize the coefficients in the A matrix in order to proceed
c in time
c
     do 41 i=1,m
      do 42 o=1,n
       e4(o)=e2(o)
       g4(o)=g2(o)
 42    continue
c
c reinitialize the coefficients in the B matrix in order to proceed
c in time
c
     do 43 q=1,m
      do 44 j=1,n
       r4(q,j)=r2(q,j)
       f4(q,j)=f2(q,j)
```

```
 44    continue
 43   continue
c
c solve entire concentration field using tridiagonal matrix solver for
c every even time step
c
     do 45 q=2,n
      e4(q)=e4(q)/f4(i,q-1)
      f4(i,q)=f4(i,q)-e4(q)*g4(q-1)
 45   continue
     do 46 q=2,n
      r4(i,q)=r4(i,q)-(e4(q)*r4(i,q-1))
 46   continue
     c(i,n)=r4(i,n)/f4(i,n)
      do 47 q=n-1,1,-1
       c(i,q)=(r4(i,q)-g4(q)*c(i,q+1))/f4(i,q)
 47    continue
 41   continue
     write(2,3) l,time,c(m,n),tau,r
     endif
 26   continue
     stop
     end
```

B.2.3 Code Listing for Shape 2

```
c This program calculates the concentration of enzyme in a rectangular
c shaped crevice shape 2 at any instant in time using the alternating on
c direction implicit method.
c
c234567
      double precision c,r1,r2,f1,f2,e1,e2,g1,g2,r3,r4,f3,f4,e3,e4,g3,g4
     $,d,t,dt,dx,cinf,fo,ao,w,a,a2,b,b2,r,rtwo,val,val2,vol,l1,l2,
     $vol2,wt
      integer s,h,u,j,l,k,m,n
      real lg,lgt
c
c dimension arrays for data input and output
c
      dimension c(200,200), r1(200,200),r2(200,200),f1(200),f2(200,200),
     $e1(200),e2(200),g1(200),g2(200),r3(200,200),r4(200,200),f3(200),
     $f4(200,200),e3(200),e4(200),g3(200),g4(200)
c
c input values for molecular diffusivity (cm^2/s), number of time steps,
c time step (seconds), step size (cm), and enzyme concentration on the
c outside of the crevice
c
      open(4,file='input4.dat')
      read(4,*) d,t,dt,dx,cinf
c
c open data file to store enzyme concentration output
c
c234567
      open(2,file='sqnew4.dat')
c
c calculate Fiot number for molecular diffusivity
c
      fo=d*dt/(dx**2)
c
c input size of opening in the crevice, width of bottom half of crevice
c up to node m (opening in the crevice is along its width), total width
c of crevice up to node j, length of crevice up to node n, and total
c length of crevice (all dimensions are in centimeters)
c
      read(4,*) ao,w,wt,lg,lgt
c
c calculate the number of nodes needed in both the x and y direction
```

```
c
      k=ao/dx
      m=((w-ao)/dx)+k+.1
      j=wt/dx+.1
      l=lgt/dx+.1
      n=lg/dx+.1
      vol = lgt*w + (wt-w)*(lgt-lg)
      write(2,*)'   vol    ao      w       wt      lg      lgt'
      write(2,80) vol,ao,w,wt,lg,lgt
 80   format(6f9.4,/)
c
c
c calculate characteristic length which will be equivalent to b-a for
c the cylindrical case
c
      l1=sqrt((lgt**2)+((wt-ao)**2))
c
c
c calculate the volume of the crevice
c
      vol2=lgt*w + (wt-w)*(lgt-lg)
c
c calculate the dimensionless number using the volume, area of the
c opening, and the characteristic length
c
      val=vol2/(ao*l1)
c
c calculate the apparent outer radius of the rectangular crevice
c using the two different characteristic lengths
c
      b= ((vol2/ao)-(l1/2.))/((vol2/(ao*l1))-1.)
c
c depending on the conditions specified on the outer radius calculate
c the apparent inner radius of the rectangular crevice using the
c characteristic length
c
      if (b.ge.0) then
      a= -vol2/ao + sqrt((vol2/ao)**2 + b**2)
      r=b/(b-a)
      else
      a= -vol2/ao - sqrt((vol2/ao)**2 + b**2)
      r=b/(b-a)
      endif
```

```
      write(2,*)'      ll          a          b          r
     $val'
      write(2,81)ll,a,b,r,val
 81   format(5f12.5,/)
c
c assign values to coefficients in the A matrix in order to solve by
c tridiagonal method for the first time step
c
      write(2,*)'        fo          k       m     j     n     l'
      do 10 i=2,j
       e1(i)=-fo
       f1(i)=1+(2*fo)
       g1(i-1)=-fo
 10    continue
       f1(1)=1+fo
       f1(m)=1+fo
       f1(j)=1+fo
       write(2,164) fo,k,m,j,n,l
 164   format(f15.6,5x,5i7,/)
c
c assign values to coefficients in the A matrix in order to solve by
c tridiagonal method for the second time step
c
      do 11 h=2,n
       e2(h)=-fo
        do 17 i=1,k
         f2(i,h-1)=1+(2*fo)
         f2(i,n)=1+(2*fo)
 17      continue
        do 18 i=k+1,m
         f2(i,h)=1+(2*fo)
         f2(i,1)=1+fo
 18      continue
       g2(h-1)=-fo
 11    continue
      do 50 h=n+1,l
       e2(h)=-fo
        do 51 i=1,m
         f2(i,h-1)=1+(2*fo)
         f2(i,l)=1+fo
 51      continue
        g2(h-1)=-fo
 50      continue
```

```
      do 99 h=n+2,l-1
       do 52 i=m+1,j
        f2(i,h)=1+(2*fo)
        f2(i,n+1)=1+fo
        f2(i,l)=1+fo
 52    continue
 99    continue
c
c begin progressing forward in time and calculate tau based on the
c characteristic length
c
      write(2,*)'   lt   time  concentration      tau'
      do 26 u=1,t
      time=u*dt
      tau=d*time/((b-a)**2)
c
c assign values to coefficients in the B matrix in order to solve by
c tridiagonal method for the even time steps
c
      s=mod(u,2)
      if (s.eq.0) then
      do 12 i=1,k
       r1(i,1)=((cinf+c(i,2))*fo) + (1-(2*fo))*c(i,1)
 12   continue
      do 13 i=k+1,m
       r1(i,1)=c(i,2)*fo + (1-fo)*c(i,1)
 13   continue
      do 14 i=1,m
       do 15 h=2,n
        r1(i,h)=(c(i,h-1)+c(i,h+1))*fo + (1-2*fo)*c(i,h)
 15    continue
 14   continue
      do 53 i=1,m
       r1(i,n+1)=(c(i,n)+c(i,n+2))*fo + (1-2*fo)*c(i,n+1)
 53   continue
      do 54 i=m+1,j
       r1(i,n+1)=c(i,n+2)*fo + (1-fo)*c(i,n+1)
 54   continue
      do 55 i=1,j
      do 56 h=n+2,l-1
       r1(i,h)=(c(i,h-1)+c(i,h+1))*fo + (1-2*fo)*c(i,h)
 56   continue
 55   continue
```

```
      do 16 i=1,j
       r1(i,l)=fo*c(i,l-1)+(1-fo)*c(i,l)
 16   continue
c
c assign values to coefficients in the B matrix in order to solve by
c tridiagonal method for the odd time steps
c
      else
      r2(1,1)=fo*(c(2,1)+cinf) + (1-fo)*c(1,1)
      do 19 i=2,k
       r2(i,1)= fo*(c(i-1,1)+c(i+1,1)+cinf) + (1-(2*fo))*c(i,1)
 19   continue
      do 20 i=k+1,m-1
       r2(i,1)= fo*(c(i-1,1)+c(i+1,1)) + (1-(2*fo))*c(i,1)
 20   continue
      r2(m,1)=fo*c(m-1,1) + (1-fo)*c(m,1)
      do 21 h=2,l
       r2(1,h)=(fo*c(2,h))+(1-fo)*c(1,h)
 21   continue
      do 22 i=2,m-1
      do 23 h=2,n
       r2(i,h)=fo*(c(i-1,h)+c(i+1,h)) + (1-(2*fo))*c(i,h)
 23   continue
 22   continue
      do 57 i=2,j-1
      do 58 h=n+1,l
       r2(i,h)=fo*(c(i-1,h)+c(i+1,h)) + (1-(2*fo))*c(i,h)
 58   continue
 57   continue
      do 25 h=2,n
       r2(m,h)=fo*c(m-1,h)+(1-fo)*c(m,h)
 25   continue
      do 59 h=n+1,l
       r2(j,h)=fo*c(j-1,h)+(1-fo)*c(j,h)
 59   continue
      endif
c
c begin calculating enzyme concentration in time
c
      s=mod(u,2)
      if(s.eq.0) then
c
c reinitialize the coefficients in the A matrix in order to proceed
```

```
c in time for the rectangle up to n nodes
c
      do 40 i=1,l
      if(i.le.n) then
       do 27 o=1,m
        e3(o)=e1(o)
        f3(o)=f1(o)
        g3(o)=g1(o)
 27     continue
        f3(m)=1+fo
        g3(m)=0
        e3(1)=0
c
c reinitialize the coefficients in the B matrix in order to proceed
c in time for the rectangle up to n nodes
c
       do 28 q=1,m
        do 29 h=1,n
         r3(q,h)=r1(q,h)
 29      continue
 28     continue
c
c solve entire concentration field using tridiagonal matrix solver for
c every odd time step up to n nodes
c
     do 30 q=2,m
      e3(q)=e3(q)/f3(q-1)
      f3(q)=f3(q)-e3(q)*g3(q-1)
 30   continue
     do 31 q=2,m
      r3(q,i)=r3(q,i)-(e3(q)*r3(q-1,i))
 31   continue
     c(m,i)=r3(m,i)/f3(m)
      do 32 q=m-1,1,-1
       c(q,i)=(r3(q,i)-g3(q)*c(q+1,i))/f3(q)
 32    continue
     else
c
c reinitialize the coefficients in the A matrix in order to proceed
c in time for the rectangle between n+1 nodes to l nodes
c
     do 60 o=1,j
     e3(o)=e1(o)
```

```
      f3(o)=f1(o)
      g3(o)=g1(o)
 60   continue
      f3(m)=1+2*fo
      e3(1)=0
      g3(j)=0
      g3(m)=-fo
c
c reinitialize the coefficients in the B matrix in order to proceed
c in time for the rectangle between n+1 nodes to l nodes
c
      do 61 q=1,j
       do 62 h=1,l
        r3(q,h)=r1(q,h)
 62    continue
 61    continue
c
c solve entrire concentration field using tridiagonal matrix solver for
c every odd time step up from n+1 nodes to l nodes
c
      do 63 q=2,j
       e3(q)=e3(q)/f3(q-1)
       f3(q)=f3(q)-e3(q)*g3(q-1)
 63    continue
      do 64 q=2,j
       r3(q,i)=r3(q,i)-(e3(q)*r3(q-1,i))
 64    continue
      c(j,i)=r3(j,i)/f3(j)
c     write(2,*) j,c(j,i)
       do 65 q=j-1,1,-1
        c(q,i)=(r3(q,i)-g3(q)*c(q+1,i))/f3(q)
 65    continue
      endif
 40   continue
c
c write to the data file, sqnew4.dat, the time step, the time, the
c concentration at the far back corner, and the dimensionless time
c
      write(2,3) u,time,c(j,l),tau
 3    format(i6,f8.0,f11.6,f15.6)
      else
c
c reinitialize the coefficients in the A matrix in order to proceed
```

```
c in time for the rectangle up to m nodes
c
      do 41 i=1,j
      if(i.le.m) then
       do 42 o=1,l
        e4(o)=e2(o)
        g4(o)=g2(o)
 42     continue
        e4(1)=0
        g4(l)=0
        e4(n)=-fo
        g4(n)=-fo
c
c reinitialize the coefficients in the B matrix in order to proceed
c in time for the rectangle up to m nodes
c
      do 43 q=1,m
       do 44 h=1,l
        r4(q,h)=r2(q,h)
        f4(q,h)=f2(q,h)
 44     continue
 43    continue
c
c solve entire concentration field using tridiagonal matrix solver for
c every even time step up to m nodes
c
      do 45 q=2,l
       e4(q)=e4(q)/f4(i,q-1)
       f4(i,q)=f4(i,q)-e4(q)*g4(q-1)
 45    continue
      do 46 q=2,l
       r4(i,q)=r4(i,q)-(e4(q)*r4(i,q-1))
 46    continue
      c(i,l)=r4(i,l)/f4(i,l)
       do 47 q=l-1,1,-1
        c(i,q)=(r4(i,q)-g4(q)*c(i,q+1))/f4(i,q)
 47     continue
      else
c
c reinitialize the coefficients in the A matrix in order to proceed
c in time for the rectangle from m+1 to j nodes
c
      do 66 o=n+2,l
```

```
      e4(o)=e2(o)
      g4(o-1)=g2(o-1)
 66   continue
      e4(n+1) =0
      g4(l)=0
c
c reinitialize the coefficients in the B matrix in order to proceed
c in time for the rectangle from m+1 to j nodes
c
     do 67 q=1,j
      do 68 h=1,l
       r4(q,h)=r2(q,h)
       f4(q,h)=f2(q,h)
 68    continue
 67   continue
c
c solve entire concentration field using tridiagonal matrix solver for
c every even time step from m+1 to j nodes
c
     do 70 q=n+2,l
      e4(q)=e4(q)/f4(i,q-1)
      f4(i,q)=f4(i,q)-e4(q)*g4(q-1)
 70   continue
     do 71 q=n+2,l
      r4(i,q)=r4(i,q)-(e4(q)*r4(i,q-1))
 71   continue
     c(i,l)=r4(i,l)/f4(i,l)
c    write(2,*) j,c(i,l)
      do 72 q=l-1,n+1,-1
       c(i,q)=(r4(i,q)-g4(q)*c(i,q+1))/f4(i,q)
 72    continue
     endif
 41   continue
c
c write into data file, sqnew4.dat, the time step, time, concentration
c at the far back corner, and the dimensionless time
c
     write(2,3) u,time,c(j,l),tau
     endif
 26   continue
     stop
     end
```

Appendix C

Experimental Verification of Diffusion Assumption

Two experimental methods for determining the binary liquid molecular diffusivity in small one-dimensional voids are outlined in this appendix. During this research the first method described was attempted with little success. The second method described should be more precise and therefore, was suggested this method for future work.

This experimentation was necessary to validate the assumption that the crevice opening for the one-dimensional case (hypodermic needle) was small enough such that only molecular diffusion occurs. These experiments would determine if the agitation in the tank would enhance the solute penetration due the turbulent nature of the mixing. Therefore, a solution with a known diffusion coefficient could be analyzed and then compared with the exact solution detailed in Chapter 2 to determine if the exact solution predicts the degree of solute penetration.

Experimental Method 1 *(Determination of Concentration by Visual Comparison)*

1. Obtain a solute/solvent mixture with a known diffusion coefficient. This solution needs to have a strong color at relatively low concentration. The solute which was used for this experiment was cupric sulfate which had a dark blue color when dissolved in water.

2. Obtain some clear capillary tubes. Try to obtain the tubes with a couple of different inside diameters ranging from 0.2 mm to 1 mm.

3. Make up a color coded set of capillary tubes using a different concentration in each capillary tube. The tubes may be filled with the solution by using a pipette bulb and then plugged at both ends with wax. If the tubes are aligned from low concentration to a higher concentration, they should exhibit a varying degree of "blueness", if using cupric sulfate as the electrolyte. This will be the concentration scale use to determine the concentration of electrolyte in the experimental tubes

4. Obtain a small lab top mixer and beaker. The beaker should be a variable speed mixer, in order to determine the agitator speed which has adequate mixing but does not break the capillary tubes.

5. A number of capillary tubes are then filled with water and plugged at one end with the wax. These tubes should be anywhere between one and two inches (2.54-5.08 centimeters).

6. Fill the agitation beaker with an electrolyte solution which is greater than the highest concentration in the "concentration scale" described in Step 2. However, this concentration should not be greater than 10 mole percent and preferably less than 5 mole percent, in order to obey the infinite dilution criterion.

7. Place the water filled tubes in the beaker and begin agitation. Monitor time and temperature of the bath.

8. Allow the tubes to agitate for some predetermined time (method to determine this time is given in Step 12). Then while still in the bath, plug the open end of the crevice with the wax and remove from the bath. Set the tubes aside for a couple days in order to allow the cupric sulfate to equilibrate throughout the entire tube.

9. Take the capillary tubes which were allowed to equilibrate and compare them with the capillary tube concentration scale. Match the color of the test tubes with the one which most closely matches it in the scale. This will be the equilibrium concentration of the test tube.

10. Take the average concentration of several different tubes. This will be the mean concentration.

11. This experiment should be conduct again with some capillary tubes of different inside diameters.

12. In order to determine the approximate time for diffusion, the one-dimensional model for diffusion during the batch process in Appendix A.1.1 and computer code in Appendix B.1.1 along with the equilibrium model for diffusion after the batch process in Appendix A.1.2 and computer code in Appendix B.1.2 can be utilized. The bath temperature can be used to determine the diffusion coefficient and the tube length should be used as well. Check a few different diffusion times using the one-dimensional model and then use these results as the initial condition in the equilibrium model. Use a diffusion time for the experiment which predicts an equilibrium concentration which falls within the capillary tube concentration scale.

13. Once the average concentration from several different capillary tubes is determine, this can be compared to the concentration predicted from the model for the same diffusion time.

Experimental Method 2 (UV Spectroscopy)

The following is not a procedure for an experiment because these tests have not been conducted. However, it is an outline of a proposed method by Davis [4] so all the specifics are not covered.

Determination of Absorbance/Concentration Curve

1. Obtain a solute/solvent mixture with a known diffusion coefficient. The solute needs to be an ultraviolet (UV) tracer possibly benzoic acid and the wavelength range which this solute absorbs the maximum UV light needs to be known. This can be found in the literature for UV tracers.

2. Determine the absorbance A_λ versus solute concentration curve. This is done with a UV spectrophotometer. Various solute concentration samples should be prepared.

3. Each sample is then tested in the UV spectrophotometer and the intensity of radiation which passes through the sample is measured.

$$A_\lambda \equiv \lg\left(\frac{I_{\lambda,l}}{I_{\lambda,0}}\right) = \frac{\alpha_\lambda C_B l}{2.303} \qquad \text{(C.1)}$$

4. Then, the Beer-Lambert Law is used to determine the absorbance. where $I_{\lambda,l}$ is the intensity of light passing through the sample of length l at the wavelength range determine in Step 1, $I_{\lambda,0}$ is the intensity of light which is incident on the sample, α_λ is the proportionality constant which is determined from the known concentration of the samples and the absorbance is determined from the UV spectrophotometer, C_B is the concentration of the solute in the sample, and l is the sample length [40, Levine].

5. Now prepare the absorbance versus concentration curve.

Determination of Concentration in Capillary Tubes

1. Obtain some capillary tubes. Try to obtain the tubes with a couple of different inside diameters.

2. Obtain a small lab top mixer and beaker. The beaker should be a variable speed mixer, in order to determine the agitator speed which has adequate mixing but does not break the capillary tubes.

3. A number of capillary tubes are then filled with water and capped at one end. These tubes should be anywhere between one and two inches (2.54-5.08 centimeters).

4. Fill the agitation beaker with an UV tracer solution with known concentration. This concentration should not be greater than 10 mole percent and preferably less than 5 mole percent, in order to obey the infinite dilution criterion.

5. Place the water filled tubes in the beaker and begin agitation. Monitor time and temperature of the bath.

6. Allow the tubes to agitate for some predetermined time (method to determine this time is given in Step 7). After this time has elapsed, remove the tubes and empty the solution into the UV spectrophotometer specimen test tubes. Be sure to wash the capillary tubes out carefully into the specimen tubes to remove all of the solute which has diffused into the capillary tube.

7. In order to determine the approximate time for diffusion, the one-dimensional model for diffusion during the batch process in Appendix A.1.1 and computer code in Appendix B.1.1 along with the equilibrium model for diffusion after the batch process in Appendix A.1.2 and computer code in Appendix B.1.2 can be utilized. The bath temperature can be used to determine the diffusion coefficient and the tube length should be used as well. Check a few different diffusion times using the one-dimensional model and then use these results as the initial condition in the equilibrium model. Use a diffusion time for the experiment which predicts an equilibrium concentration which falls within the concentration range of the absorbance/concentration curve.

8. Fill the UV spectrophotometer tubes with water to the needed volume to test in the spectrophotometer.

9. Determine the absorbance of each sample with the UV spectrophotometer and determine the concentration of each sample from the absorbance/concentration curve or from the Beer-Lambert Law, equation (C.1).

10. Take the average concentration of several different tubes. This will be the mean concentration. There will probably be a high degree of variation in the sample concentration since the sample volume of the capillary tubes is very small.

11. This experiment should be conducted again with some capillary tubes of different inside diameters.

Validity of Assumption

Remember that this experiment was used to validate the assumption that small crevices only experience mass transfer through diffusion. These guidelines should be followed to determine the validity of this assumption.

1. Experimental conc. = Theoretical conc. ---------- diffusion only

2. Experimental conc. > Theoretical conc. ---------- diffusion + other

If condition 2 is satisfied then tubes with smaller inside diameters should be used to determine limiting diameter for the diffusion only assumption. This limiting diameter can then be compared to the diameter of most hypodermic needles to determine if the diffusion only assumption was valid in this research.

Appendix D

Sector-Rectangular Comparison for Shape 2

Figure D.1 shows the series of curves for τ versus *Vo* for $\theta = 0.1$ and a length ratio of 0.25. The series of curves is for various values of width ratios. Similar curves are shown in Figures D.2 and D.3 except that these figures are for length ratios of 0.50 and 0.75, respectively.

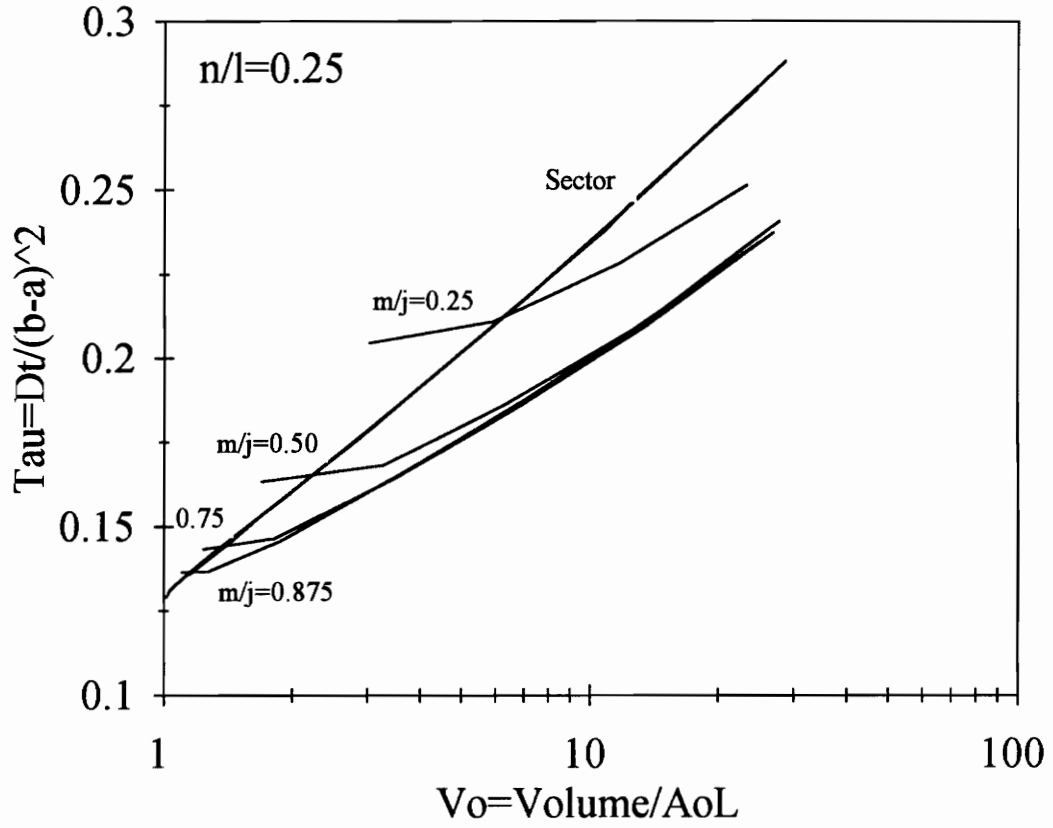

Figure D.1 - Sector - Shape 2 Comparison for a Length Ratio of 0.25.

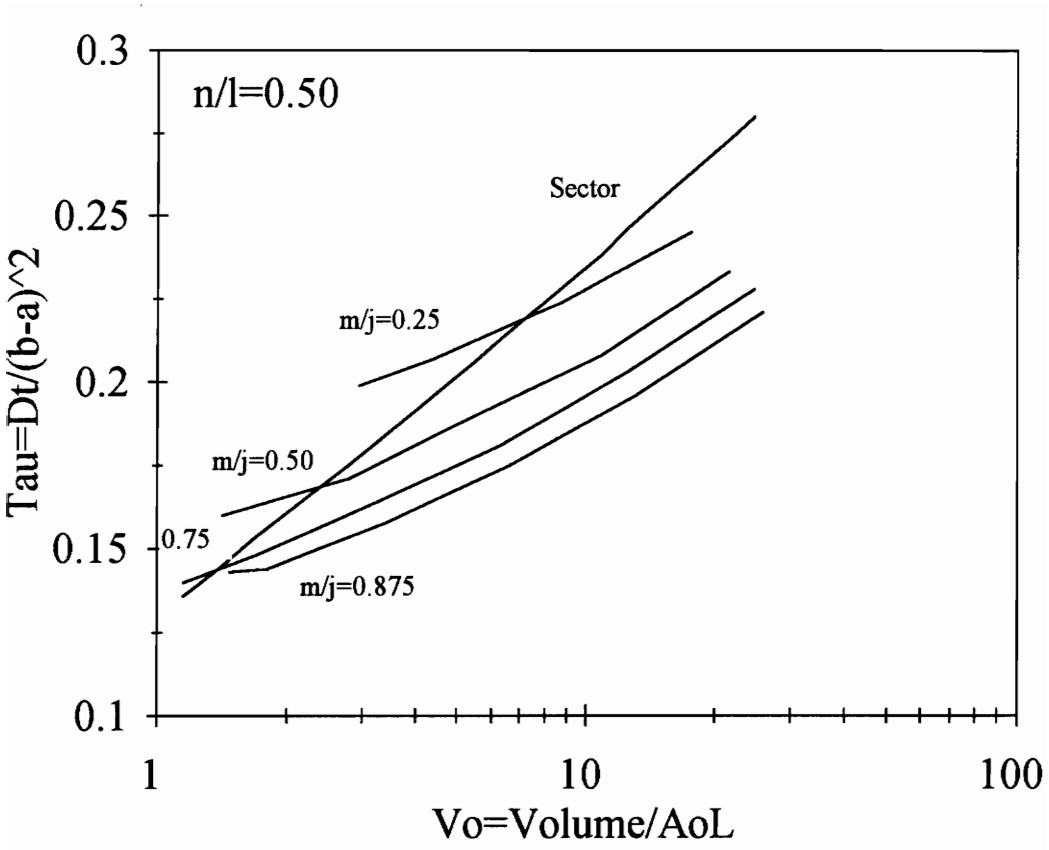

Figure D.2 - Sector - Shape 2 Comparison for a Length Ratio of 0.50.

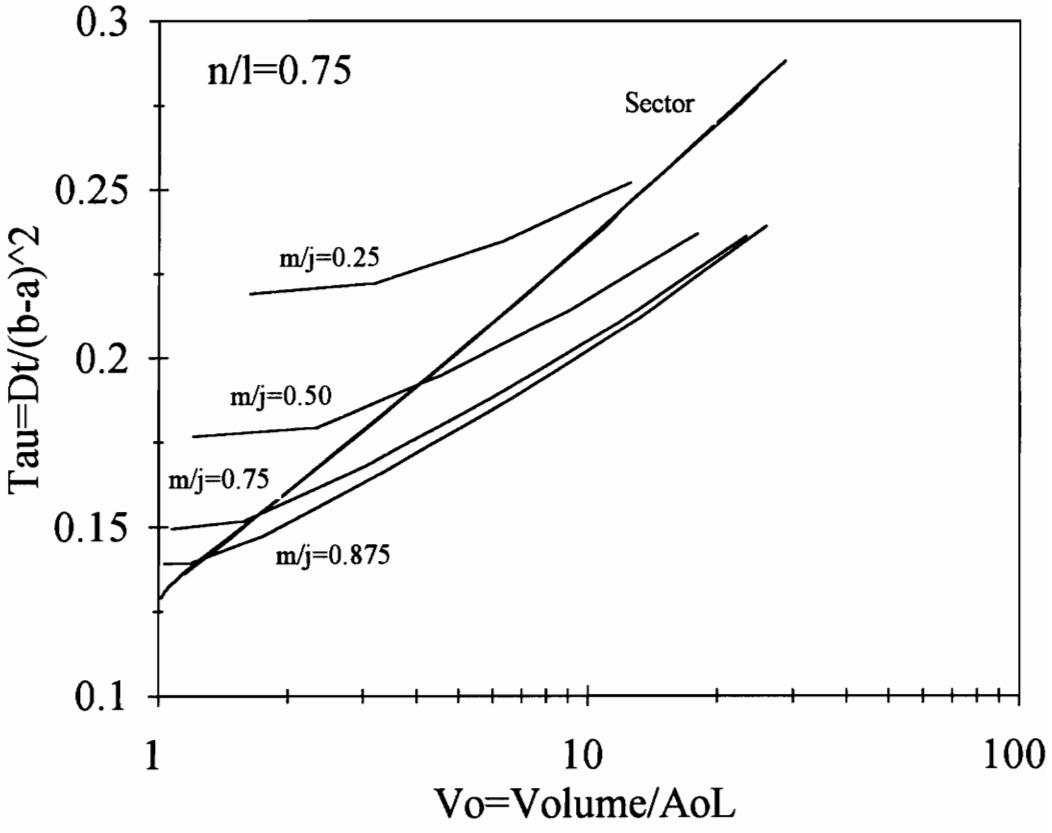

Figure D.3 - Sector - Shape 2 Comparison for a Length Ratio of 0.75.

References

1. Malloy, Michael G. (1992) "Medical Waste Treatment: A Status Report." Waste Age. pp 66-75. Aug.

2. Hershkowitz, Allen. (1990) "Without a Trace. Handling Medical Waste Safely." Technology Review. Vol 93, No 6.

3. Carpenter, William K. (1992) "Design of Medical Waste Treatment Systems Employing Bioremediation." M.S. Thesis, Virginia Polytechnic Institute and State University, Blacksburg, Virginia.

4. Davis, Richey M., personal communication.

5. Ottesen, Martin and Ib Svendsen (1969) "The Subtilisins." Proceedings from the Conference on the Serine Proteases, Vol 8, pp 199-215.

6. Shane, Erica S., John L. Anderson, and Michael M. Domach, (1990) "Enhanced Protein Diffusion in a Solvent Gradient." Ind. Eng. Chem. Res. Vol 29, No 2, pp 309-312.

7. Northrop, J.N. and M.L. Anson (1928) Journal of General Physiology. Vol 12, pp 543-565.

8. Taylor, G. (1953) Proc. R. Soc. A. Vol 219, pp 186-202.

9. Cummins, H.Z. and E.R. Pike (1974) "Photon Correlation and Light Beating Spectroscopy." NATO Advanced Study Institute Series. Plenum Press, London.

10. Heflinger, L.O., R.F. Wuerker, and R.E. Brooks (1966) Journal of Applied Physics. Vol 37, pp 642-656.

11. Anderson, J. and K. Saddington (1949) Journal of Chemical Society. Vol S, pp 381-384.

12. Mills, R and J. W. Kennedy (1953) Journal of American Chemical Society. Vol 75, pp 5696-6000.

13. Mills, R. (1955) Journal of American Chemical Society. Vol 77, pp 6116-6122.

14. Seilliere, G. (1906) Compt. Rend. Soc. Biol. Vol 61, pp 205-207.

15. Reese, E.T., R.G.H. Siu, and H.S. Levinson (1950) "Biochemical Degradation of Soluble Cellulase Derivatives and Its Relation to the Mechanism of Cellulose Hydrolysis." Journal of Bacteriology. Vol 59, pp 485-492.

16. Emert, G.H., E.K. Gum, J.A. Lang, T.H. Liu and R.D. Broun, Jr. (1974) "Cellulases." Food Related Enzymes. Advances in Chemistry Series, Vol 136, American Chemical Society Publications, Washington, D.C., pp 79-100.

17. Ramachandran, K.B. and M.A. Hashim (1990) "Simulation studies on simultaneous saccharification and fermentation of cellulose to ethanol." The Chemical Engineering Journal. Vol 45, pp B27-B34.

18. Roy, Samir K., Ramkrishna Sadhukhan, Syamal K. Raha, and S.L. Chakrabarty (1991) "Enzymatic hydrolysis of pretreated cellulosic wastes by the cellulase complex of *Myceliophthora thermophila* D-14 to produce ethanol." Fuel. Vol 70, pp 757-760.

19. Philippidis, George P., Tammy K. Smith, and Charles E. Wyman (1993) "Study of the Enzymatic Hydrolysis of Cellulose for Production of Fuel Ethanol by the Simultaneous Saccharification and Fermentation Process." Biotechnology and Bioengineering. Vol 41, pp 846-853.

20. Mukataka, Sukekuni, Nobuyuki Kobayashi, Seigo Sato, and Joji Takahashi (1988) "Variation in Cellulase-Constituting Components from *Trichoderma reesei* with Agitation Intensity." Biotechnology and Bioengineering. Vol 32, pp 760-763.

21. Wase, D.A.J., W.J. McManamey, S. Raymahasay, and A.K. Vaid (1985) Biotechnology and Bioengineering. Vol 27, pp 1166-1169.

22. Tiraby, G., M. Clanet, and H. Durand (1988) "Enzymatic Saccharification of Municipal Wastes." Biotechnology and Bioengineering. Vol 32, pp 930-934.

23. Sattler, W., H. Esterbauer, O. Glatter, and W. Steiner (1989) "Effect of enzyme concentration on the rate of the hydrolysis of cellulose." Biotechnology and Bioengineering. Vol 33, pp1221-1234.

24. Reid, Robert C., John M. Prausnitz, and Bruce E. Poling (1987) The Properties of Gases and Liquids. McGraw-Hill, New York, pp 577-631.

25. Bird, R.B., W.E. Stewart, and E.N. Lightfoot (1960) Transport Phenomena. Wiley, New York, chap 16.

26. Cussler, E.L. (1984) Diffusion: Mass Transfer in Fluid Systems. Cambridge, Cambridge, chaps 3,7.
27. Boyce C.O.L. (1986) Novo's Handbook of Practical Biotechnology. Novo Industri A/S, Bagsvaere, Denmark, pp 77-89.

28. Therien, Ned C. (1993) Recommendations for State Regulatory Oversight of Medical Waste Treatment Technologies. Department of Environmental Quality, Washington, D.C., p 1.

29. Toth, Thomas E., personal communication.

30. Sriranganathan, N., personal communication.

31. Özişik, M.N. (1980) Heat Conduction. Wiley, New York, chaps 2,3.

32. Peaceman D.W. and H. H. Rachford (1955) "The Alternating Direction Implicit Method." The Journal Society for Industrial Applied Mathematics. Vol 3, pp 28-41.

33. Cowling, E.B. and W. Brown (1969) "Structural Features of Cellulosic Materials in Relation to Enzymatic Hydrolysis." Cellulases and Their Applications. Advances in Chemistry Series, Vol 95, American Chemical Society Publications, Washington, D.C., pp 152-187.

34. Malcolm, Alan D.B. (1971) Enzymes. Methuen Educational Ltd, London, chaps. 1-3.

35. King, K.W. and Mahmood I. Vessal (1969) "Enzymes of the Cellulase Complex." Cellulases and Their Applications. Advances in Chemistry Series, Vol 95, American Chemical Society Publications, Washingtion, D.C., pp 7-25.

36. Wood, T.M. and S.I. McCrae (1979) "Synergism Between Enzymes Involved in the Solubilization of Native Cellulose." Hydrolysis of Cellulose: Mechanism of Enzymatic and Acid Catalysis. Advances in Chemistry Series, Vol 181, American Chemical Society Publications, Washington, D.C., pp 181-210.

37. Nissan, Alfred H. (1980) Basic Principles of Pulp and Paper. Westvaco, Charleston, chap 2.

38. Britt, Kenneth W. (1964) Handbook of Pulp and Paper Technology. Van Nostrand Reinhold Company, New York, pp 4-5.

39. Press, William H., Brian P. Flannery, Saul A. Teukolsky, William T. Vetterling (1989) Numerical Recipes (FORTRAN Version). Cambridge University Press, Cambridge, pp 170-179.

40. Levine, Ira N. (1983) Physical Chemistry. McGraw Hill, New York, chap 21.

Bibliography

American Paper and Pulp Association (1965) The Dictionary of Paper. George Banta Company, Inc., New York.

Casey, James P. (1980) Pulp and Paper Chemistry and Chemical Technology. Wiley, New York.

Cornish-Bowden, Athel (1976) Principles of Enzyme Kinetics. Butterworths and Co., London.

Kirkaldy, J.S. and D.J. Young (1987) Diffusion in the Condensed State. The Institute of Metals, London.

Laidler, Keith J. and Peter S. Bunting (1973) The Chemical Kinetics of Enzyme Action. Clarendon Press, New York.

Robinson, R.A. and R.H. Stokes (1959) Electrolyte Solutions. Butterworths Scientific Publications, London.

Tyrrell, H.J.V. and K.R. Harris (1984) Diffusion in Liquids. Butterworths and Co., London.

Young, Raymond A. and Roger M. Rowell (1986) Cellulose: Structure, Modification and Hydrolysis. Wiley, New York.

Vita

Douglas Bland Hudgins was born 15 October 1969 in Richmond, Virginia. He lived in Mathews County, Virginia where he graduated from high school. Douglas attended Virginia Polytechnic Institute and State University in Blacksburg from 1987 to 1992 and received a Bachelor of Science degree in Mechanical Engineering. During his undergraduate studies, Douglas worked for E. I. DuPont in Richmond, Virginia under the Cooperative Education Program and also worked for DuPont as an engineer during the summer following graduation. Following the summer of 1992, Douglas attend the graduate school of Virginia Polytechnic Institute and State University from August of 1992 until his graduation with a Master of Science degree in Mechanical Engineering in the spring of 1994. Upon graduation, Douglas will pursue graduate studies in the Department of Environmental Engineering at Virginia Polytechnic Institute and State University.

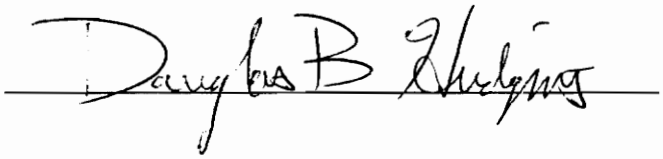

Douglas B. Hudgins